Wisconsin Highway Research Program

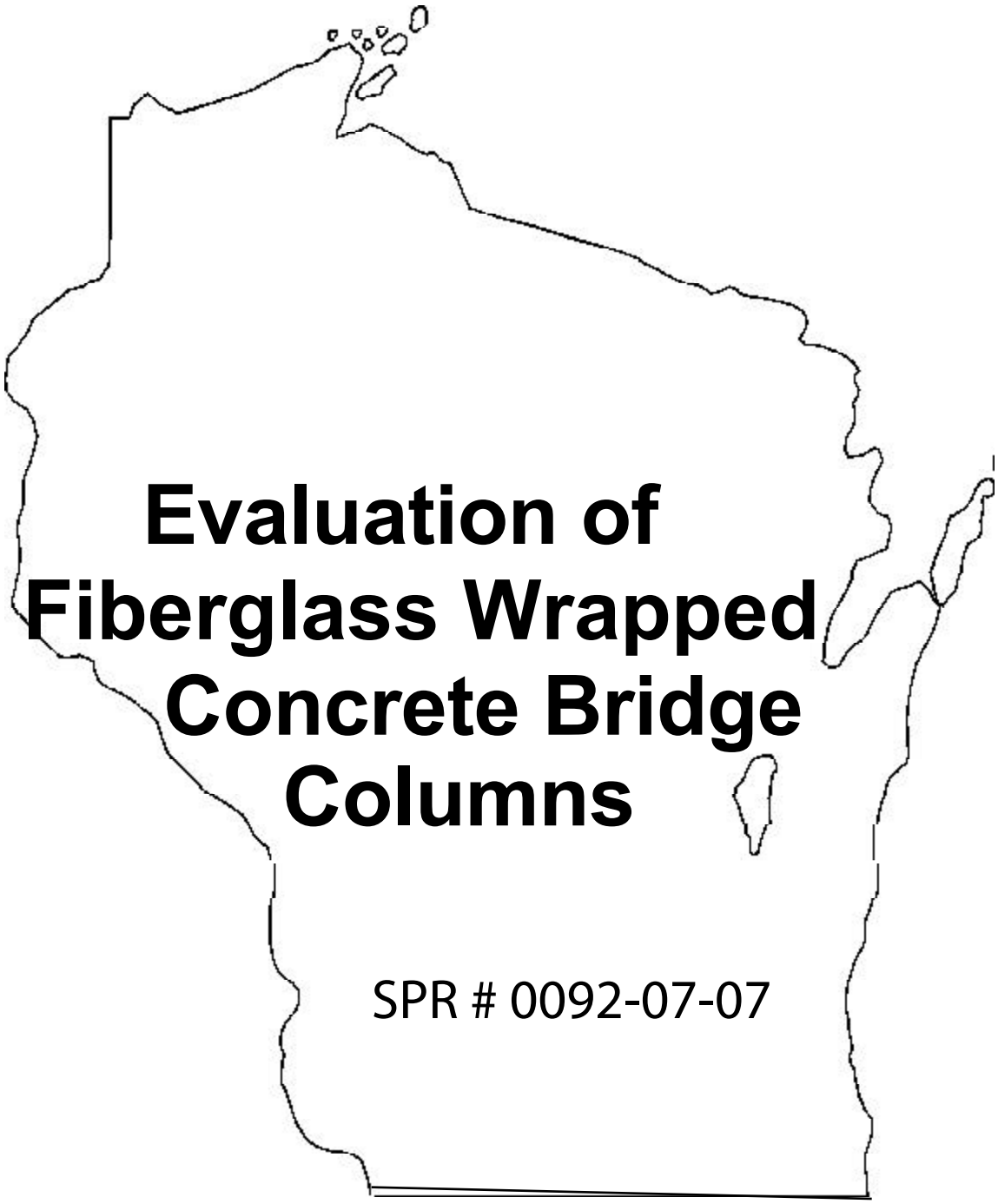

Evaluation of Fiberglass Wrapped Concrete Bridge Columns

SPR # 0092-07-07

Dante Fratta and Jose Pincheira
Department of Civil and Environmental Engineering
University of Wisconsin Madison

December 2008

WHRP 08-06

WISCONSIN HIGHWAY RESEARCH PROGRAM #0092-07-07

EVALUATION OF FIBERGLASS WRAPPED CONCRETE BRIDGE COLUMNS

Final Report

By

Principal Investigators: Dante Fratta and Jose A. Pincheira

Graduate Research Assistants: Kyu-Sun Kim

Department of Civil and Environmental Engineering
University of Wisconsin-Madison

Submitted to the
Wisconsin Department of Transportation

December 2008

DISCLAIMER

This research was funded through the Wisconsin Highway Research Program by the Wisconsin Department of Transportation and the Federal Highway Administration under Project 0092-07-07. The contents of this report reflect the views of the authors who are responsible for the facts and accuracy of the data presented herein. The contents do not necessarily reflect the official views of the Wisconsin Department of Transportation or the Federal Highway Administration at the time of publication.

This document is disseminated under the sponsorship of the Department of Transportation in the interest of information exchange. The United States Government assumes no liability for its contents or use thereof. This report does not constitute a standard, specification or regulation.

The United States Government does not endorse products or manufacturers. Trade and manufacturers' names appear in this report only because they are considered essential to the object of the document.

TECHNICAL REPORT DOCUMENTATION PAGE

1. Report No. WHRP 08-06	2. Government Accession No.	3. Recipient's Catalog No.
4. Title and Subtitle Evaluation of Fiberglass Wrapped Concrete Bridge Columns		5. Report Date December 2008 6. Performing Organization Code Wisconsin Highway Research Program
7. Authors Dante FRATTA, Jose A. PINCHEIRA, and Kyu-Sun KIM		8. Performing Organization Report No.
9. Performing Organization Name and Address Department of Civil and Environment Engineering University of Wisconsin-Madison 1415 Engineering Drive, Madison, WI		10. Work Unit No. (TRAIS) 11. Contract or Grant No. WisDOT SPR# 0092-07-07
12. Sponsoring Agency Name and Address Wisconsin Department of Transportation Division of Business Services Research Coordination Section 4802 Sheboygan Ave., Room 104 Madison, WI 53707		13. Type of Report and Period Covered Final Report, 2006-2008 14. Sponsoring Agency Code
15. Supplementary Notes		

16. Abstract

The main purpose of this project is to assess the effectiveness of the fiberglass wrapping in reducing the corrosion degradation rate of the columns. To evaluate the effectiveness of the technique, the research team will use both non-destructive and destructive test methods. The results of the study will provide show that the wrapping while protecting the columns from further ingress of chloride ions, it does not help deter the corrosion activity when already present. Recommendation for future use fiber wraps complemented with other remediation techniques and maintenance practices are provided.

17. Key Words Concrete columns, rebar corrosion, fiberglass, non-destructive testing, half-cell potential, chlorine ion content		18. Distribution Statement No restriction. This document is available to the public through the National Technical Information Service 5285 Port Royal Road Springfield VA 22161	
19. Security Classification (of this report) Unclassified	20. Security Classification (of this page) Unclassified	21. No. of Pages	22. Price

Form DOT F 1700.7 (8-72) Reproduction of completed page authorized

EXECUTIVE SUMMARY

The service life of concrete elements in highway bridges is often limited by the corrosion deterioration of reinforcing bars. In cold regions, the corrosion rate of concrete bridge decks and columns is accelerated by the use of deicing solutions during the winter driving season. The corrosion process in steel rebars causes cracking, spalling, and delamination of the reinforced concrete structures and increases the cost of rehabilitation and maintenance operations. In Wisconsin, fiberglass wrapping has been used for corrosion protection of reinforced concrete columns. In this technique, a fiberglass wrap creates a barrier intending at reducing the detrimental effect of traffic splashing of deicing solutions and therefore controlling the rate of corrosion while extending the service life of concrete columns. This report describes a study aimed at evaluating the effectiveness of fiberglass wrapping in controlling and reducing the rate of corrosion in concrete columns. Field tests including visual surveys, P-waves and electromagnetic wave propagation methods, tomographic imaging, half-cell potential surveys, and measurements of chloride ion intrusion were run in eight concrete columns of three Wisconsin bridges to assess the effectiveness of the fiberglass wrapping in reducing the corrosion degradation rate of the reinforced concrete columns. Field and laboratory data show that fiberglass wrapping may help deter the ingress of chloride ions into the repaired concrete, but it does not reduce or stop the corrosion rate in the bars if the corrosion conditions (e.g., high chlorine ion content) remain inside the concrete columns or moisture and chlorine ion have access the columns through paths along areas above and below fiberglass wrap.

TABLE OF CONTENTS

TECHNICAL REPORT DOCUMENTATION PAGE 2
EXECUTIVE SUMMARY 3
TABLE OF CONTENTS 4
ACKNOWLEDGMENTS 6
Chapter 1. Introduction 7
1.1. Problem Statement 7
1.2. Project Background and Research Objectives 8
1.3. Organization of the Report 8
Chapter 2. Literature Review 10
2.1. Introduction 10
2.2. Corrosion Process 10
2.3. Corrosion Repair and Prevention Methods 13
2.4. Field and Laboratory Methods for Bridge Column Assessment 16
2.4.1 P-wave Travel Time Profiling 16
2.4.2 Ground Penetrating Radar 17
2.4.3 Travel-time Tomographic Imaging 18
2.4.4 Half-cell potential (ASTM C876-91) 20
2.4.5 Chlorine Ion Concentration (AASHTO T 260-97) 22
Chapter 3. Description of Bridges and Columns Surveyed 26
3.1. Introduction 26
3.2. Wisconsin Inspection Reports and Visual Surveys 28
3.2.1 Bridge B-11-17 29
3.2.2 Bridge B-13-113 32
3.2.3 Bridge B-13-144 33
3.2.4 Bridge B-13-172 35
3.2.5 Bridge B-28-35 37
3.2.6 Bridge B-28-40 39
3.2.7 Bridge B-28-43 42
3.2.8 Bridge B-28-45 44
3.2.9 Bridge B-28-50 45
3.2.10 Bridge B-53-65 47
3.2.11 Bridge B-53-66 50
3.2.12 Bridge B-53-71 52
3.2.13 Bridge B-53-75 54
3.3. Selection of Columns for Testing 55
Chapter 4. Field Testing and Data Interpretation 58
4.1. Introduction 58
4.2. P-wave velocity measurements 58
4.2.1 Bridge B-28-45: P-wave velocity results 61
4.2.2 Bridge B-53-71: P-wave velocity results 66
4.2.3 Bridge B-13-144: P-wave velocity results 70
4.3. Ground Penetrating Radar Measurements 73
4.3.1 Bridge B-28-45: GPR tomography results 74
4.2.2 Bridge B-13-144: GPR tomography results 77

4.4. Half-Cell Potential Measurements 78
4.4.1 Bridge B-28-45: Half-cell potential results 79
4.4.2 Bridge B-53-71: Half-cell potential results 85
4.4.3 Bridge B-13-144: Half-cell potential results 88
4.5. Half-Cell Potential Measurements 88
4.5.1. Sample collection 89
4.5.2. Conceptual interpretation 90
4.5.3. Cl^- Concentration Results 91
Chapter 5. Summary and Conclusions 95
References 98

ACKNOWLEDGMENTS

Mr. A. Summitt collaborated in the field data collection. Funds were provided by the Wisconsin Highway Research Program (WHRP Project 0092-07-07) and by Midwest Regional University Transportation Center (MRUTC). The content of this report does not necessarily reflect the views of the funding agencies.

Chapter 1. Introduction

1.1. Problem Statement

The Wisconsin Department of Transportation (WisDOT) has been using fiberglass wrapping as part of maintenance operations for standard circular reinforced concrete columns built in the 1970s or before. These columns were built with uncoated, black steel bars and thus are susceptible to corrosion caused by the splashing of saline solutions used during winter (Figure 1.1). Over the years, the progression of steel corrosion has led to cracking and spalling of the concrete causing concerns over the loss of serviceability and structural integrity of bridge columns. A maintenance strategy used by the WisDOT throughout the state is to remove the deteriorated concrete, clean the damaged area, patch it with grout, and to wrap the columns with a thin layer of a fiberglass composite material cemented with epoxy resin. The use of fiberglass wrapping intents at providing a barrier to moisture and deicing salts in the splash zone of the columns. This barrier should help in arresting or reducing the corrosion rate of the steel reinforcement. Thus, the fiberglass wrap should extend the service life of the columns. However, the premature failure of some of these wraps has cast doubts on their effectiveness fiberglass wrapping and there is a concern that the corrosion process has continued even after the application of the wraps.

Figure 1.1: Snow and deicing solution splash on bridge columns (Interstate I-94 East bound – December 2008).

1.2. Project Background and Research Objectives

The main purpose of this research project is to assess the effectiveness of fiberglass wrapping in arresting or reducing the corrosion degradation rate of concrete columns in Wisconsin bridges. To evaluate the effectiveness of the technique, the research team used several assessment tools:

- Visual inspection to assess the overall condition of wrapped and unwrapped concrete columns in selected Dane, Jefferson, Columbia and Rock Counties, WI bridges
- P-wave travel time measurements to evaluate the general structural integrity of selected wrapped and unwrapped columns
- P-wave travel time tomographic imaging of cross-sections of selected columns to constrained damage areas in the concrete
- Electromagnetic wave travel time tomographic imaging of cross-sections of selected column to estimate moisture and chlorine ion concentration distribution.
- Half-cell potential measurements to assess corrosion activity in selected columns
- Chloride ion content measurements to evaluate the ingress of the chloride ion into the wrapped columns

1.3. Organization of the Report

This report documents the results of a study aimed at evaluating the effectiveness of fiberglass wrapping on reducing the exposure of concrete bridge columns to chloride ion contamination by field inspection, nondestructive testing, and laboratory chloride ion content measurements.

The report describes the different activities performed during the study, the testing methodology, data analysis and interpretation, and recommendations. Chapter 2 documents a comprehensive literature review of the corrosion process in concrete columns, remediation techniques, and past experiences on the use of fiberglass as corrosion remediation technique for reinforced concrete elements. Chapter 2 also describes concepts and applications related to the use of nondestructive evaluation techniques for the health monitoring of civil infrastructure. Chapter 3 describes and analyzes the results of the WisDOT regular inspection and the research team field surveys. The chronological evaluation of the WisDOT regular inspection documents the degradation and repairing actions followed on selected bridges and columns; while the research team field survey documents the overall health of the columns and the selection of columns for field testing.

Chapter 4 describes the field testing methodology used in the selected wrapped and unwrapped reinforced concrete columns. The details of the field testing as well as the data interpretation are presented and discussed. To evaluate the degraded quality of concrete, three testing methods were used: elastic wave propagation and tomographic imaging, electromagnetic wave propagation and tomographic imaging, and half-cell potential measurements. Tomographic imaging permitted locating deteriorated concrete areas of concrete while half-cell potential readings allowed a qualitative evaluation of corrosion active areas. Chapter 5 describes the laboratory experiments used to measure chloride ion content concentrations. These results were used to monitor one of the most important corrosion-driving mechanisms of reinforced bars; that is, if high chlorine ion content is present, corrosion would continue even if the column is protected with fiberglass wrap. For this study, the research team collected concrete powder samples both in wrapped and unwrapped columns. Finally, Chapter 6 provides a summary of the research activities, conclusions, and recommendations for the use of fiberglass wraps in Wisconsin bridges.

Chapter 2. Literature Review

2.1. Introduction

The service life of reinforced concrete elements in highway bridges is limited by corrosion deterioration. Rebar corrosion processes cause cracking, spalling, and delamination of the cover concrete in reinforced concrete structures. Corrosion damage increases the maintenance and rehabilitation expenses of structural concrete elements. In northern states, corrosion rates in bridge decks and columns are accelerated by the use of chloride ion-rich deicing solutions. The required use of deicing solutions urges the development of alternative methodologies for preventing and/or controlling the corrosion deterioration process. Fiberglass wrapping is one of the alternatives used for corrosion protection of reinforced concrete columns in bridges. In this methodology, the application of fiberglass creates an impervious barrier intending to reduce the detrimental effect of traffic splashing of deicing solutions on bridge columns (Figure 2.1). That is, the fiberglass wrap barrier reduces the access of moisture and chloride ion into the concrete structure preventing and/or controlling the corrosion process (Teng et al. 2003).

2.2. Corrosion Process

Corrosion of black steel rebars is one of the major causes of deterioration of reinforced concrete elements. The chloride ion concentration, temperature, relative humidity, concrete cover depth, and concrete quality are critical factors affecting corrosion rates of reinforcing bars. For example, chloride ions cause the local failure of the passive film in the cement past that naturally protects the reinforcing steel in the concrete from corrosion activity (Neville 1996).

During winters, sodium chloride (NaCl) aqueous solution is applied to pavements and bridge decks to reduce the freezing point of water and to prevent frost/black ice, sleet/freezing drizzle, or freezing rain and to improve drivers' safety. However, the exposure of concrete elements to chloride ions (Cl^-) and water creates the conditions for corrosion attack on reinforcing steel bars and the degradation of the concrete structure through cracking, spalling, and delamination. This progressive advance of the corrosion damage, if left unattended, can cause loss of serviceability and the overall deterioration of the infrastructure (Li et al. 2005).

2.2.1. Corrosion phenomena in reinforced concrete

Corrosion is an electrochemical process. In reinforced concrete structures, the electrochemical potential is generated by the concentration of dissolved ions near the steel in the concrete. Chemical changes at the anodic and cathodic areas are as follows (Figure 2.1 - Baiyasi 2000; Bentur et al. 1997; Broomfield 1997; Mehta et al. 1986):

anodic reactions:

$$Fe \rightarrow Fe^{2+} + 2e^{-}$$

$$Fe^{2+} + 2OH^{-} \rightarrow Fe(OH)_2 \qquad \textit{ferrous hydroxide}$$

$$4Fe(OH)_2 + 2H_2O + O_2 \rightarrow 4Fe(OH)_3 \qquad \textit{ferric hydroxide}$$

cathodic reaction:

$$4e^{-} + O_2 + 2H_2O \rightarrow 4(OH)^{-}$$

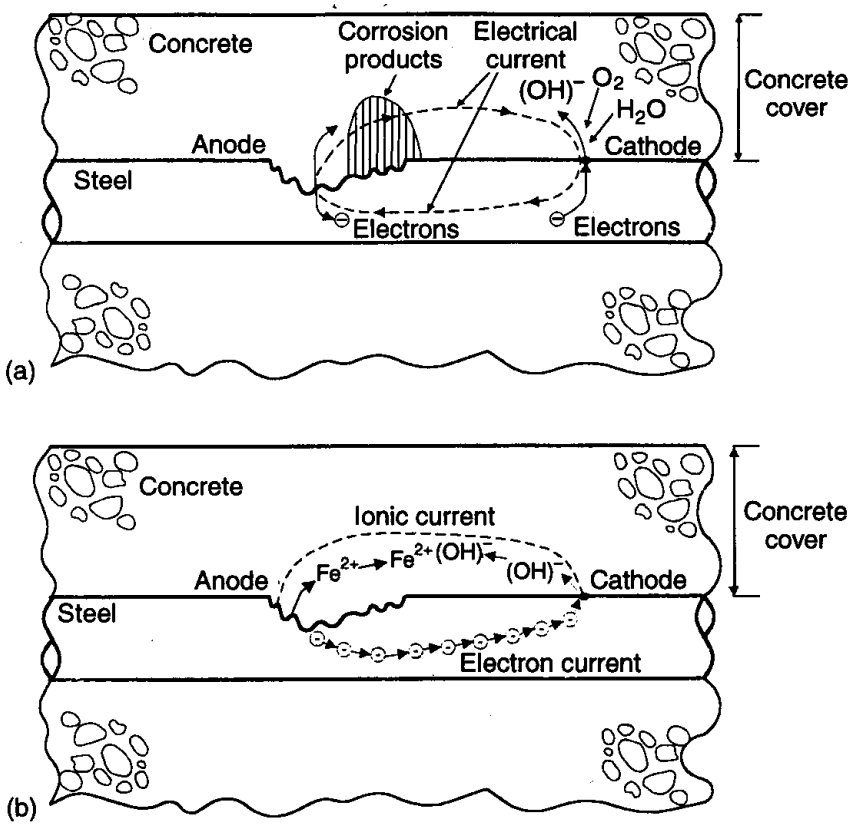

Figure 2.1: Corrosion process on the surface of steel: (a) reactions at anodic and cathodic sites and the electric current loop. (b) Flow of electrical charge during corrosion process (Bentur et al. 1997).

During these chemical reactions, large tensile stresses are generated in the concrete due to the increase in volume of the corroding steel bars. The hydrated ferric oxide ($Fe(OH)_3$) molecules

occupy a much larger volume than the original iron atom (Fe). These corrosion-generated tensile stresses cause cracking, spalling, debonding, and delamination in concrete elements (Figure 2.2 - Broomfield 1997; Neville 1996). To avoid these problems, the American Concrete Institute recommends limits in the chloride ion concentration in new concrete structures (Table 2.1).

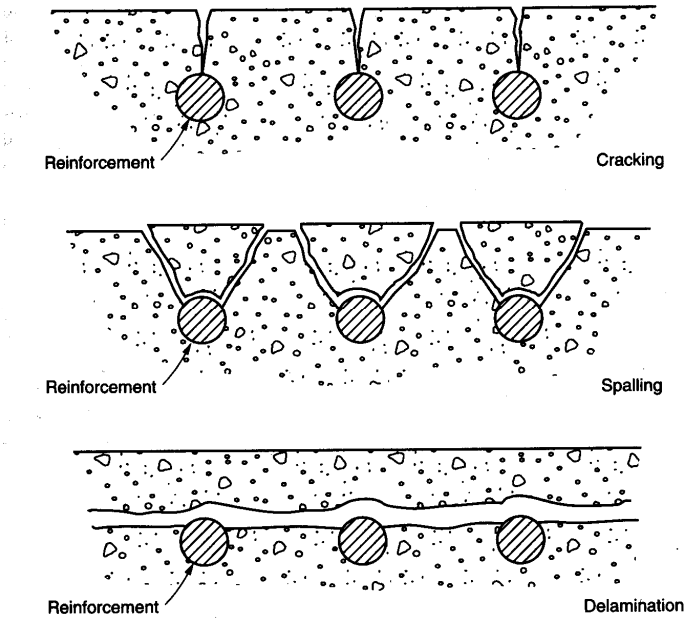

Figure 2.2: Conceptual view of the concrete damage caused by the corrosion process in the rebars (Neville 1996).

Table 2.1: Recommended limits for chloride ion content in concrete (Berver et al. 2001; ACI 201.2R-77)

Type of concrete element	**Maximum water-soluble chloride ion content [% by weight of cement content]**
Prestressed concrete	0.06
Conventionally reinforced concrete in a moist environment and exposed to chloride	0.10
Conventionally reinforced concrete in a moist environment but not exposed to chloride	0.15
Above ground construction where concrete will stay dry	No limit for corrosion

2.3. Corrosion Repair and Prevention Methods

Corrosion caused by chemical attacks from deicing salt and sea water environments needs to be repaired and maintained to prevent serviceability loss. Vaysburd and Emmons (2000) proposed a holistic model for assessing concrete damage and repair operations of degrading reinforced concrete elements (Figure 2.3).

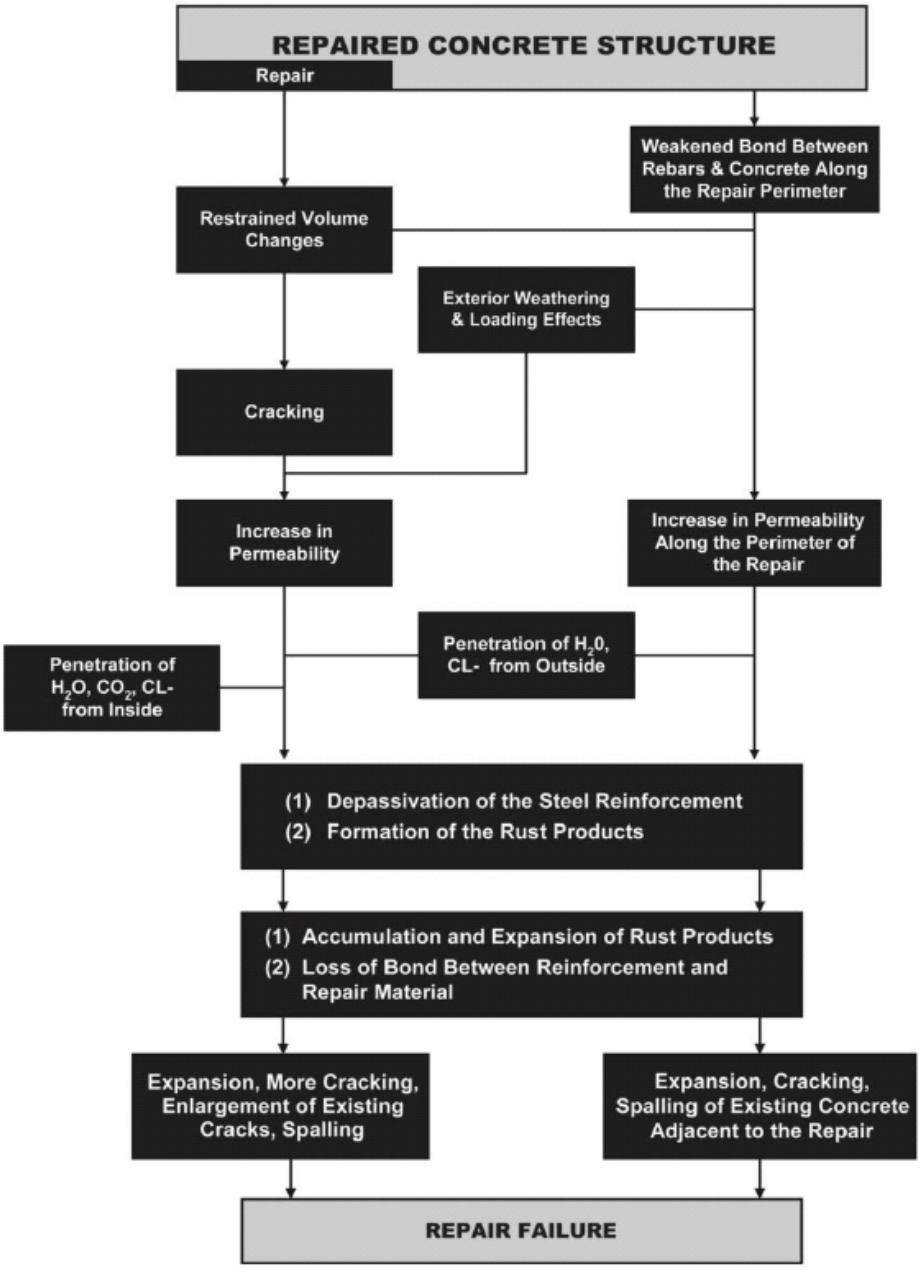

Figure 2.3: A holistic model for concrete infrastructure maintenance operation (Vaysburd and Emmons 2000).

The most common repair technique used in corrosion-attacked reinforced concrete elements is to (1) remove the cracked, spalled, or delaminated concrete; (2) clean the corroded reinforcing steel; and (3) place a concrete patch. Most reinforced concrete structural elements in bridges are repaired less than two years after to rebar corrosion damage has been detected (Watson 2000; Berver et al. 2001). When replacing the degraded concrete, latex-rich admixtures are added to the repairing mortar helping to create a low permeability mortar that will prevent the access of water and chloride ions by acting as a corrosion barrier (Allen et al. 1993). When the damage involves surface cracks, injections are used to fill deep cracks to improve the strength of the concrete. Common injection chemicals include epoxy, polyurethane, or polyester resins. These resins are injected after dust, dirt, grit or corrosions by-products are removed from the crack. The polymer resin bonds crack faces and seals cracks preventing the water, chloride ions and carbon dioxide to enter the concrete and rebar (Perkins 1997).

Fiber reinforced polymers

Fiber reinforced polymer (FRP) systems are also used to repair and prevent corrosion processes in reinforce concrete columns. The technique has been presented as an innovative and cost-effective repair and retrofit method that could extend service life of and improve serviceability of reinforced concrete structures. Most FRP materials are made of continuous fibers of aramid, carbon fiber, and glass fiber reinforced polymers impregnated in a resin matrix (Mirmiran et al. 2004). Advantages of FRP reinforcement include (Erki and Rizkalla 1993):

- high ratio of strength to mass density
- good fatigue characteristics (carbon and aramid fiber reinforcement)
- corrosion resistance
- electromagnetic neutrality
- low thermal extension in the axial direction
- light weight

Neale et al. (2005) investigated three different types of protection using FRPs and showed that FRP materials provide good protection against corrosion even for already corrosion-damaged concrete specimens. Wootton et al. (2003) indicated that the concrete chloride ion content measurements provide strong evidence that the epoxy type and the number of wraps influence

the ingress of chloride content. After testing concrete specimens submerged/splashed in salt solutions, Wootton et al. (2003) showed that the unwrapped specimens had a higher chloride ion concentration than the wrapped control specimens. They also observed that just a single layer of epoxy treatment is not as beneficial in preventing corrosion process as two or three layers of epoxy treatment (Figure 2.4 and 2.5).

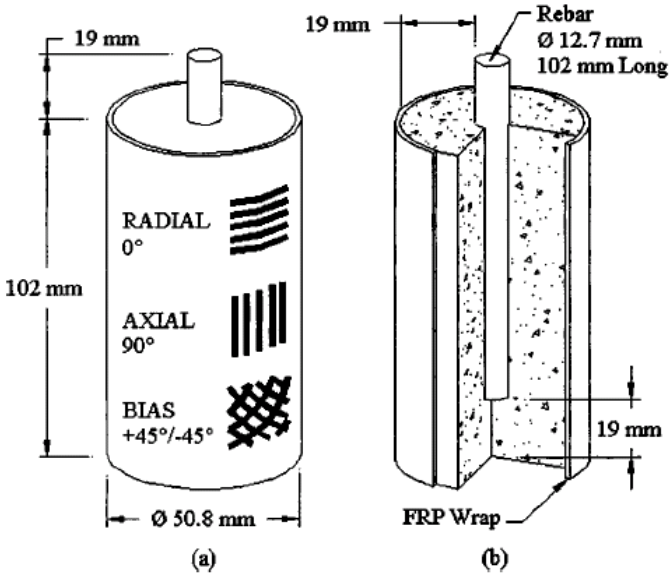

Figure 2.4: Laboratory specimens tested by Wootton et al. (2003): (a) wrap fiber orientation and (b) sectional view.

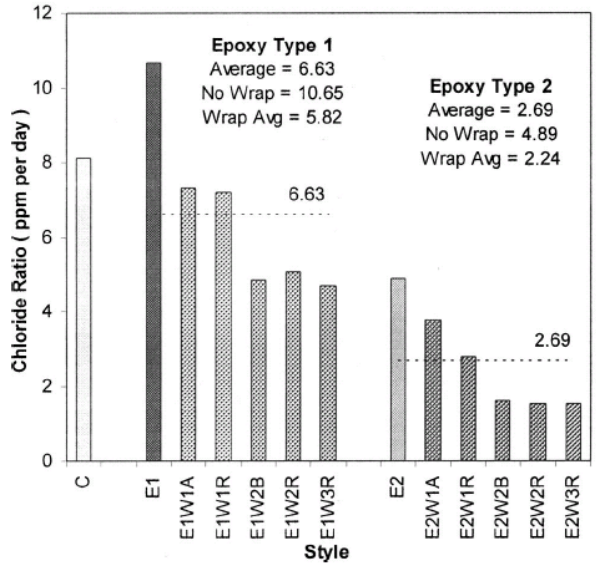

Style	Number of fiber-reinforced polymer wraps	Thermoset resin	Wrap fiber orientation	Number of samples	Average coating thickness (mm)
C	0	None	None	3	—
E1	0	Epoxy 1	None	3	—
E1W1A	1	Epoxy 1	Axial-90°	3	1.55
E1W1R	1	Epoxy 1	Radial-0°	4	1.09
E1W2R	2	Epoxy 1	Radial-0°	3	2.31
E1W2B	2	Epoxy 1	Bias-±45°	4	2.23
E1W3R	3	Epoxy 1	Radial-0°	4	3.37
E2	0	Epoxy 2	None	3	—
E2W1A	1	Epoxy 2	Axial-90°	3	1.88
E2W1R	1	Epoxy 2	Radial-0°	3	1.78
E2W2R	2	Epoxy 2	Radial-0°	3	2.57
E2W2B	2	Epoxy 2	Bias-±45°	3	3.30
E2W3R	3	Epoxy 2	Radial-0°	3	4.09

Figure 2.5: Reduction of concrete chloride content in specimen wrapped with fiberglass wrap (Epoxy 1: marine grade epoxy; Epoxy 2: thick gray epoxy intended for high-build, corrosion-resistant, moisture-insensitive coating - Wootton et al. 2003)

The fiberglass wrap repairing method's advantages over other corrosion damage repairs include low cost and simple installation (Tang 2003; Teng et al. 2003). The treatment of reinforced concrete columns with FRP have following additional advantages: (1) provides confinement for the repaired sections; (2) acts as a barrier to prevent from chloride attack of deicing salt, and (3) compensates for the sectional loss of corroded rebar (Watson 2000). Basic properties of a fiberglass wrapped are presented in Table 2.2.

Table 2.2: Basic properties of common fiberglass wraps (source: Tyfo Fiberwrap Systems 2008)

Composite Property	SCH-41	SEH-51	SEH-51A
Primary Fiber	Unidirectional Carbon Fabric	Unidirectional Glass	Unidirectional Glass
Laminate Thickness	1.0 mm (0.04 in)	1.3 mm (0.05 in)	1.3 mm (0.05 in)
Ultimate Tensile Strength [1]	876 MPa (127 ksi)	575 MPa (83.4 ksi)	575 MPa (83.4 ksi)
Ultimate Transverse Tensile Strength [1]	34.5 MPa (5 ksi)	34.5 MPa (5 ksi)	25.8 MPa (3.75 ksi)
Ultimate Strain [1]	0.0121	0.022	0.022
Elastic Modulus [1]	72.4 GPa (10,500 ksi)	26.1 GPa (3,790 ksi)	26.1 GPa (3,790 ksi)

[1] Test Standard ASTM D-3039

2.4. Field and Laboratory Methods for Bridge Column Assessment

Several different test methodologies were used to assess the condition of the concrete columns and fiberglass wrapping. These methodologies include: P-wave travel time profiling, P-wave travel-time tomographic imaging, ground penetrating radar tomographic imaging, half-cell potential measurements, and chlorine ion concentration determination. A brief description of the techniques follows.

2.4.1 P-wave Travel Time Profiling

The average P-wave velocity of concrete elements can be obtained by calculating the ratio of the distance of the traveling of P-wave to the measured travel time. The measured P-wave velocity

depends on the density and elastic properties of the concrete along the length of the wave propagation path (Krautkrämer and Krautkrämer 1990; Ryall 2001):

$$V = \sqrt{\frac{E}{\rho}\frac{1-\nu}{(1+\nu)(1-2\nu)}} \tag{2.1}$$

where E is the elastic modulus, ν is the Poisson's ratio, and ρ is the mass density. Concrete quality is not only related to the cement paste quality but it is also related to the homogeneity of the mix and the presence of cracks and voids. In non-destructive evaluation (NDE) applications, the quality of the concrete is related to the concrete P-wave velocity (Leslie and Chessman 1949). This qualitative indication assumes that the elastic properties of the concrete are related to the overall properties of the concrete. Table 2.3 summarizes the relationship between measured P-wave velocities and the estimate quality of the concrete.

Table 2.3: Relationship between local P-wave velocity and concrete quality (Ryall 2001).

Longitudinal pulse velocity (m/s)	Quality of concrete
> 4500	Excellent
3500 – 4500	Good
3000 – 3500	Doubtful
2000 – 3000	Poor
< 2000	Very poor

2.4.2 Ground Penetrating Radar

The ground penetrating radar (GPR) technique is based on the monitoring of transmitted and reflected high-frequency electromagnetic (EM) waves. The attenuation α_{EM} and velocity V_{EM} of EM waves depend on the electrical conductivity σ and the relative real dielectric permittivity κ' of the medium where the wave propagates (Santamarina et al. 2001):

$$\alpha_{EM} = \frac{2\pi f}{V_{EM}} \cdot \sqrt{\frac{1}{2} \cdot \left[\sqrt{1 + \left(\frac{\sigma}{2\pi f \cdot \kappa' \cdot \varepsilon_o} \right)^2} - 1 \right]} \tag{2.2}$$

$$V_{EM} = \frac{c}{\sqrt{\kappa'}} \tag{2.3}$$

where f is the frequency, ε_o is the permittivity of free space, and c is the electromagnetic speed in free space. The presence of Cl^- increases the conductivity σ and higher water content increases the relative real permittivity κ'. Changes in these properties can be detected by monitoring travel time and amplitudes. The GPR systems generated EM waves in the MHz to GHz frequency range. GPR antennae and their frequency are selected based on resolution and depth of penetration. These frequencies range from 12.5 to 3,000 MHz. In structural engineering health monitoring surveys, high frequency GRP systems are commonly used to help obtaining high resolution images. These surveys can be used for locating the presence and depth of rebars (in bridge decks using high frequency antennae) and for identifying the degree and extent of deterioration caused by corrosion beneath the concrete cover (Sbartai 2007).

2.4.3 Travel-time Tomographic Imaging

Travel-time tomographic imaging is a powerful tool in the interpretation of wave propagation data for the non-destructive monitoring of the civil engineering infrastructure. In this technique, elastic or electromagnetic waves are sent in different directions along the section or volume to be imaged. For each wave ray, the wave travel time is measured. The combination of all measured travel times is the used to calculate the distribution of wave velocity throughout the medium.

Travel-time is defined as the integral of the inverse of the wave velocity along the wave travel length. If the medium is discretized into pixels of constant wave velocity, the problem can be expressed as the summation of the length of ray i in pixel k, $L_{i,k}$ times the slowness (inverse of velocity) of pixel k, s_k along the whole ray length (Figure 2.6):

$$t_i = \sum_k \frac{L_{i,k}}{V_k} = \sum_k L_{i,k} \cdot s_k \tag{2.4}$$

where t_i is the measured travel time for ray i, $L_{i,k}$ is the travel length of ray i on pixel k, and s_k is the unknown pixel slowness of pixel k (Prada et al. 2000, Santamarina and Fratta 2005). In matrix form, equation 2.4 can be expressed as:

$$\underline{t} = \underline{\underline{L}} \cdot \underline{s} \qquad (2.5)$$

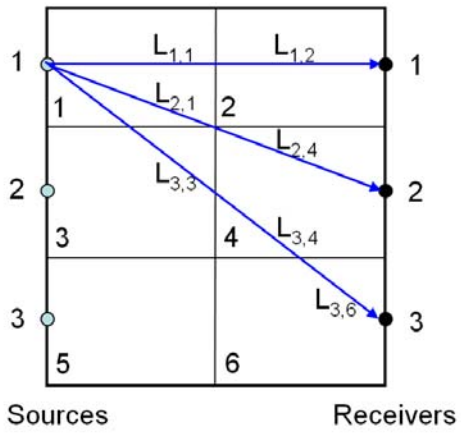

Figure. 2.6: Pixel representation of the medium for tomographic analysis of the data.

In most NDE applications, tomographic data are not equally distributed over the testing space. Therefore, information content is denser in some areas (over-determined areas) while in other areas the information content is much smaller (underdetermined areas). This combination of areas with greater and lower information yields a mix-determined problem. These types of problems are ill-conditioned; that is, the solution to the problem is not unique, the solution is unstable, or the solution cannot be found. Most of these problems are solved by using techniques such as singular value decomposition (SVD) or by applying regularization techniques (Aster et al. 2005).

When regularization techniques are used, additional information is added to the problem. For example, the solution is found by smoothing the final image or by forcing the final result to adopt a certain characteristic. One of the simplest regularization techniques is obtained by forcing a smooth variation of the solution field. An example of this solution technique is the damped least squares solution (DLLS - Fernandez and Santamarina 2003; Aster et al. 2005):

$$\underline{s} = \underbrace{(\underline{\underline{L}}^T \cdot \underline{\underline{L}} + \eta^2 \cdot \underline{\underline{I}})^{-1} \cdot \underline{\underline{L}}^T}_{\underline{\underline{L}}^{-g}} \cdot \underline{t} \qquad (2.6)$$

where $\underline{\underline{L}}^{-g}$ is the generalized inverse and $\underline{\underline{I}}$ is the identity matrix. The degree of smoothness in solution field is controlled by the regularization (or damping) coefficient η.

In this study, P-wave and EM-wave data were collected in different directions to obtain tomographic images of the concrete columns. Data analyses follow the same interpretation presented in equations 2.4 to 2.6. The main difference to the P-wave travel time tomography is that EM-wave travel time tomography yield images that depend on the distribution of the concrete electromagnetic properties while P-wave tomography captures the distribution of P-wave velocity.

2.4.4 Half-cell potential (ASTM C876-91)

The half-cell potential is a method based on measuring the electrochemical potential that drives the corrosion process. The measurements reflect the tendency of the anode to corrode. The more negative the half-cell potential readings are, the greater the tendency of the corroding metal to lose electrons is. The standard procedure for measuring half-cell potential is presented in ASTM C876-91 as illustrated in Figure 2.7. The testing instrument consists of copper-copper sulfate half-cell, wires, and a high-impedance voltmeter. Table 2.4 summarizes the typical interpretation of the half-cell potential readings. For example, the potential which is more negative than -350 mV, can be evaluated as a 90% probability of corrosion (Teng et al. 2003). It should be noted, however, that these values should be only considered as reference values. Half-cell potential readings depend on many other concrete properties, including level of carbonation, Cl^- concentration, water content, and concrete permeability that limits the absolute interpretation of the half-cell potential readings (Gu and Beaudoin 1998).

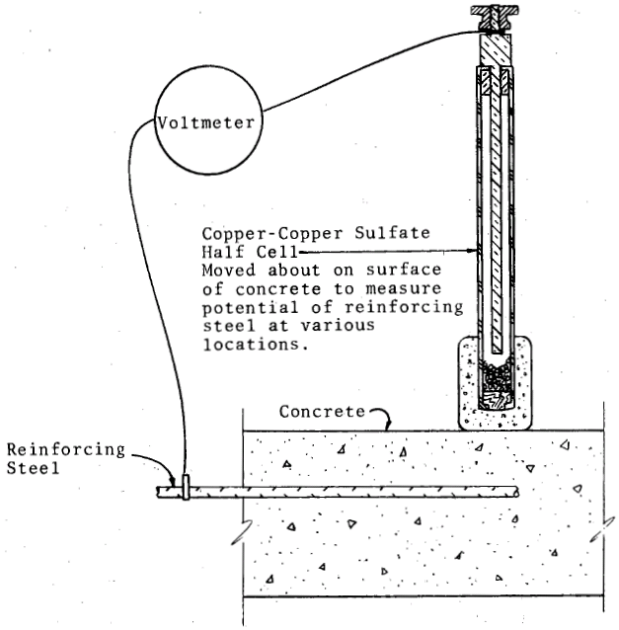

Figure 2.7: Half-cell potential circuitry (ASTM C876-91)

Table 2.4: ASTM criteria for corrosion of steel in concrete for standard half-cell potential method (Khan 1991; Teng et al. 2003).

Corrosion state	Situation/ half-cell potential measurements
Passive state	Absence of chloride ions. The passive potential range is very wide, from +200mV to -600mV at pH=13. In aerated concrete, steel normally exhibits a potential ranging between +100 and -200 mV.
Pitting corrosion	Pitting typically results from the presence or ingress of chloride ions. The average potential is typically –between 200 and -500mV.
General corrosion	General corrosion is the result of the general loss of passivity (caused by the carbonation of the concrete or by excessive amounts of chloride ions). The potentials range between -450 and -600 mV
Active, low potential corrosion	In environments where oxygen is very limited, the passive film cannot be maintained. Embedded steel may corrode even in high alkaline environment. The potentials can be as low as -1000 mV

Risk of corrosion	Half-cell potential measurements
Low (10% risk of corrosion)	>-200 mV
Uncertain (intermediate)	-350 mV < value < -200 mV
High (90% risk of corrosion)	< -350 mV
Severe corrosion	< -500 mV

2.4.5 Chlorine Ion Concentration (AASHTO T 260-97)

Chloride ions attack the passive layer between concrete and steel reinforcement. The removal of the protective passive layer is one of main causes of corrosion in the reinforced concrete elements. The chloride ion contamination progresses by diffusion in concrete. Therefore, the chloride ion content in depth is a good indicator of the corrosion potential of reinforcing bars in concrete. The AASHTO Designation: T 260-97 (2001) standard "Standard Method of Test for Sampling and Testing for Chloride Ion in Concrete and Concrete Raw Materials" is a methodology used to evaluate the chloride ion concentration in concrete elements. AASHTO T-260 describes the methodology for determining the water-soluble or acid soluble chloride ion content of aggregates, cement, mortar, or concrete. The chloride ion content can be determined by potentiometric titration method.

Instrumentation and chemicals. The primary equipment for chloride ion test is a voltmeter with the electrode (Figure 2.7). The procedure to determine the acid-soluble chloride ion content required several chemical reagents and solutions. Concentrated nitric acid (HNO_3) was used in the initial stages of the procedure to decompose the concrete sample. Methyl orange indicator was used to verify the acidity of the solution. An ionic strength adjuster and chloride activity standard of a known concentration were used to calibrate the electrode (0.01 normal solutions of sodium chloride (NaCl) and silver nitrate ($AgNO_3$) were selected).

Figure 2.7: Testing set-up for measuring chloride ion content.

Sample Preparation. A 3.0-g pulverized concrete material is transferred from a sample container to a 100-mL beaker. The 10-mL of distilled (or deionized) water is added to the beaker containing the sample, which was swirled to bring the concrete powder into suspension. After adding 3-mL of concentrated nitric acid (HNO_3), and the composite solution is swirled for 3-4 minutes. Hot distilled (or deionized) water is added up to the volume of 50-mL. To check acidity of the solution, five drops of methyl orange indicator are added into the solution and the color of solution is observed. Additional nitric acid can be dropped until the solution is changed to a faint pink or red color. The beaker containing solution is heated to boiling on a hot plate at 250 to 400°C for 1 minute.

After boiling the solution, the solution is filtered through a funnel double-lined with filter paper, Whatman No. 41 over No. 40, into a clean 250-mL beaker. The filter paper is continuously washed with hot distilled water, until the volume of the filtered solution can be reached to 150-mL. The prepared sample solution is allowed to cool to room temperature before performing tiltration test.

Tiltration test. The 4-mL of 0.01 normality sodium chloride solution (NaCl) and 3-mL of the ionic strength adjuster (ISA) are stirred into the test sample. The electrode is immersed in the test sample solution, and the beaker-electrode assembly was placed beneath the spout of a 25-mL calibrated buret containing 0.01 normality silver nitrate solution ($AgNO_3$). With continuous stirring using a rod, 0.01 normality silver nitrate solution is added and the volume recorded to bring the millivoltmeter reading to within 40mV below the equivalence point determined in distilled water. And then, the 0.01 normality silver nitrate solution is added in 0.20-mL increments. As the equivalence point is approached, equal additions of silver nitrate solution ($AgNO_3$) caused to large changes in the millivoltmeter readings. After reaching the equivalence point, the variation in the millivoltmeter readings can be decreased.

Data Reduction. The amounts of infiltration of silver nitrate solution ($AgNO_3$) and the corresponding millivoltmeter readings are recorded. The endpoint of the titration used to calculate the percent chloride ion can be determined by plotting the volume of silver nitrate

solution added and the millivoltmeter readings. The endpoint of the titration corresponded to the point of inflection of the resultant curve.

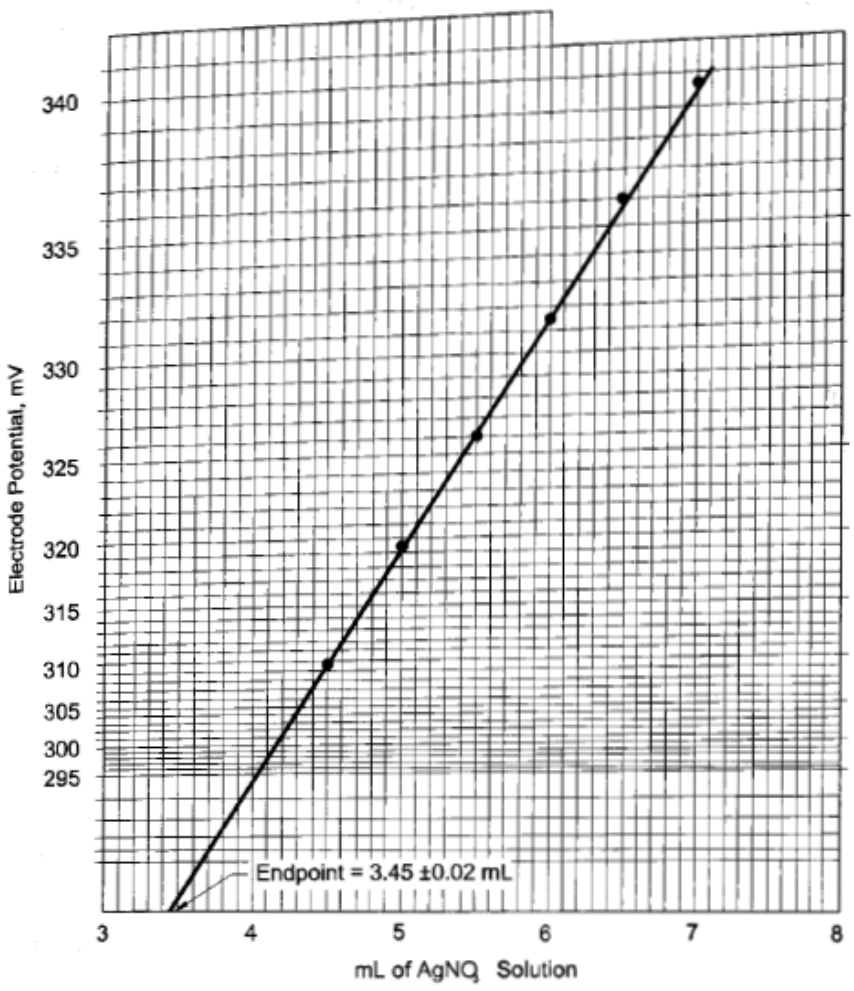

Figure 2.8: Use of grain method to determine endpoint in the potentionmetric tiltration of an acid extract of concrete (AASHTO T 260).

The volume of silver nitrate, V_1, added to reach the endpoint of the titration (inflection point) was used to calculate the percent chloride ion in each concrete sample using the following equation:

$$Cl^{-}(\%) = 3.5453\frac{V_1N_1 - V_2N_2}{W} \qquad (2.7)$$

where V_1 is the endpoint in mL of $AgNO_3$, N_1 is the normality of $AgNO_3$, W is the mass of original concrete sample (g), V_2 is the volume of NaCl solution added (mL), and N_2 is the normality of NaCl solution.

Chapter 3. Description of Bridges and Columns Surveyed

3.1. Introduction

Wisconsin Department of Transportation (WisDOT) officials identified a number of bridges that have been treated fiberglass wraps. The location of all these bridges is summarized in Table 3.1. The aim of this maintenance operation was to arrest or at least reduce the corrosion activity in steel reinforcement and to prevent the further degradation of the concrete cover. These bridges were visited by the research team during the spring-fall 2007 period. The survey included visual inspection, digital photography, and light-tapping with a mallet to evaluate the integrity of the fiberglass-wrapped columns. During the visual inspection, the research team identified several heavily damaged fiberglass wrapped columns (e.g., bulged failure at the column bottom, complete wrapping failure, etc.). Examples of the identified damaged columns are shown in Figure 3.1 while Table 3. 2 summarizes the visual survey results.

During the initial visual survey, the research team also evaluated traffic levels and the available working space to help decide which columns would be selected for testing during the research program. The research team also requested input from WisDOT officials regarding:

(a) WisDOT's salt application protocol and schedule
(b) Year of construction of the bridge, year of fiberglass wrap application, and the condition of the columns at the time of fiberglass wrap application
(c) The specifications of fiberglass wraps used in all surveyed bridges

Table 3.1: Location of bridges with columns treated with fiberglass wrap.

Bridge No.	Date of fiberglass application	Location
B-11-17	Mid-1990's	On I-90/94 under county road K (Columbia Co., WI)
B-13-113	Mid-1990's	On I-90 under county road AB (Dane Co., WI)
B-13-144	2006	On I-90 under county Church St. (Dane Co., WI)
B-13-172	2006	On I-90WB under US highway 51NB (Dane Co., WI)
B-28-35	Mid-1990'	On I-94 under Airport Rd. (Jefferson Co., WI)
B-28-40	Mid-1990's	On I-94 under state highway 89 (Jefferson Co., WI)
B-28-43	Mid-1990's	On I-94 under county road Q (Jefferson Co., WI)
B-28-45	Mid-1990's	On I-94 under Ziebell Rd. (Jefferson Co., WI)
B-28-50	Mid-1990's	On I-94 under county road F (Jefferson Co., WI)
B-53-65	Mid-1990's	On I-90EB under US highway 14 (Rock Co., WI)
B-53-66	1994	On I-90WB under US highway 14 (Rock Co., WI)
B-53-71	Mid-1990's	On I-90 under sate highway 59 (Rock Co., WI)
B-53-75	Mid-1990's	On county road M under I-90WB (Rock Co., WI)

Figure 3.1: Evidence of corrosion activity in fiberglass wrapped column in bridge B-53-71 (I-39/90 under State highway 59). (a) May 2007 and (b) September 2007. After 10 years, WisDOT needed to re-wrap the column because corrosion continued under the fiberglass wrap.

Table 3.2: Summary of visually inspected bridge and columns

Bridge	Bridge Columns			Wrapped column location
	Total columns	Fiberglass-wrapped columns	Damaged wrapped columns	
B-11-17	9	3	0	North bound: 2 South bound: 1
B-28-35	9	2	0	East bound: 2
B-28-40	9	3	0	East bound: 2 West bound: 1
B-28-43	9	1	0	West bound: 1
B-28-45	9	2	0	East bound: 2
B-28-50	9	2	0	East bound: 1 West bound: 1
B-13-113	9	9	0	North bound: 3 South bound: 3 Median: 3
B-13-144	9	6	0	North bound: 3 South bound: 3
B-13-172	8	4	0	West bound: 4
B-53-71	9	4	1	North bound: 3 Median: 1
B-53-75	8	4	0	East bound: 4
B-53-65	12	5	2	East bound: 3 West bound: 2
B-53-66	15	5	0	East bound: 3 West bound: 2

3.2. Wisconsin Inspection Reports and Visual Surveys

Wisconsin bridges are regularly inspected in two-year intervals. During these regular inspection operations, WisDOT officials document the condition of bridge and make recommendations for required follow-up inspections or for maintenance operations. In this report, the information from the inspection reports was summarized by ranking the condition of the concrete in columns in four categories based in the level of deterioration of the structural element (Table 3.3). The description of all visually inspected bridges and the summary of the inspection reports are presented next.

Table 3.3: Qualitative description of the columns deterioration

Condition category	Description	Suggested action
No deterioration	Possible discoloration, efflorescence, or superficial cracking. This deterioration does not affect strength or serviceability of the structural element	None
Minor cracks and spalls	Minor cracking and spalling may be present. There are no exposed reinforced bars or surface evidence of rebar corrosion.	Seal cracks, apply minor patch
Deterioration	Some delamination and/or spalls may be present. Some reinforcing bars may be exposed. Possible rebar corrosion but section loss is incidental and it does not significantly affect strength or serviceability.	Clean rebar, patch and/or seal
Advanced deterioration	Corrosion of reinforcing bars and/or loss of concrete section. The level of deterioration is sufficient to warrant analysis to evaluate the impact on the strength and/or serviceability of either the element or the bridge.	Rehab unit or replace unit

3.2.1 Bridge B-11-17

This bridge is located under county road K on interstate highway I-90/94 in Columbia Co., WI. The bridge has nine concrete columns and three of these columns have been repaired using fiberglass wraps (Figure 3.2). In this bridge, WisDOT has used the fiberglass wraps in at least two different maintenance operation cycles. The wrap applications on these bridge columns were implemented between years 1997~1998 and 2003~2005 to upgrade the structural condition of the bridge following regular inspections. Table 3.4 summarizes the inspection findings for this bridge and the timeline of degradation and repairs is summarized in Figure 3.3.

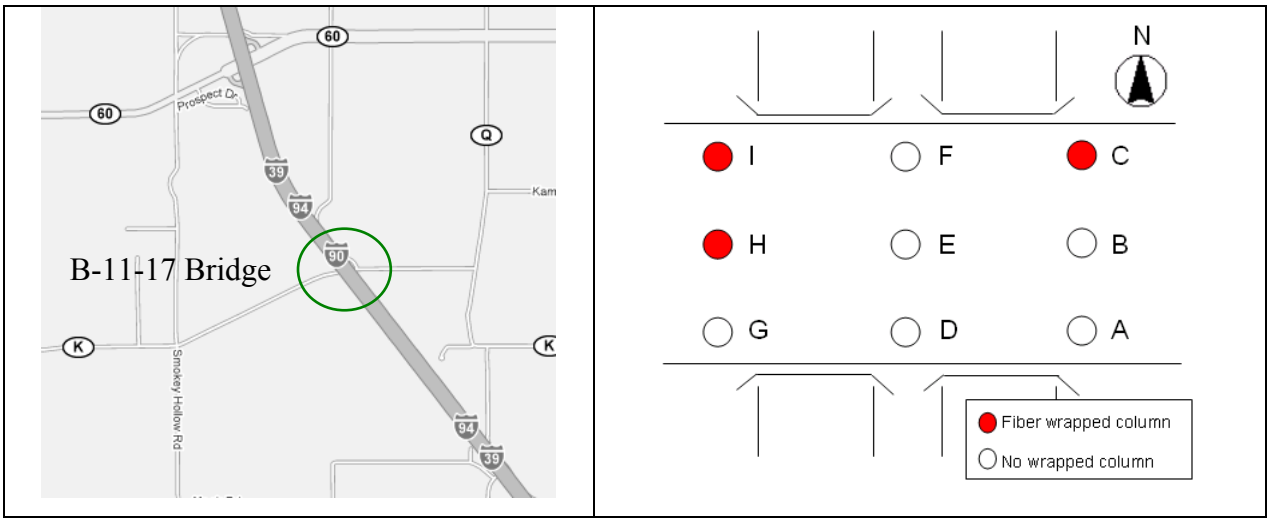

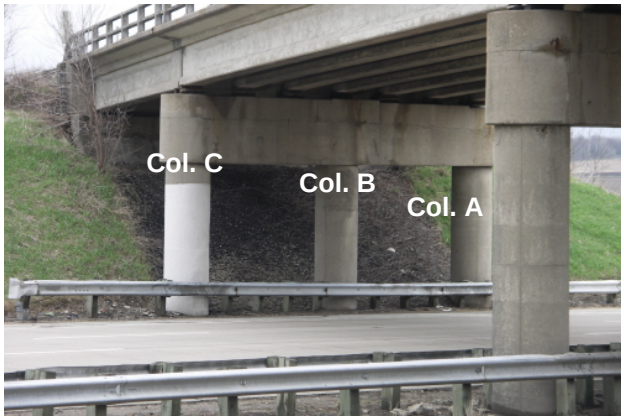

Figure 3.2: Location of B-11-17 bridge in Columbia Co., WI and arrangement of columns (map: after Google Maps 2008).

Table 3.4: Summary of B-11-17 Bridge inspection reports

Year	Relevant inspection report comments
12/1996 ~ 4/1999	Columns G, H, and I have been repaired and look good. Columns A, B, and C have spalls and delaminated areas with exposed rusty rebar.
7/2001	Columns G, H, and I have been repaired and look good. Columns A, B, and C have spalls and delaminated areas with exposed rusty rebar. Delamination/spall at columns G, H and I (pier 1) and at columns A, B, and C (pier 3)
6/2003	Columns H and I have 2" by 2" spalls with exposed rebar. Column C has a 2" by 2" spalls with exposed rebar.
6/2005	Columns G and H have spalled areas repaired. Column C have spalled areas repaired Three columns are wrapped with fiber wrap.
6/2007	Vertical cracks in column G. Four columns are wrapped with fiber wrap. *Note: New fiberglass wrapping was applied column G after this research team initial visual survey.*

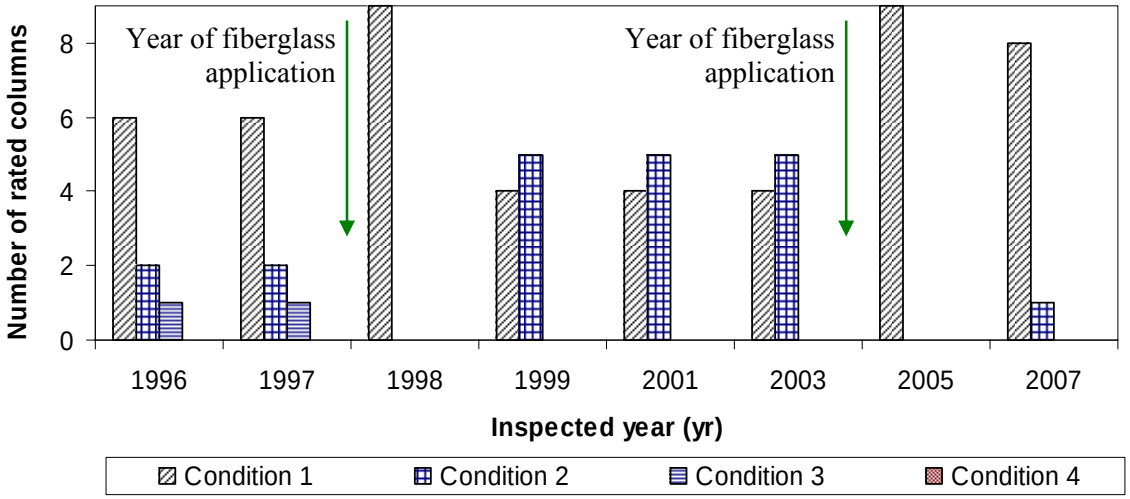

Figure 3.3: Timeline of inspected conditions of columns and maintenance operations in B-11-17 bridge (Condition rating definitions are summarized in Table 3.3).

3.2.2 Bridge B-13-113

This bridge is located under county road AB on interstate highway I-90 (Figure 3.4). The bridge has nine concrete columns and all of them have been repaired using fiberglass wraps. WisDOT has used the fiberglass wraps in two occasions. The wrap applications on these bridge columns were implemented between years 1996-1997 and 2001-2003 to upgrade the structural condition of the bridge columns following the regular inspection reports documented in Table 3.5. The timeline of degradation and repairs is summarized in Figure 3.5.

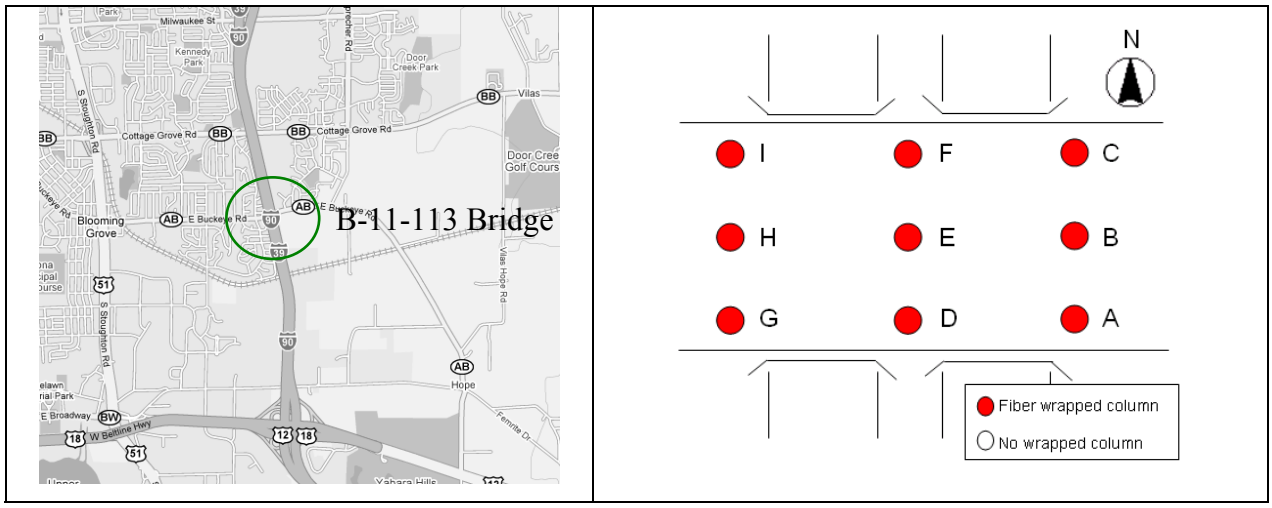

Figure 3.4: Location of B-11-113 bridge in Dane Co., WI and arrangement of columns (map: after Google Maps 2008).

Table 3.5: Summary of B-11-113 Bridge inspection reports

Year	Relevant inspection report comments
3/1996 ~ 11/2001	All columns are repaired and have fiber wraps on them (look good).
12/2003 ~ 12/2005	All columns have fiber wraps on them (sound solid).

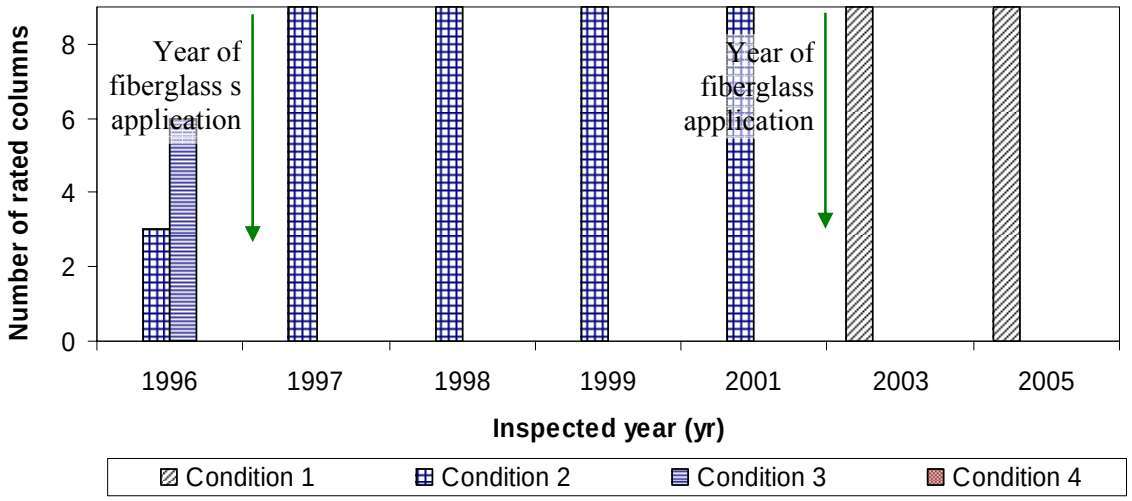

Figure 3.5: Timeline of inspected conditions of columns and maintenance operations in the B-13-113 bridge (Condition rating definitions are summarized in Table 3.3).

3.2.3 Bridge B-13-144

This bridge is located under Church St. on interstate I-90 in Dane Co., WI. The bridge has nine concrete columns and six of these columns have been repaired using fiberglass wrap as shown in Figure 3.6. WisDOT has used the fiberglass wraps in two different occasions to repair the columns in this bridge. WisDOT wrapped the columns 2002-2004 and in 2006 to upgrade the structural condition. Table 3.6 and Figure 3.7 summarize the timeline of degradation and repairs in the columns.

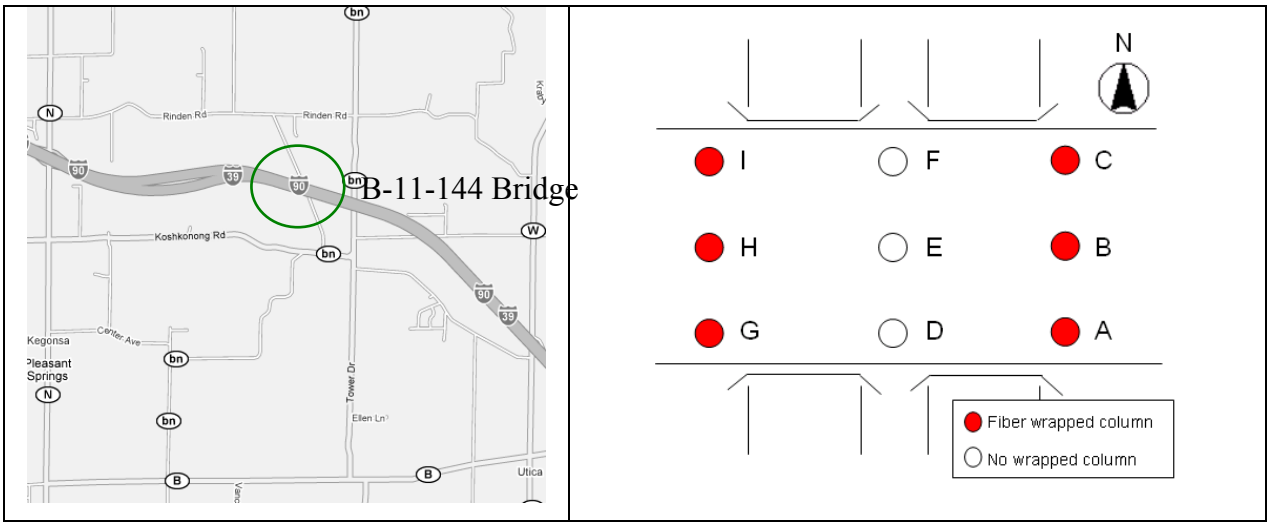

Figure 3.6: Location of B-11-144 bridge in Dane Co., WI and arrangement of columns (map: after Google Maps 2008).

Table 3.6: Summary of B-11-114 bridge inspection reports

Year	Relevant inspection report comments
12/1996 ~ 11/2000	Columns A, B, and C have fiber wraps, all look good. Columns G, H, and I have fiber wraps, all look good.
2/2002	Columns A, B, and C have fiber wraps, all look good. Columns G, H, and I have fiber wraps, all look good. Fiber wrap at column G is starting to break open.
2/2004	Columns A, B, and C have fiber wraps, all look good. Columns G, H, and I have fiber wraps, all look good.
9/2004	Columns A, B, and C have fiber wraps. Columns G, H, and I have fiber wraps.
9/2006	Columns A, B, and C have fiber wraps, all look good. Columns G, H, and I have fiber wraps, all look good.

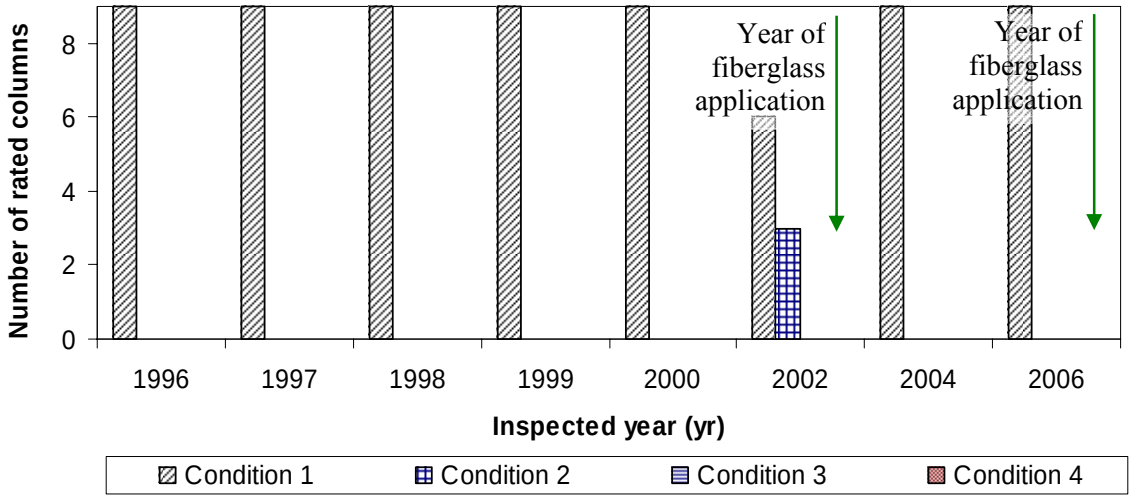

Figure 3.7: Timeline of inspected conditions of columns and maintenance operations in the B-13-144 bridge (Condition rating definitions are summarized in Table 3.3).

3.2.4 Bridge B-13-172

This bridge is located under interstate highway I-90 Westbound on US road 51 Northbound. The bridge has eight concrete columns and four of them have been repaired using fiberglass wraps as shown in Figure 3.8. WisDOT has used the fiberglass wraps in two occasions. The wrap applications on these bridge columns were implemented between years 2002-2004 and in 2006

to upgrade the structural condition of the bridge columns following the regular inspection reports documented in Table 3.7. The timeline of degradation and repairs is summarized in Figure 3.9.

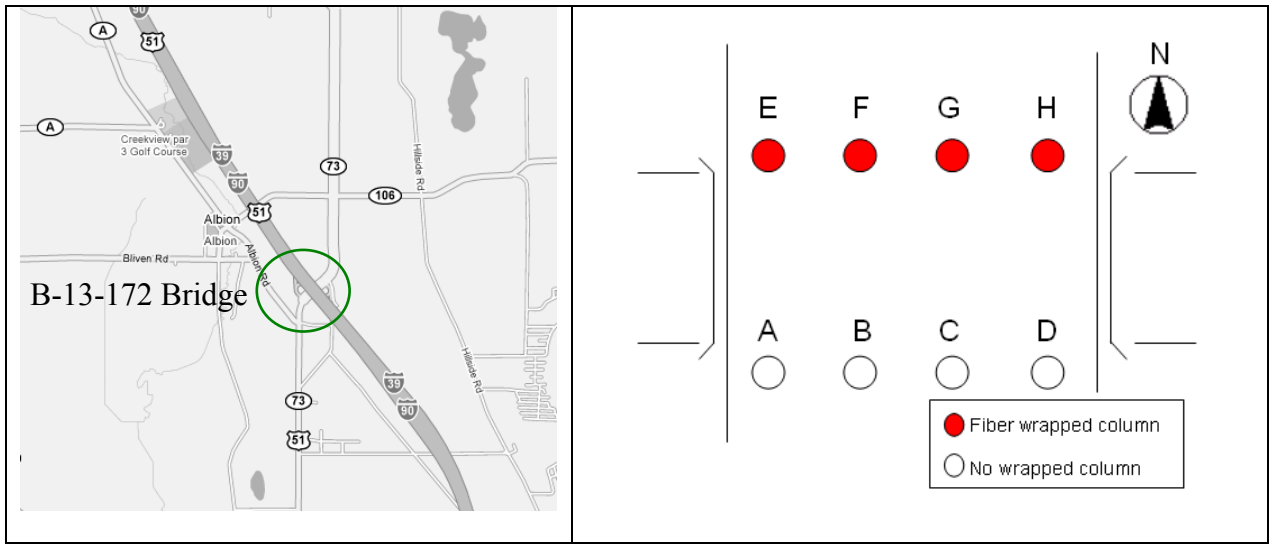

Figure 3.8: Location of B-11-172 bridge in Dane Co., WI and arrangement of columns (map: after Google Maps 2008).

Table 3.6: Summary of B-13-172 bridge inspection reports

Year	Relevant inspection report comments
11/1996 ~ 2/2002	Columns E, F, G, and H have concrete patches. These patches have some cracks and sound hollow.
1/2004	Columns E, F, G, and H have concrete patches and patches have random cracks and sound hollow. All columns were wrapped and sealed.
9/2004	Columns E, F, G, and H have fiber wraps. Delamination/cracking in column F (or G?).
9/2006	Columns E, F, G, and H have fiber wraps. All columns look good.

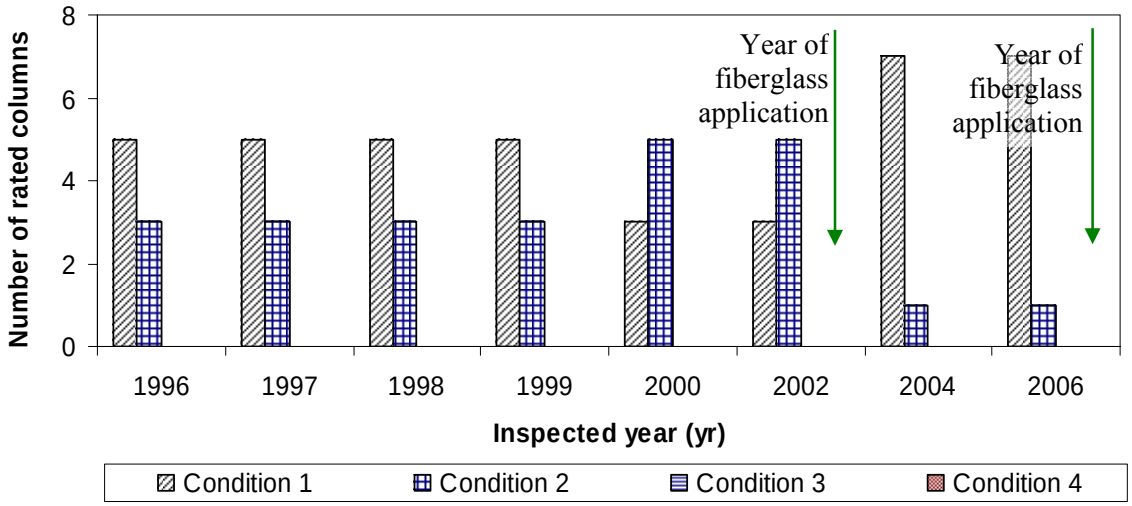

Figure 3.9: Timeline of inspected conditions of columns and maintenance operations in the B-13-172 bridge (Condition rating definitions are summarized in Table 3.3).

3.2.5 Bridge B-28-35

This bridge is located under Airport Road on interstate highway I-94 in Jefferson Co. The bridge has nine concrete columns and two of them have been repaired using fiberglass wraps as shown in Figure 3.10. WisDOT has used the fiberglass wraps in two occasions. The wrap applications on these bridge columns were implemented in the mid 1990s to upgrade the structural condition of the bridge columns as documented in Table 3.7. The timeline of degradation and repairs is summarized in Figure 3.11.

Figure 3.10: Location of B-28-35 bridge in Jefferson Co., WI and arrangement of columns (map: after Google Maps 2008).

Table 3.7: Summary of B-28-35 bridge inspection reports

Year	Relevant inspection report comments
6/1996 ~ 6/2005	Columns A, B, and C have fiber wrap and look good. Other columns look good.

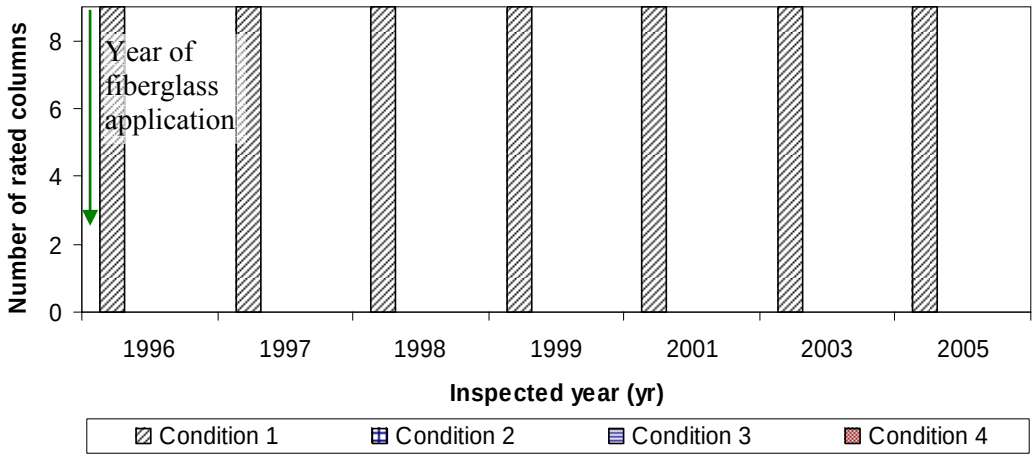

Figure 3.11: Timeline of inspected conditions of columns and maintenance operations in the B-28-35 bridge (Condition rating definitions are summarized in Table 3.3). Mid 1990s is the estimated wrapping year.

3.2.6 Bridge B-28-40

This bridge is located under state highway 89 on interstate highway I-94 in Jefferson Co., WI. The bridge has nine concrete columns and three of them have been repaired using fiberglass wraps as shown in Figure 3.12. WisDOT has used the fiberglass wraps in two occasions. The wrap applications on these bridge columns were implemented in the mid 1990s and then again in 1999 to upgrade the structural condition of the bridge columns as documented in Table 3.8. The timeline of degradation and repairs is summarized in Figure 3.13.

Figure 3.12: Location of B-28-40 bridge in Jefferson Co., WI and arrangement of columns (map: after Google Maps 2008).

Table 3.8: Summary of B-28-40 bridge inspection reports

Year	Relevant inspection report comments
10/1996 ~ 11/1999	Columns A, B, and I are wrapped. There a few cracks in the three columns (A, B, I).
5/2000	Columns A, B, and I are wrapped
2/2002 ~ 2/2004	Columns A, B and I have fiberglass wraps. Column F has high rust steel, popout spalls. Column H has vertical cracks at bottom.
9/2004	Columns A, B and I have fiber wraps. Column F has high rust steel popout spalls. Column H has vertical cracks and delamination at bottom.
9/2006	Column A & B has fiber wraps and both columns look good. Column A has a couple rust stains. Column F has high rust steel popout spalls. Column H has vertical cracks and delamination at bottom. Column I has fiber wrap 1/3 up and it looks good.

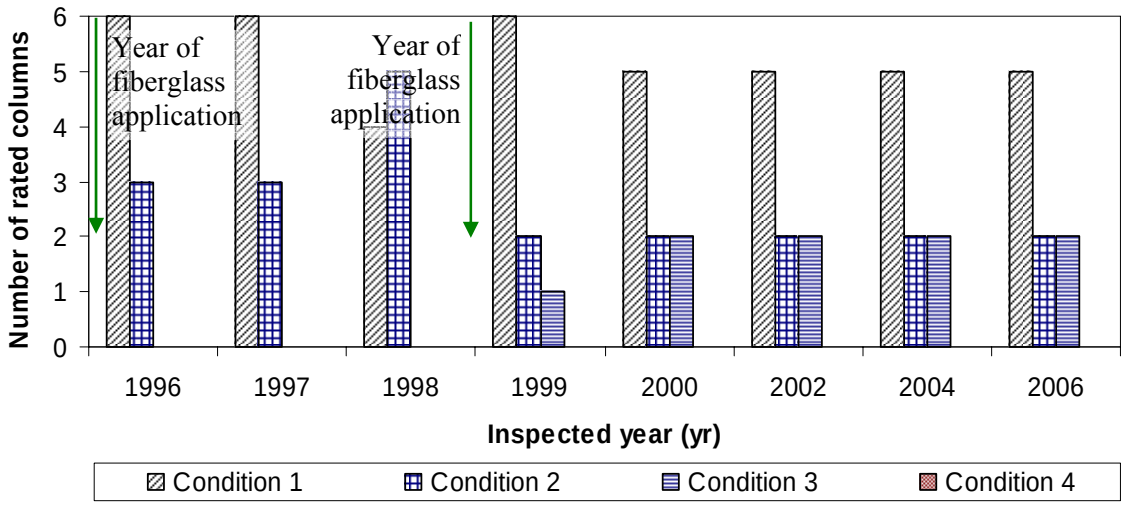

Figure 3.13: Timeline of inspected conditions of columns and maintenance operations in the B-28-40 bridge (Condition rating definitions are summarized in Table 3.3).

3.2.7 Bridge B-28-43

Bridge B-28-43 is located under county road Q on interstate highway I-94 in Jefferson Co., WI. The bridge has nine concrete columns and one of them have been repaired using fiberglass wraps as shown in Figure 3.14. WisDOT has used the fiberglass wraps in one occasion. The wrap application on the bridge column was implemented in the mid 1990s to upgrade the structural condition of the bridge columns as documented in Table 3.9. The timeline of degradation and repairs is summarized in Figure 3.18.

Figure 3.14: Location of B-28-43 bridge in Jefferson Co., WI and arrangement of columns (map: after Google Maps 2008).

Table 3.9: Summary of B-28-43 bridge inspection reports

Year	Relevant inspection report comments
6/1996 ~ 6/2005	Columns A, B, and C have concrete collars one third up. Column G has a fiber wrap one third up. Column I has numerous cracks in concrete collars.

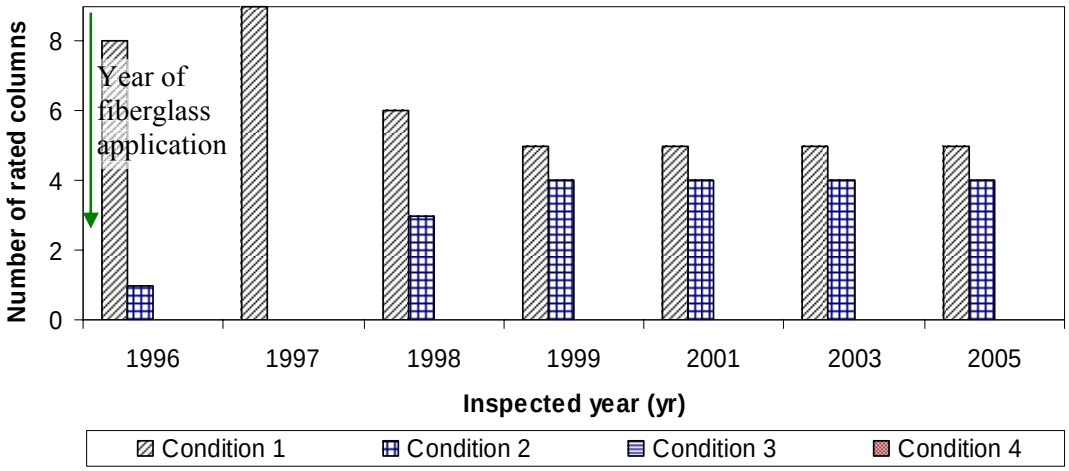

Figure 3.15: Timeline of inspected conditions of columns and maintenance operations in the B-28-43 bridge (Condition rating definitions are summarized in Table 3.3).

3.2.8 Bridge B-28-45

This bridge is located under Ziebell Road on interstate highway I-94 in Jefferson Co., WI. The bridge has nine concrete columns and two of them have been repaired using fiberglass wraps as shown in Figure 3.16. WisDOT has used the fiberglass wraps in one occasion. The wrap application on the bridge column was implemented in the mid 1990s to upgrade the structural condition of the bridge columns as documented in Table 3.10. The timeline of degradation and repairs is summarized in Figure 3.17.

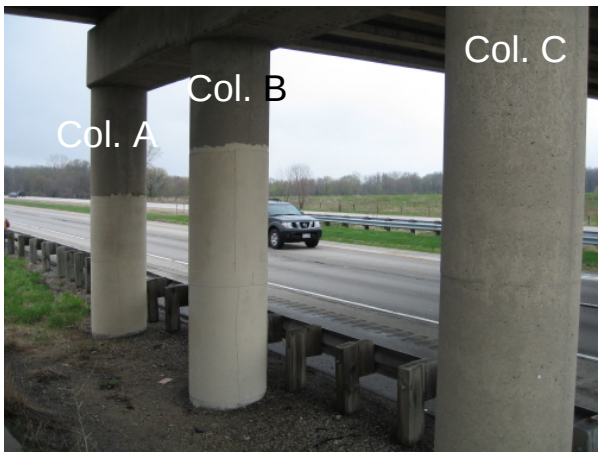

Figure 3.16: Location of B-28-45 bridge in Jefferson Co., WI and arrangement of columns (map: after Google Maps 2008).

Table 3.10: Summary of B-28-45 bridge inspection reports

Year	Relevant inspection report comments
7/1997	Columns A and B are wrapped.
3/1998 ~ 3/1999	Columns A and B are wrapped.
6/2001 ~ 6/2005	Columns A and B have been wrapped halfway up. Column D has a small spalledout area half way up, no exposed rebar.

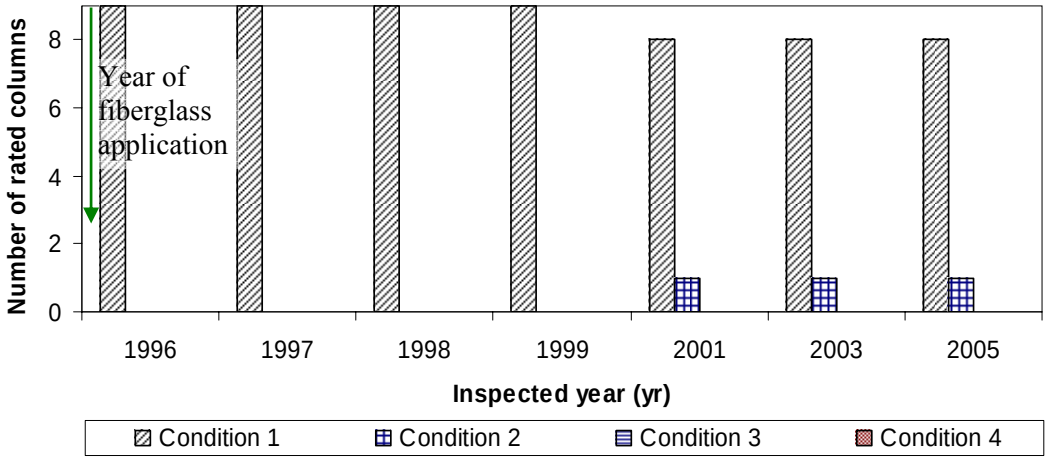

Figure 3.17. Timeline of inspected conditions of columns and maintenance operations in the B-28-45 bridge (Condition rating definitions are summarized in Table 3.3).

3.2.9 Bridge B-28-50

This bridge is located under county road F on interstate highway I-94 in Jefferson Co., WI. The bridge has nine concrete columns and two of them have been repaired using fiberglass wraps as shown in Figure 3.18. WisDOT has used the fiberglass wraps in on occasion. The wrap application on the bridge column was implemented in the mid 1990s to upgrade the structural condition of the bridge columns as documented in Table 3.11. The timeline of degradation and repairs is summarized in Figure 3.19.

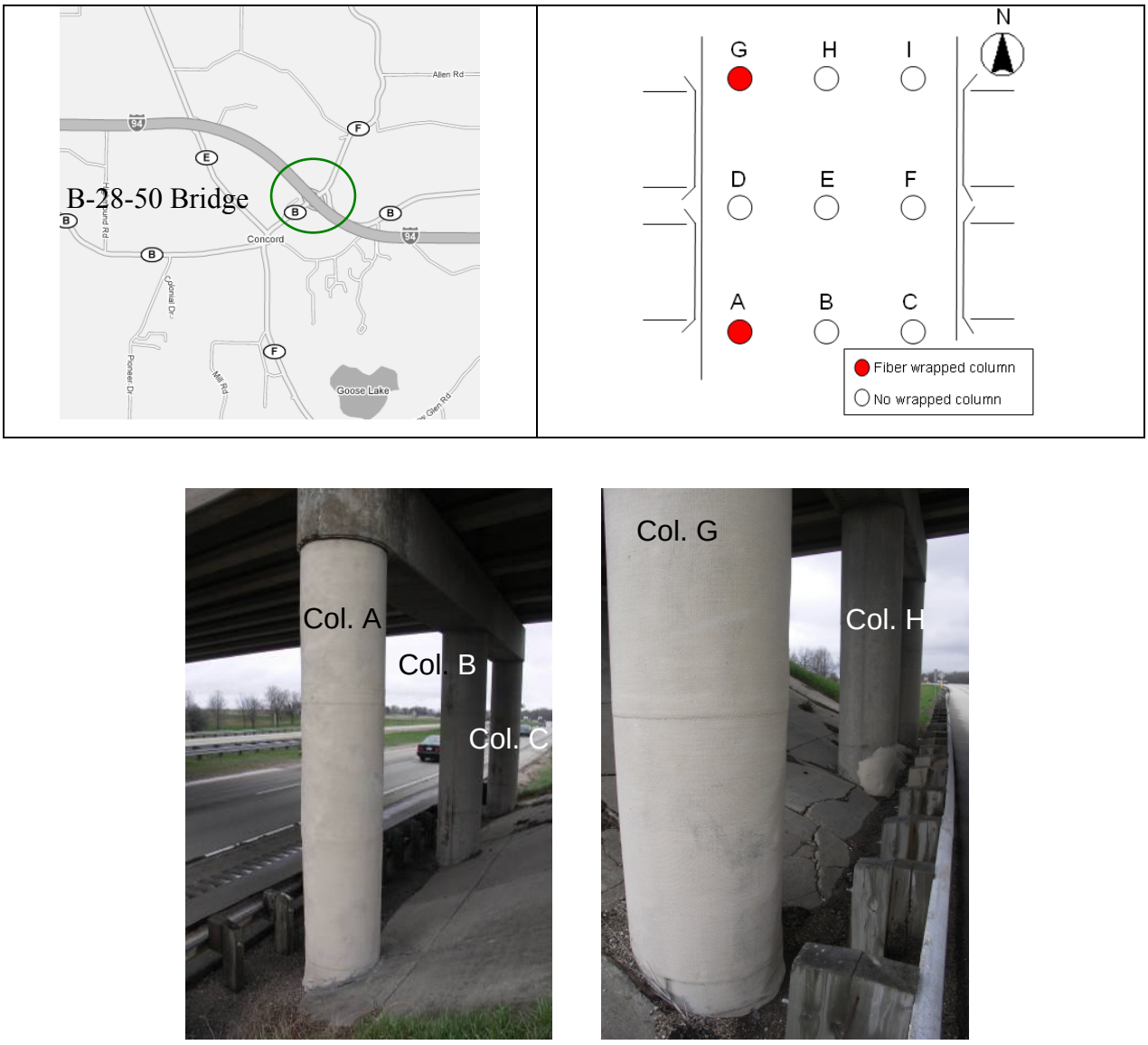

Figure 3.18: Location of B-28-50 bridge in Jefferson Co., WI and arrangement of columns (map: after Google Maps 2008).

Table 3.11: Summary of B-28-50 bridge inspection reports

Year	Relevant inspection report comments
3/1996 ~ 3/1999	Fiberglass wrap on column A looks good. Fiberglass wrap on column G looks good.
5/2000 ~ 9/2006	Fiberglass wrap on column A looks good. Couple of vertical cracks remaining. Fiberglass wrap on column G looks good. Couple of vertical cracks remaining.

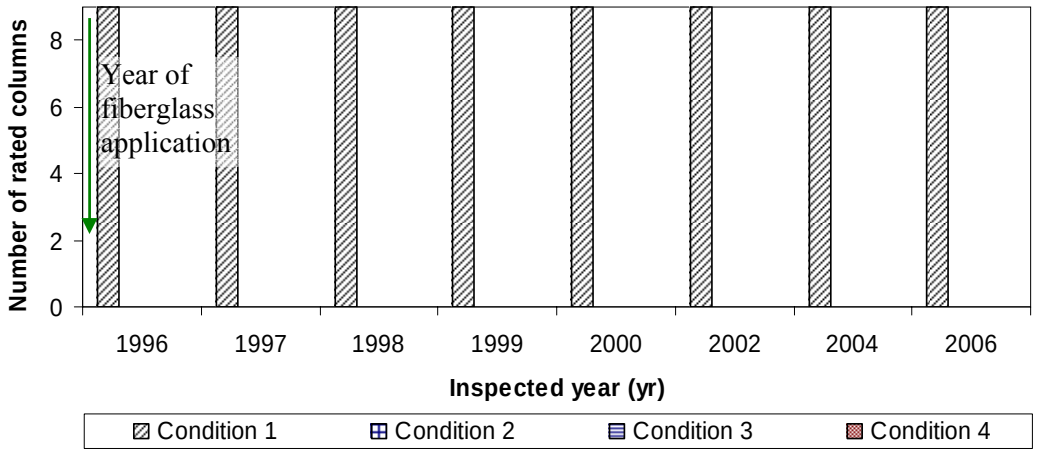

Figure 3.19: Timeline of inspected conditions of columns and maintenance operations in the B-28-50 bridge (Condition rating definitions are summarized in Table 3.3).

3.2.10 Bridge B-53-65

This bridge is located under US highway 14 on interstate highway I-90EB in Rock Co., WI. This bridge has twelve concrete columns and five of them have been repaired using fiberglass wrapping (Figure 3.20). WisDOT has used the fiberglass wraps in two occasions: in the mid 1990s and in the 2001-2002 to upgrade the structural condition of the bridge columns. The timeline of degradation and repairs is summarized in Table 3.12 and Figure 3.10.

Figure 3.20: Location of B-53-65 bridge in Rock Co., WI and arrangement of columns (map: after Google Maps 2008).

Table 3.12: Summary of B-53-65 bridge inspection reports

Year	Relevant inspection report comments
11/1996 ~ 9/2005	Columns I and K are wrapped with fiberglass. Columns A, C and D are wrapped with fiberglass. These columns have cracks and delaminations.
12/2005	Columns I & K are wrapped with fiberglass. The fiberglass wrap in column I is debonding and column is spalling. Columns A, C and D are wrapped with fiberglass. The fiberglass wrap in column A is debonding and column is spalling. The fiberglass wrap in column C is starting to debond. The fiberglass wrap in column D is in ok condition. Column B has hairline cracks & delaminations. There is no fiberglass wrap on it.

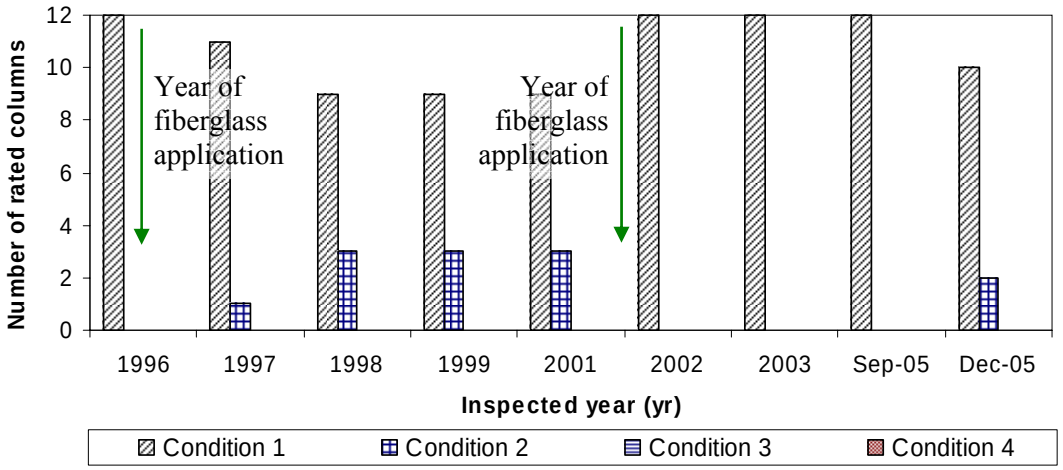

Figure 3.21: Timeline of inspected conditions of columns and maintenance operations in the B-53-65 bridge (Condition rating definitions are summarized in Table 3.3).

3.2.11 Bridge B-53-66

Bridge B-53-66 is located under US highway 14 on interstate highway I-90WB in Rock Co., WI. This bridge has fifteen concrete columns and five of them have been repaired using fiberglass wrapping (Figure 3.22). WisDOT has used the fiberglass wraps in two occasions: in 1994 and in the 2001-2002 to upgrade the structural condition of the bridge columns. The timeline of degradation and repairs is summarized in Table 3.13 and Figure 3.23.

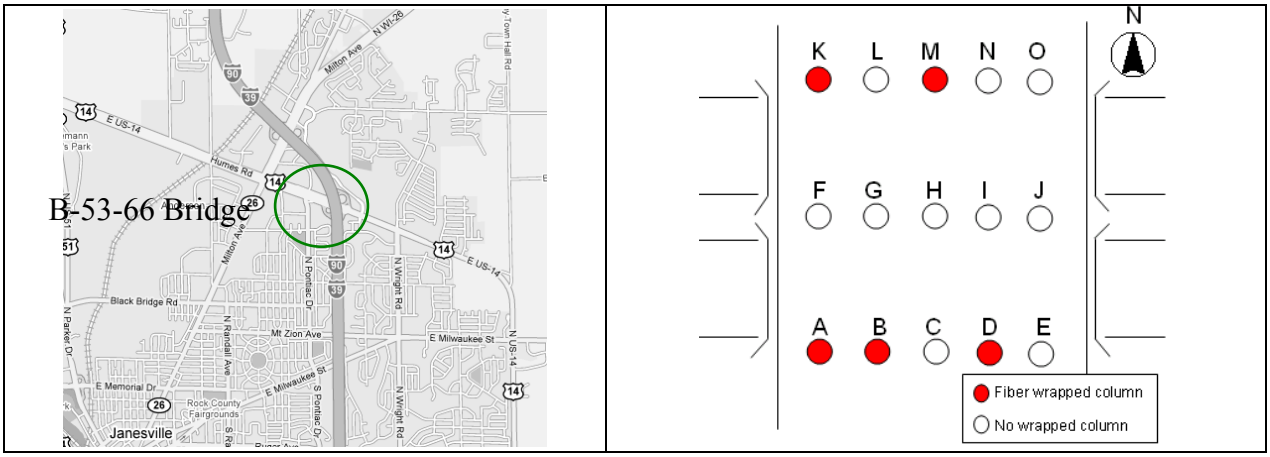

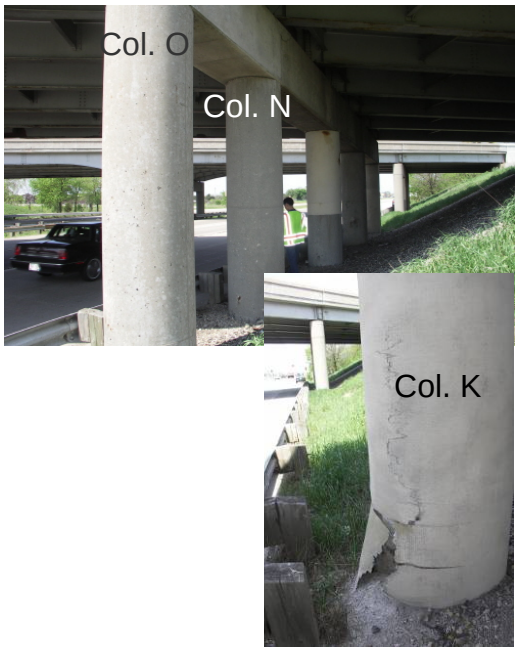

Figure 3.22: Location of B-53-66 bridge in Rock Co., WI and arrangement of columns (map: after Google Maps 2008).

Table 3.13: Summary of B-53-66 bridge inspection reports

Year	Relevant inspection report comments
11/1996 ~ 11/1999	Fiberglass wrapped columns K and M have some vertical cracks. Column L has delaminated area.
7/2001	Columns A, B and D were fiber wrapped in 2000 and painted gray. They look good.
10/2002 ~ 10/2004	Column K has old fiberglass wrap and the wrap is busting out.
10/2006	Column K and M have old fiberglass wraps and are busting out at bottom. Columns A, B & D were fiber wrapped in 2000 and painted gray. They look good.

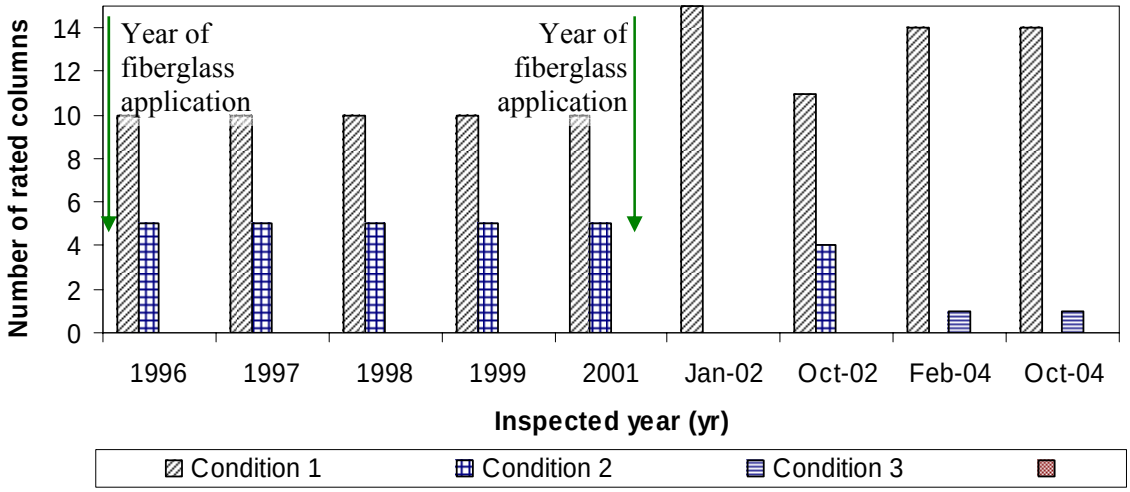

Figure 3.23: Timeline of inspected conditions of columns and maintenance operations in the B-53-66 bridge (Condition rating definitions are summarized in Table 3.3).

3.2.12 Bridge B-53-71

This bridge is located under state highway 59 on interstate highway I-90 in Rock Co., WI. The bridge has nine concrete columns and four of them have been repaired using fiberglass wraps as shown in Figure 3.24. WisDOT has used the fiberglass wraps in two occasions: in the mid 1990s and in 2001-2003.The timeline of degradation and repairs is summarized in Table 3.14 and Figure 3.25.

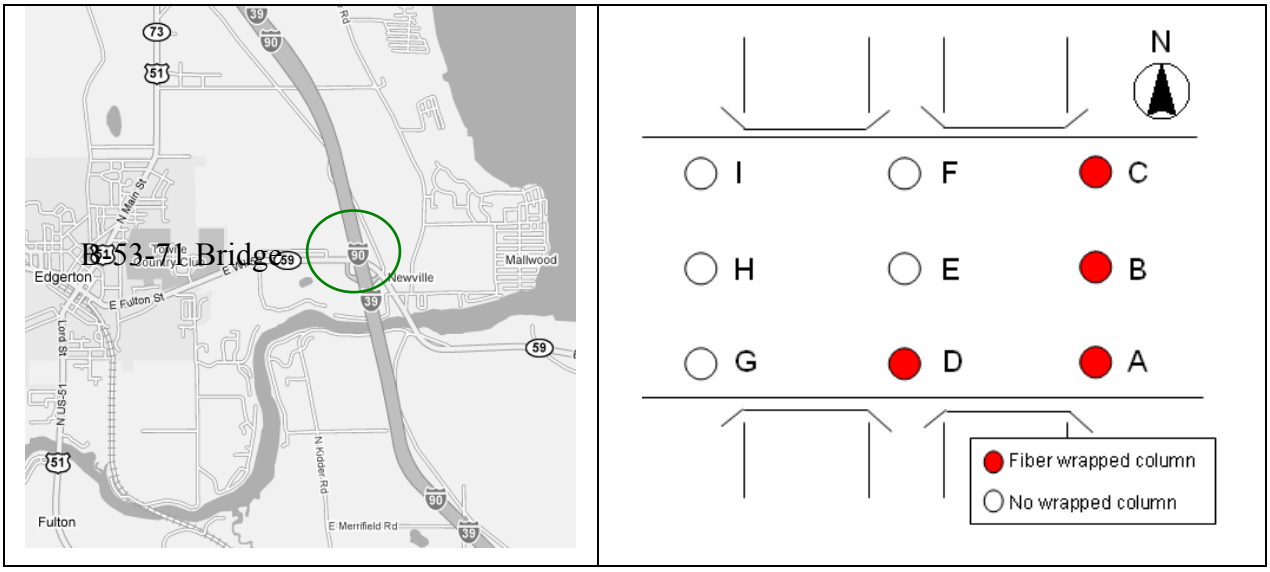

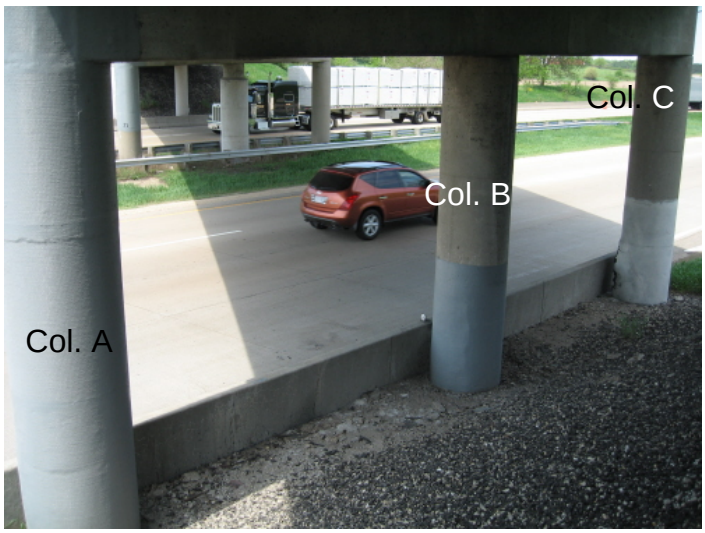

Figure 3.24: Location of B-53-71 bridge in Rock Co., WI and arrangement of columns (map: after Google Maps 2008).

Table 3.14: Summary of B-53-71 bridge inspection reports

Year	Relevant inspection report comments
10/1996	Columns A, B, and C are all fiberglass wrapped. Column E has one concrete collar has several cracked rust stains
10/1997	Columns A, B, and C are all fiberglass wrapped. Column C has several cracks with rust stains. Column E has a concrete collar has horizontal cracks, sounding was good.
4/1998	Columns A and B have fiberglass wrap on the lower half. Columns C has a complete fiberglass wrap.
3/1999	Columns A and B have fiberglass wrap on the lower half. Columns C has a complete fiberglass wrap.
7/2003	Columns A, B, C, and D are wrapped. The fiberglass wrapping in column C has failed near the ground line. Column E has a collar.
7/2005	Columns G and H both have bottom half spalling out. Column E has a collar. Column A is completely wrapped in fiberglass. Columns B and C are wrapped half height in fiberglass. The wrap in column C is coming off.

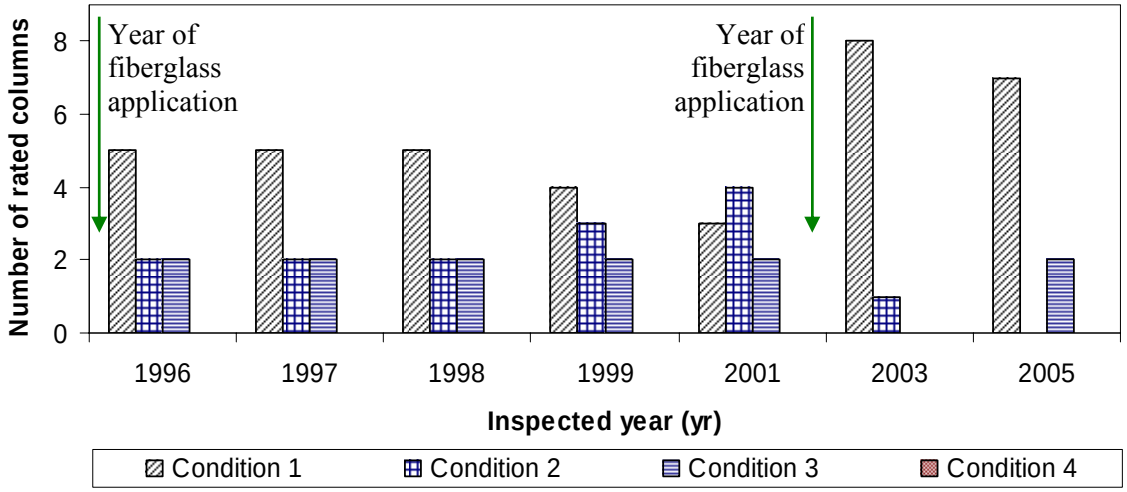

Figure 3.25: Timeline of inspected conditions of columns and maintenance operations in the B-53-71 bridge (Condition rating definitions are summarized in Table 3.3).

3.2.13 Bridge B-53-75

This bridge is located under interstate highway I-90WB on county road M in Rock Co., WI. The bridge has eight concrete columns and four of them have been repaired using fiberglass wraps as shown in Figure 3.25. WisDOT has used the fiberglass wraps in two occasions. The wrap applications on these bridge columns were implemented in the mid 1990s and 2001-2003 to upgrade the structural condition of the bridge columns as documented in Table 3.13. The timeline of degradation and repairs is summarized in Figure 3.26.

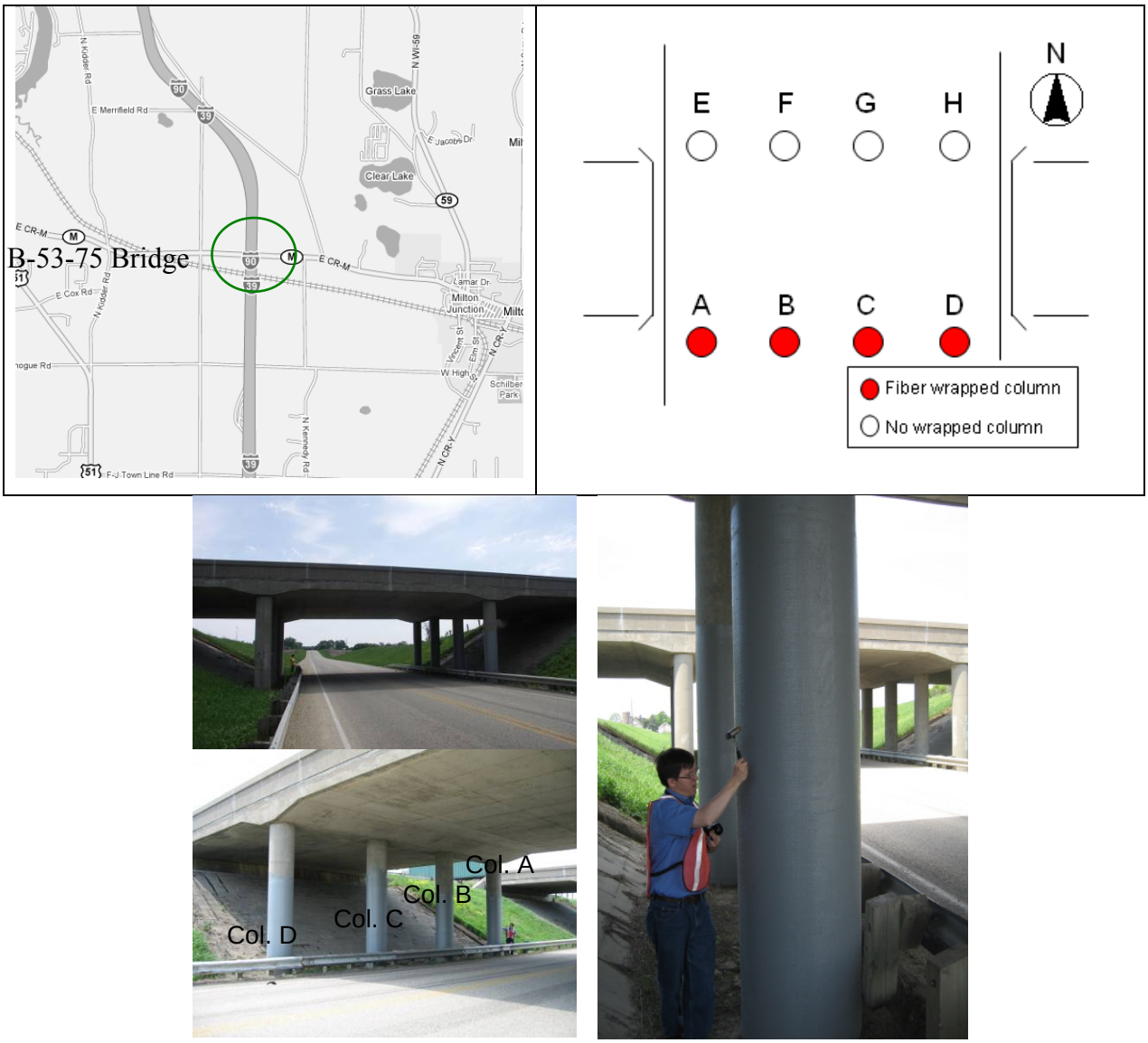

Figure 3.26: Location of B-53-75 bridge in Rock Co., WI and arrangement of columns (map: after Google Maps 2008).

Table 3.15: Summary of B-53-75 bridge inspection reports

Year	Relevant inspection report comments
10/1996 ~ 7/2001	Columns A, B, C, and D are cracked and delaminated in the bottom half. Column G is delaminated, exposed rusty rebar.
7/2003 ~ 7/2005	Columns A, B, C, and D are wrapped.

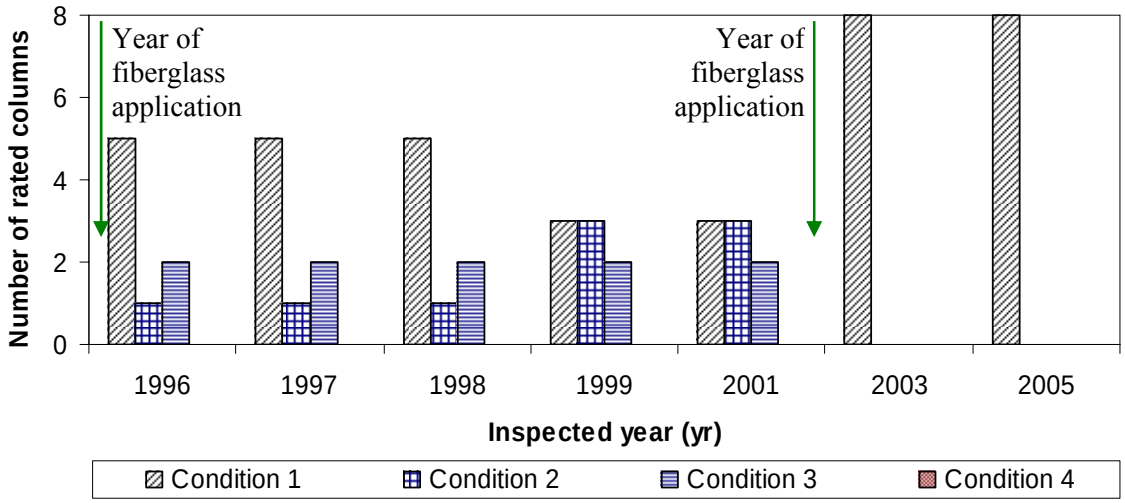

Figure 3.27: Timeline of inspected conditions of columns and maintenance operations in the B-53-75 bridge (Condition rating definitions are summarized in Table 3.3)

3.3. Selection of Columns for Testing

The research team used the information from the WisDOT bridge inspection and from its own visual inspection to select eight columns for in-depth evaluation (e.g, sonic testing, travel time tomographic imaging, half-cell potential readings, and chloride ion content). This selection was based on the overall range of column conditions, column and wrap types, wrap ages, testing environment, safety of the working crew, and minimal traffic disruption. In this report, results for the eight representative columns are presented. Table 3.16 and Figures 3.28 and 3.29 summarize the location and views of the selected bridges and columns.

Table 3.16. Summary of tested columns for field and laboratory testing

Bridge	Location (Lane Direction)	Column	Wrap Color	Wrap Height
B-28-45	Ziebell Rd. / IH-94 (EB)	A	cream wrap	1/2 column
		B	cream wrap	2/3 column
		C	No wrap	No warp
B-53-71	STH59 / IH90 (NB)	A	gray wrap	complete column
		B	gray wrap	1/3 column
		C	cream wrap	2/3 column
B-14-144	Church St. / IH-90 (NB)	H	gray wrap	2/3 column
		G	gray wrap	2/3 column

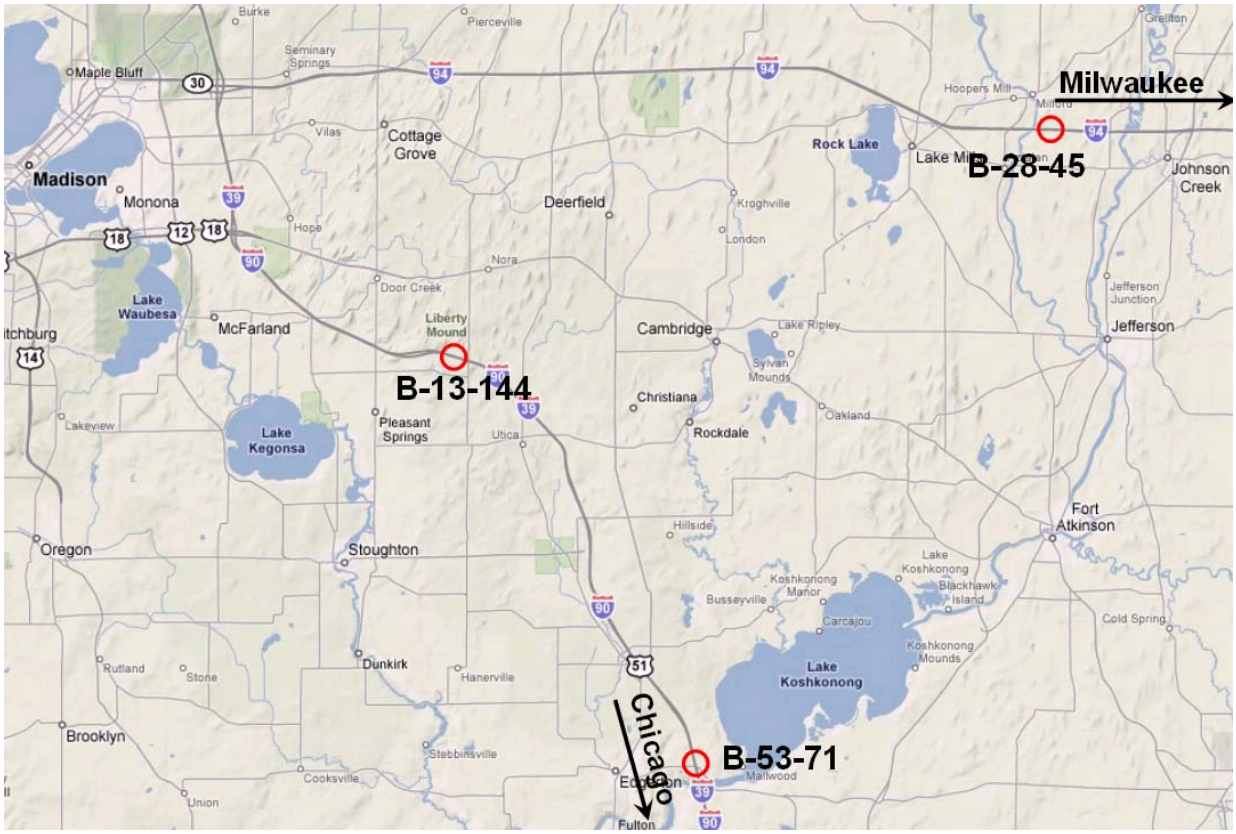

Figure 3.28. Geographic location of the selected bridges for the performance assessment of fiberglass wrapped columns (Dane County, Wisconsin - after Google map 2008).

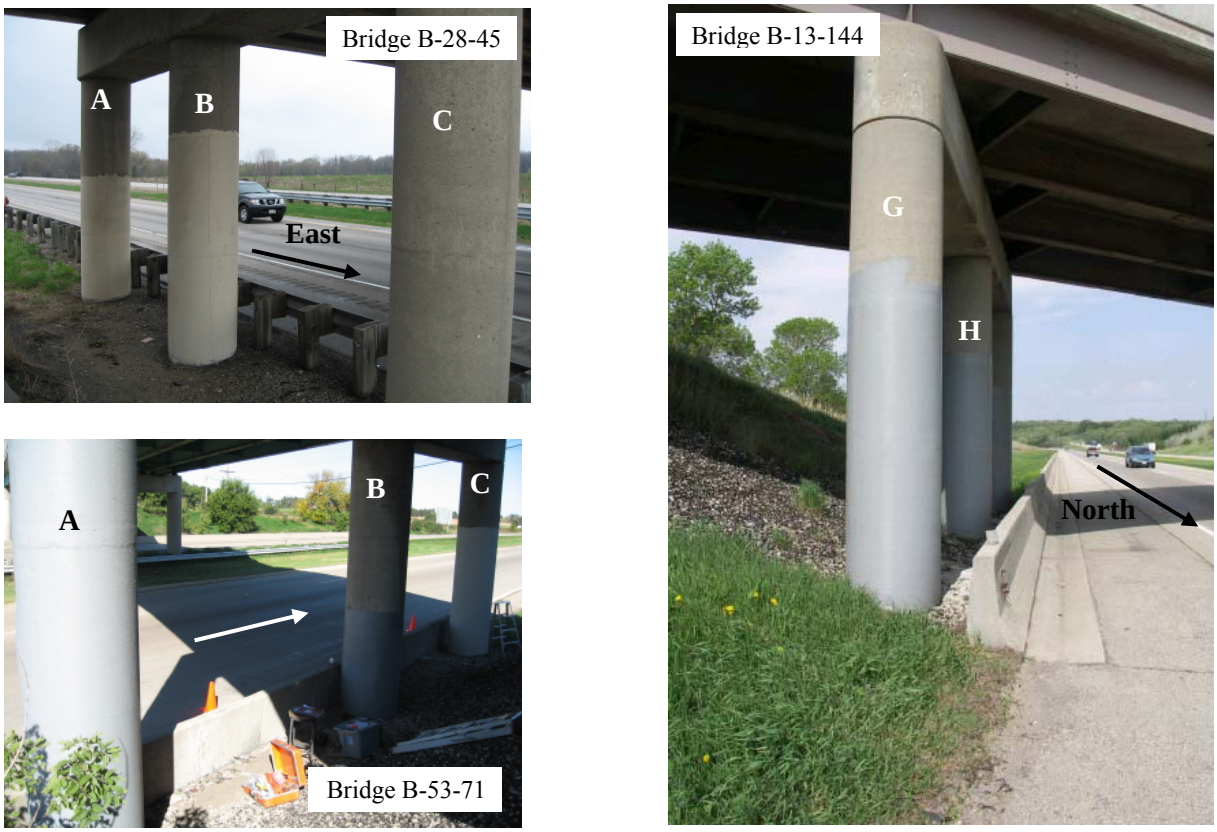

Figure 3.29. View of tested columns in the three selected different bridges.

Chapter 4. Field Testing and Data Interpretation

4.1. Introduction

The research team tested a total of eight different bridge columns to evaluate the integrity of the reinforced concrete in fiberglass-wrapped and non-wrapped columns. These tests include: P-wave velocity measurements, P-wave and ground penetrating radar tomographic imaging, half-cell potential, and determination of chloride ion content. A brief description of the test and test results are presented next.

4.2. P-wave velocity measurements

Internal concrete deterioration was evaluated by profiling P-wave velocity at 0.2 m intervals along a longitudinal plane. Measurements were taken at 20-cm intervals from just above the soil level to above the fiberglass wrapping height. This test was used to evaluate the overall structural health of the concrete in the column (see Table 2.3). Overall reductions in the wave velocity provide an indication of the internal deterioration of the concrete (Prada et al. 2000; Nanni and Lopez 2004; Daigle et al. 2005).

P-wave velocity data were taken along vertical and horizontal cross sections. Figure 4.1a shows the instrumentation used in the P-wave data collection. The instrumentation includes piezoelectric accelerometers, instrumented hammer, signal conditioning system, oscilloscope, and laptop computer for data storage and interpretation. Figure 4.1b presents the simple vertical profiling setup where P-wave traces were collected along horizontal propagation lines to quickly evaluate the overall concrete quality.

The data collected along the horizontal profiles yield average P-wave velocity information. However, visual surveys of columns have shown that the damaged caused by the corrosion of the reinforcing bars was mainly localized along the lower third of the columns, in an area facing the traffic direction (see Figures 3.1, 3.2, 3.18, 3.22, and 3.24). For this reason, data were also collected by sending P-waves in several directions on vertical and horizontal planes as shown in Figure 4.2 and 4.3. These data sets permitted obtaining tomographic images of the P-wave

velocity field and the evaluation of the local damaged concrete. A summary of these results are presented next

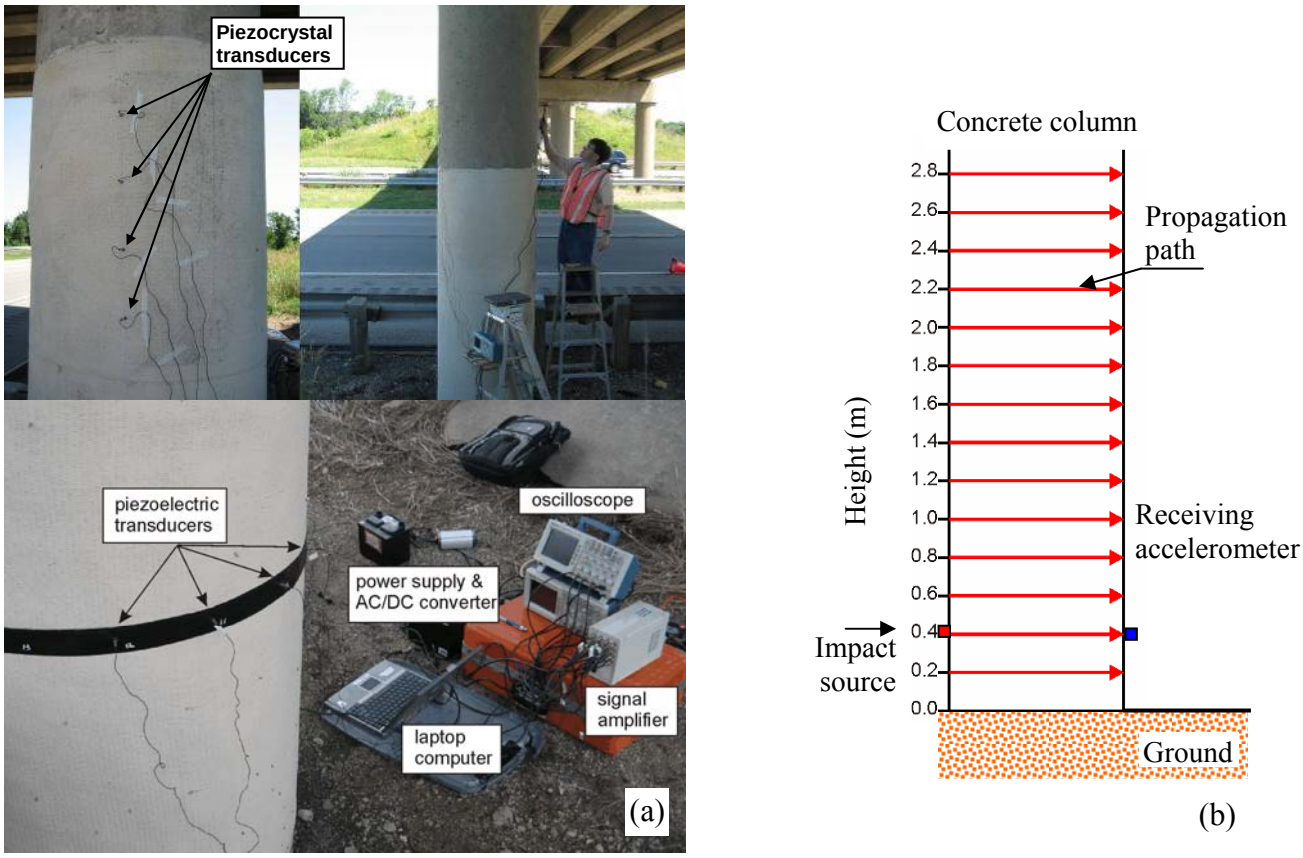

Figure 4.1: (a) Field instrumentation used for P-wave travel time data collection. (b) Test setup for P-wave velocity profiling along longitudinal plane.

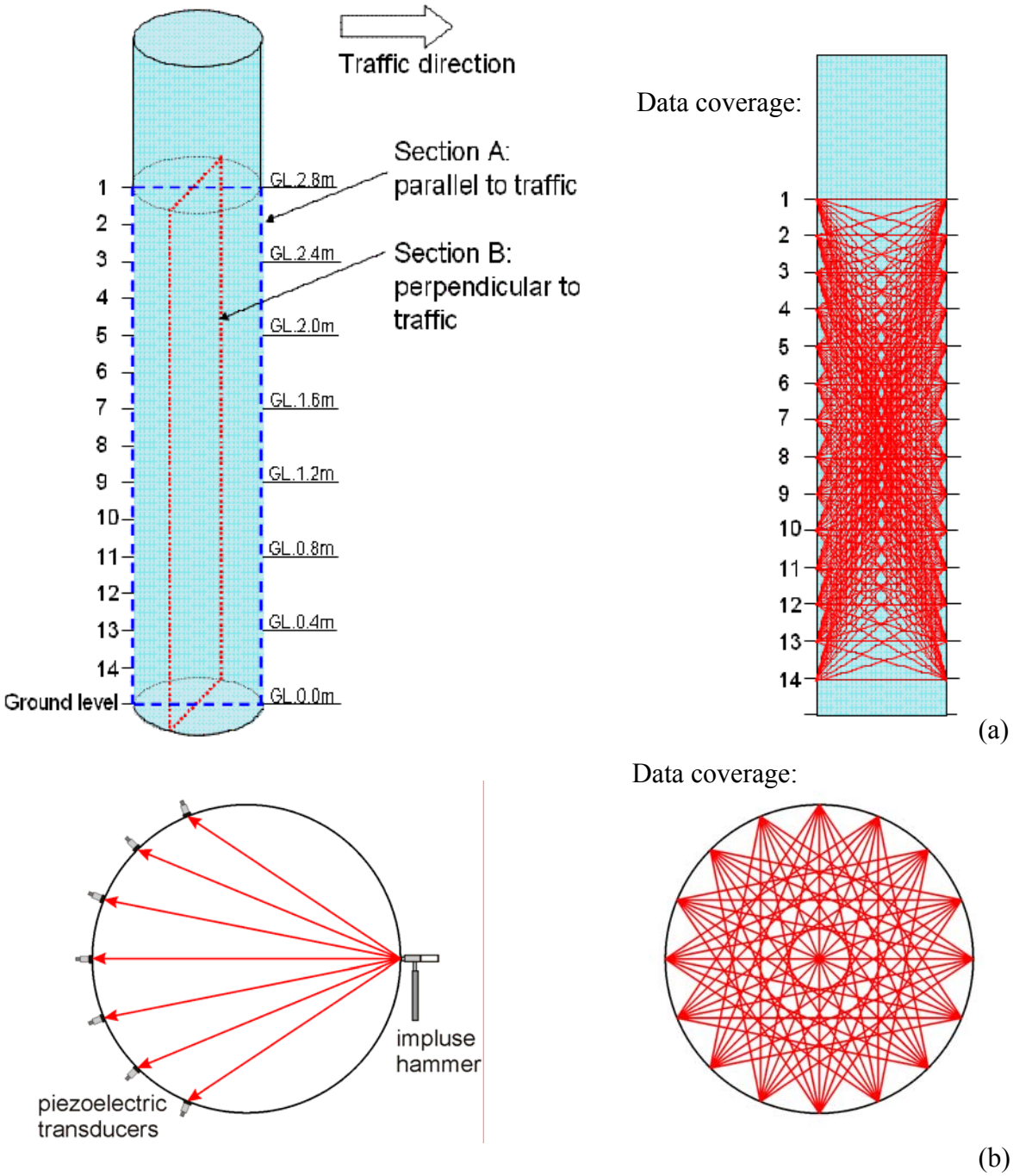

Figure 4.2: Test setups for the collection of tomographic data along (a) vertical and (b) horizontal planes. An impact hammer was used to trigger the P-waves used in the study.

4.2.1 Bridge B-28-45: P-wave velocity results

P-wave velocity profiles and tomographic images were collected on three columns along of eastbound shoulder of Bridge B-28-45. Two of these columns (columns A and B) were coated with fiberglass wraps while the third column (Column C) was in its as-built condition, as shown in Figure 4.3. Columns A and B did not show external signs of distress while Column C showed cracks on the surface facing traffic.

Average P-wave velocity profiles along vertical planes parallel and perpendicular to the traffic direction for column A are presented in Figure 4.4. The figure shows a significant reduction in the P-wave velocity and thus areas of weaker concrete at 1.2 m and 1.5 m high in the vertical plane parallel to the traffic direction. Because these measurements provide average P-wave velocities only and the local position of the weaker concrete material cannot be determined (e.g., how far from the concrete surface), P-wave data were also collected to obtain tomographic images of the vertical planes. These tomographic images are presented in Figure 4.5. The local distribution of P-wave velocity shown in Figure 4.5b indicates that the areas of degraded concrete facing the traffic direction.

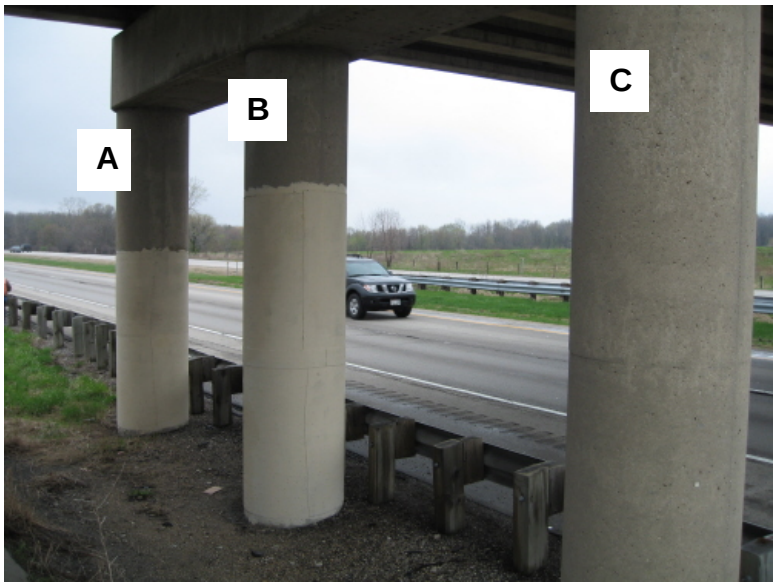

Figure 4.3: Tested columns in the Bridge B-28-45 (Eastbound).

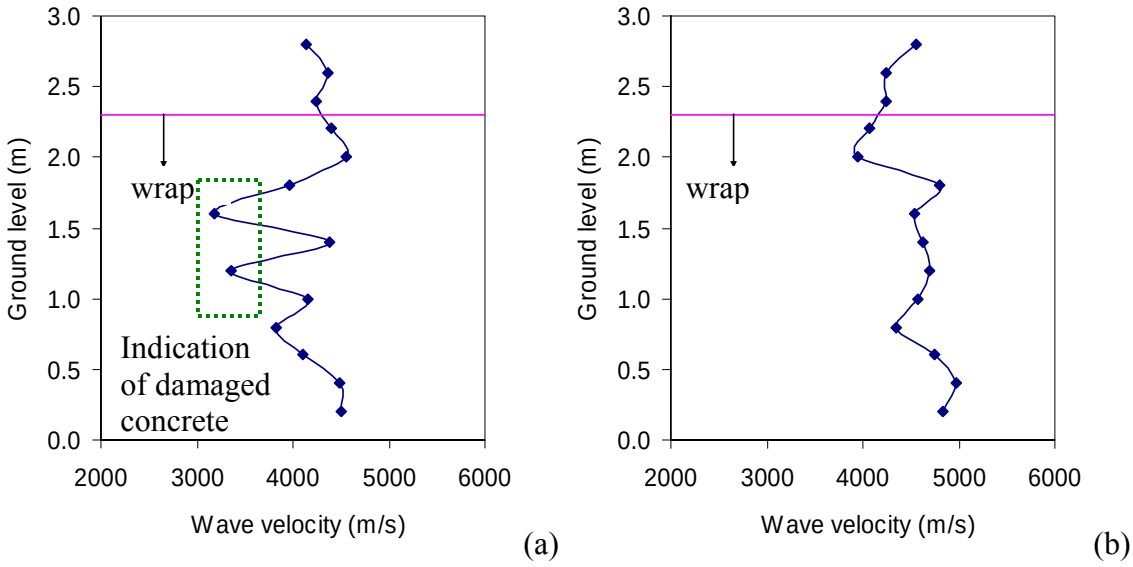

Figure 4.4: Horizontal P-wave velocity profiles on Bridge B-28-45 column A: (a) vertical parallel to traffic and (b) vertical plane perpendicular to traffic.

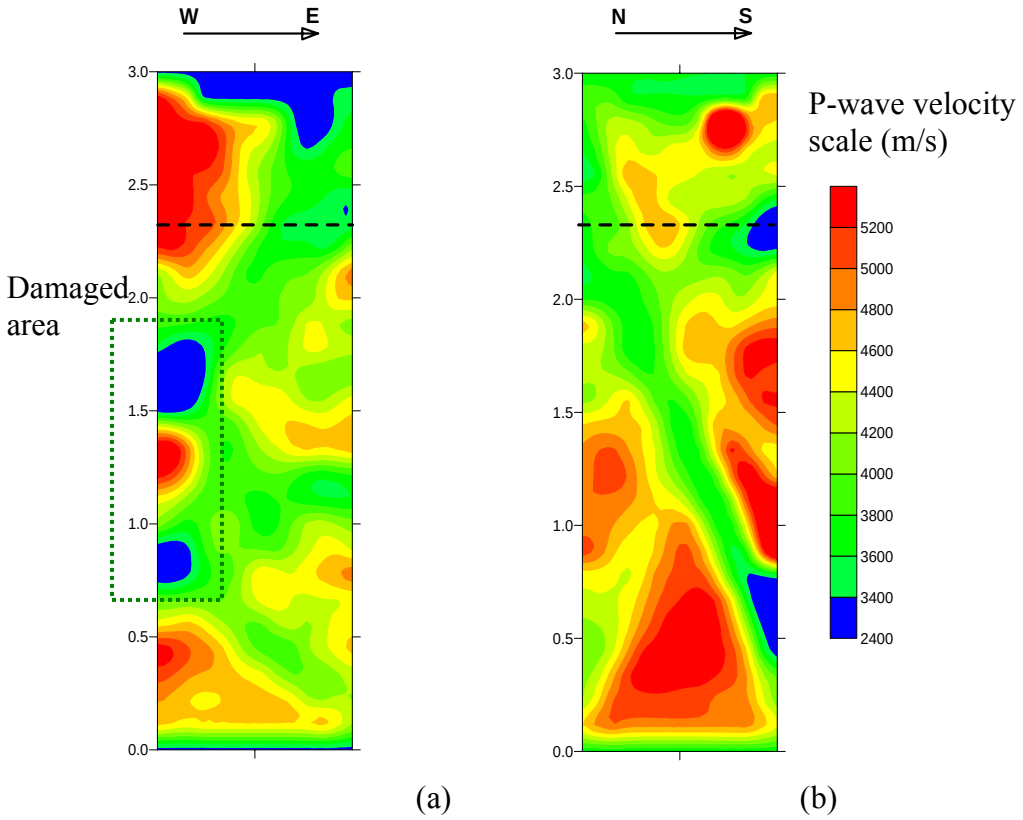

Figure 4.5: P-wave velocity tomographic images on Bridge B-28-45 column A: (a) vertical plane parallel to traffic and (b) vertical plane perpendicular to traffic.

Similar P-wave velocity profiles and tomographic images along vertical planes were collected for Bridge B-28-45 column B, as shown in Figure 4.6. While the tomographic images presented in Figure 4.7 do not seem to indicate definite locations of the damaged concrete areas, the tomographic images along two horizontal cross-sections (Figure 4.8) clearly constrain the location of damaged area on the concrete facing the traffic direction.

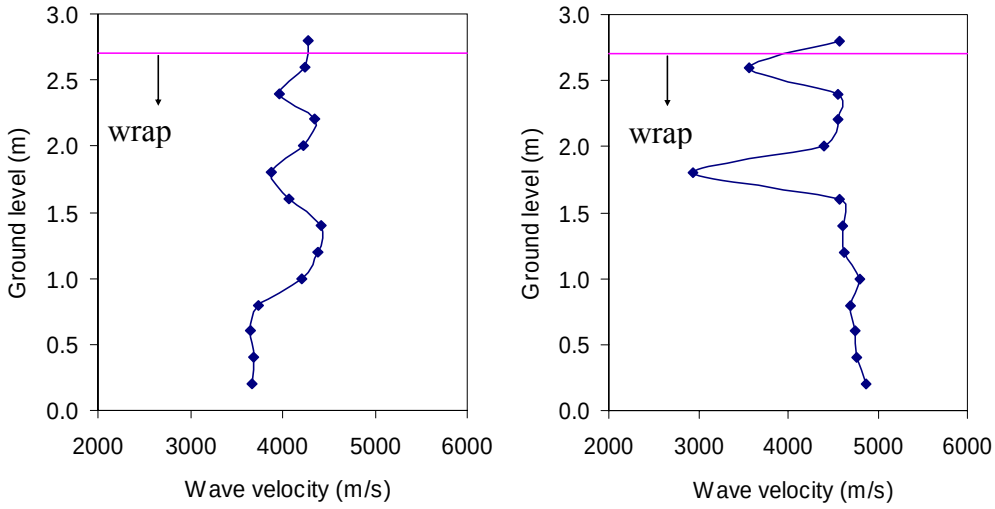

Figure 4.6: Horizontal P-wave velocity profiles on Bridge B-28-45 column B: (a) vertical parallel to traffic and (b) vertical plane perpendicular to traffic.

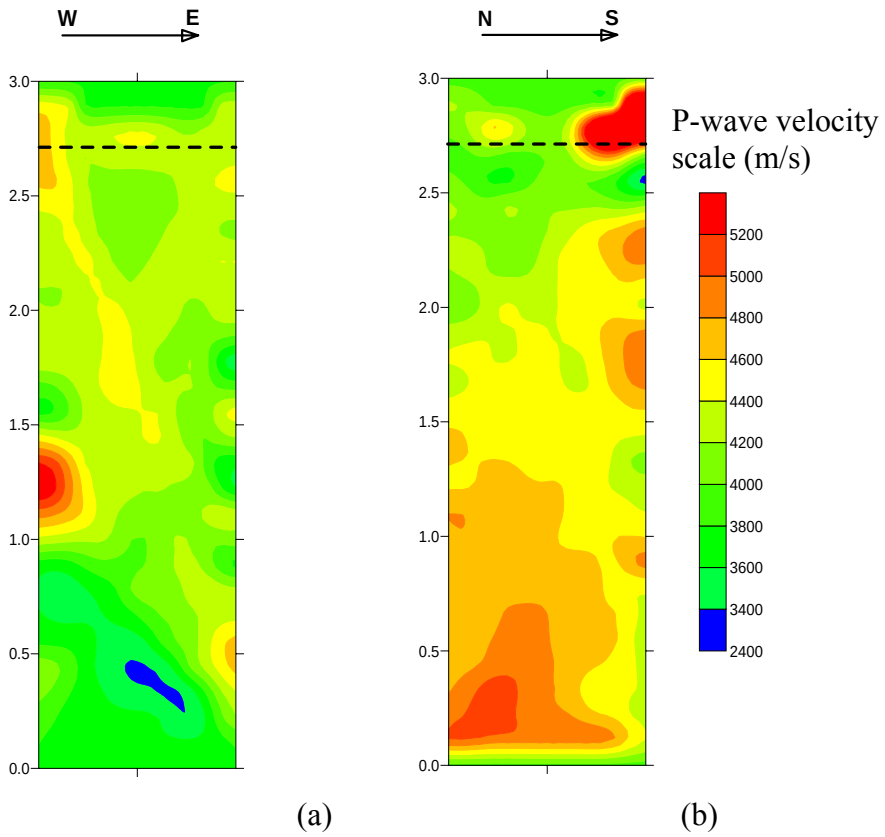

Figure 4.7: P-wave velocity tomographic images on Bridge B-28-45 column B: (a) vertical plane parallel to traffic and (b) vertical plane perpendicular to traffic.

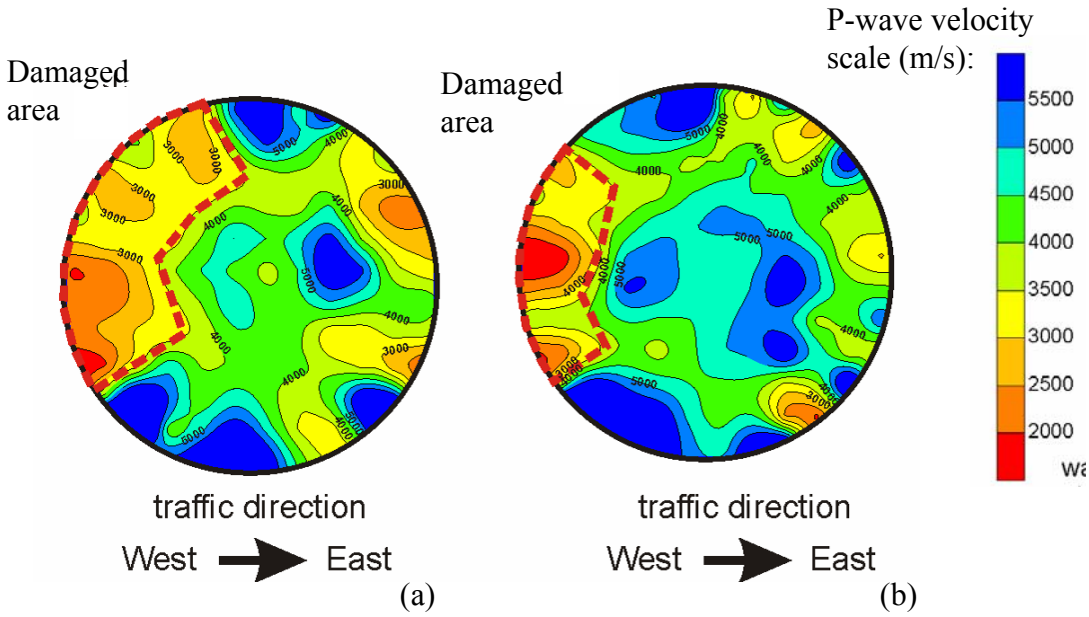

Figure 4.8: P-wave velocity tomographic images on Bridge B-28-45 column B: (a) Section at 0.8 m high (b) Section at 0.4 m high (The dashed line limits damaged areas).

To provide a benchmark to the measurements conducted on the fiberglass wrapped columns A and B, P-wave velocity tests were also conducted on column C (unwrapped column) of Bridge B-28-45. Both horizontal P-wave velocity profiles (Figure 4.9) and tomographic images (Figure 4.10) along vertical planes parallel and perpendicular to traffic directions coincide in the locating areas of degrading concrete. These concrete areas face the traffic direction. Thus, it is likely that the damage observed in columns A and B using the wave propagation techniques reflect the degradation caused by the rebar corrosion even after the columns were treated with fiberglass wrap.

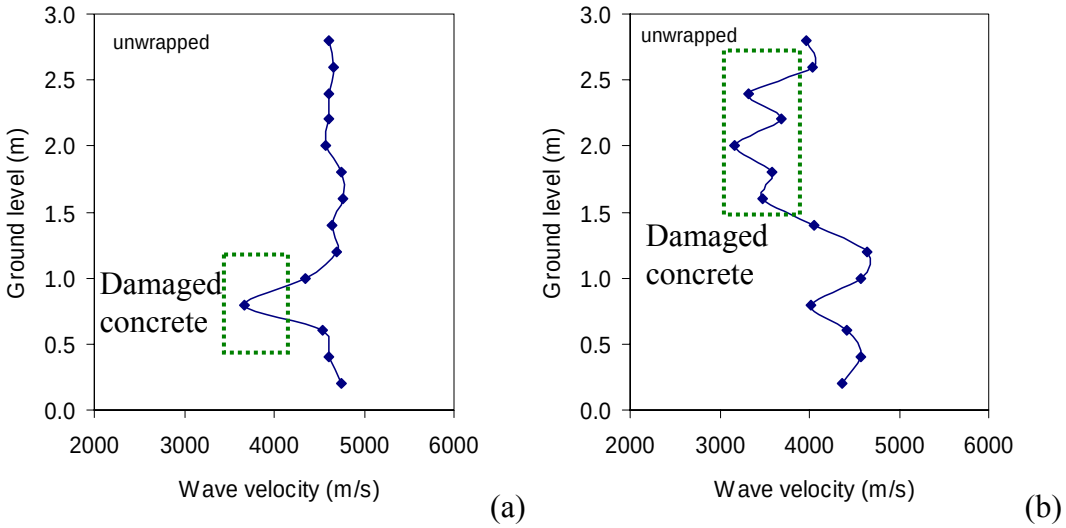

Figure 4.9: Horizontal P-wave velocity profiles on Bridge B-28-45 column C: (a) vertical parallel to traffic and (b) vertical plane perpendicular to traffic.

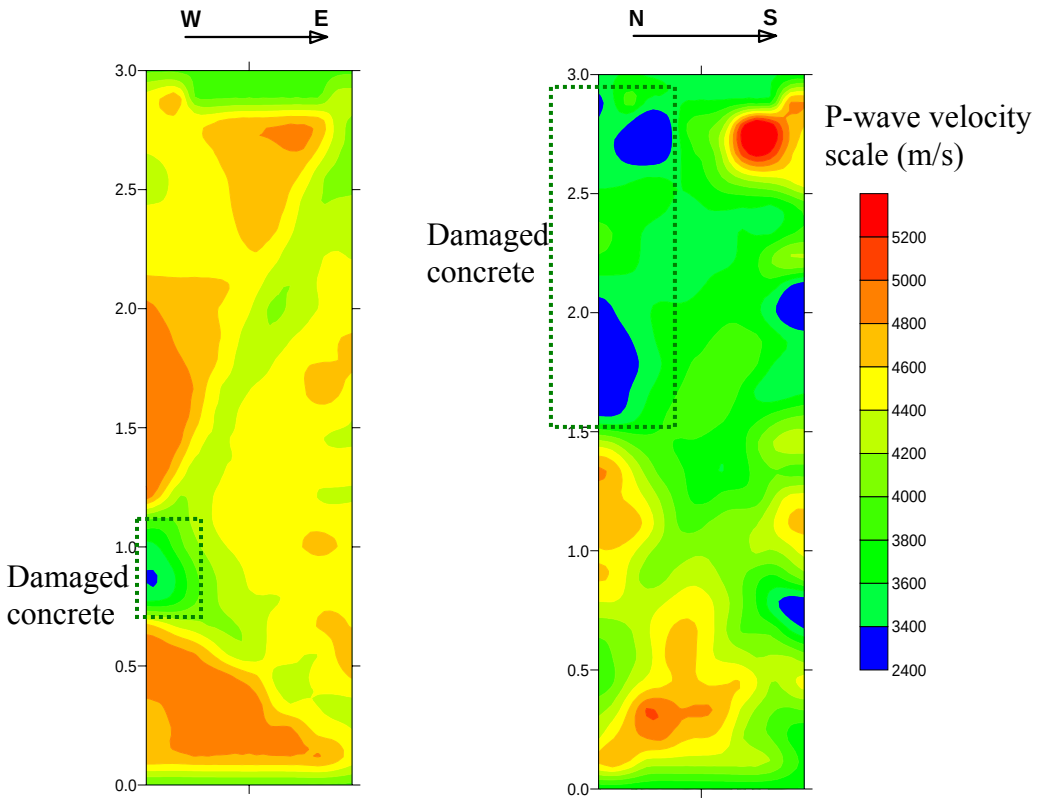

Figure 4.10: P-wave velocity tomographic images on Bridge B-28-45 column C: (a) vertical plane parallel to traffic and (b) vertical plane perpendicular to traffic.

4.2.2 Bridge B-53-71: P-wave velocity results

P-wave velocity profiles and tomographic images were collected on three columns along of eastbound shoulder of Bridge B-53-71. Two of these columns (columns A and C) were treated with fiberglass wrap along at least two third of the column high, while the third B was treated to less than half its height as shown in Figure 4.11. Column C was re-wrapped in 2007 due to corrosion damage at the bottom of the column (see Figure 3.1)

The average P-wave velocity profile and a tomographic image collected along a vertical plane parallel to traffic direction in column A are presented in Figure 4.12. These results show areas of weaker concrete at 0.6 to 1.2 m levels above ground. The results seem to show that despite of the repairs done with fiberglass wrapping (including replacing damage concrete with new mortar), areas of damaged concrete remains.

Figure 4.11: Tested columns in the Bridge B-53-71 (Northbound).

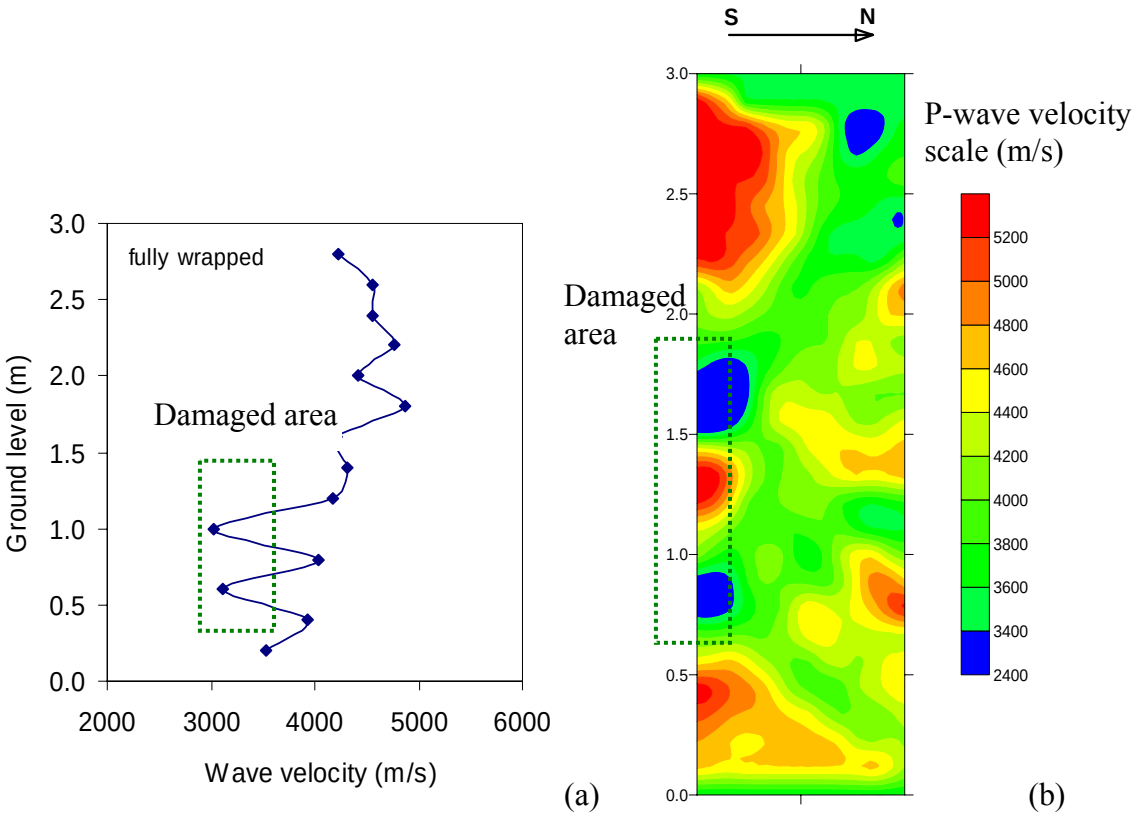

Figure 4.12: P-wave velocity results in Bridge B-53-71 column A along vertical plane parallel to traffic: (a) P-wave velocity profile and (b) tomographic imaging.

Figures 4.13 and 4.14 summarize the P-wave velocity profiles and tomographic images obtained in Bridge B-53-71 column B. This column shows relative low P-wave velocities along the vertical plane parallel to the traffic direction (Figures 4.13a and 4.14a) and higher P-wave velocities in the vertical plane perpendicular to the traffic direction. However even this plane shows pockets of low P-wave velocity both in areas above and below the fiberglass wrap level (see for example the drop on P-wave velocity at the 1.8 m level in Figures 4.13b and 4.14b).

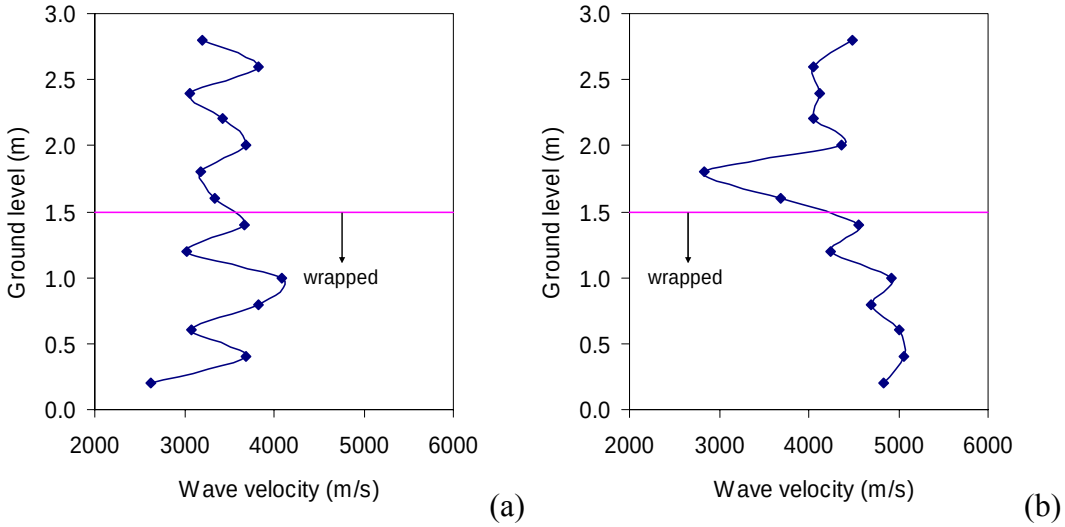

Figure 4.13: Horizontal P-wave velocity profiles in Bridge B-53-71 column B: (a) vertical parallel to traffic and (b) vertical plane perpendicular to traffic.

Finally, Figures 4.15 and 4.16 show the horizontal P-wave velocity profiles and tomographic images along vertical planes parallel and perpendicular to traffic directions coincide in the locating areas of degrading concrete for column C. This column was treated twice with fiberglass warp, most recently in 2007. Overall, the P-wave velocity profiles indicate good concrete quality

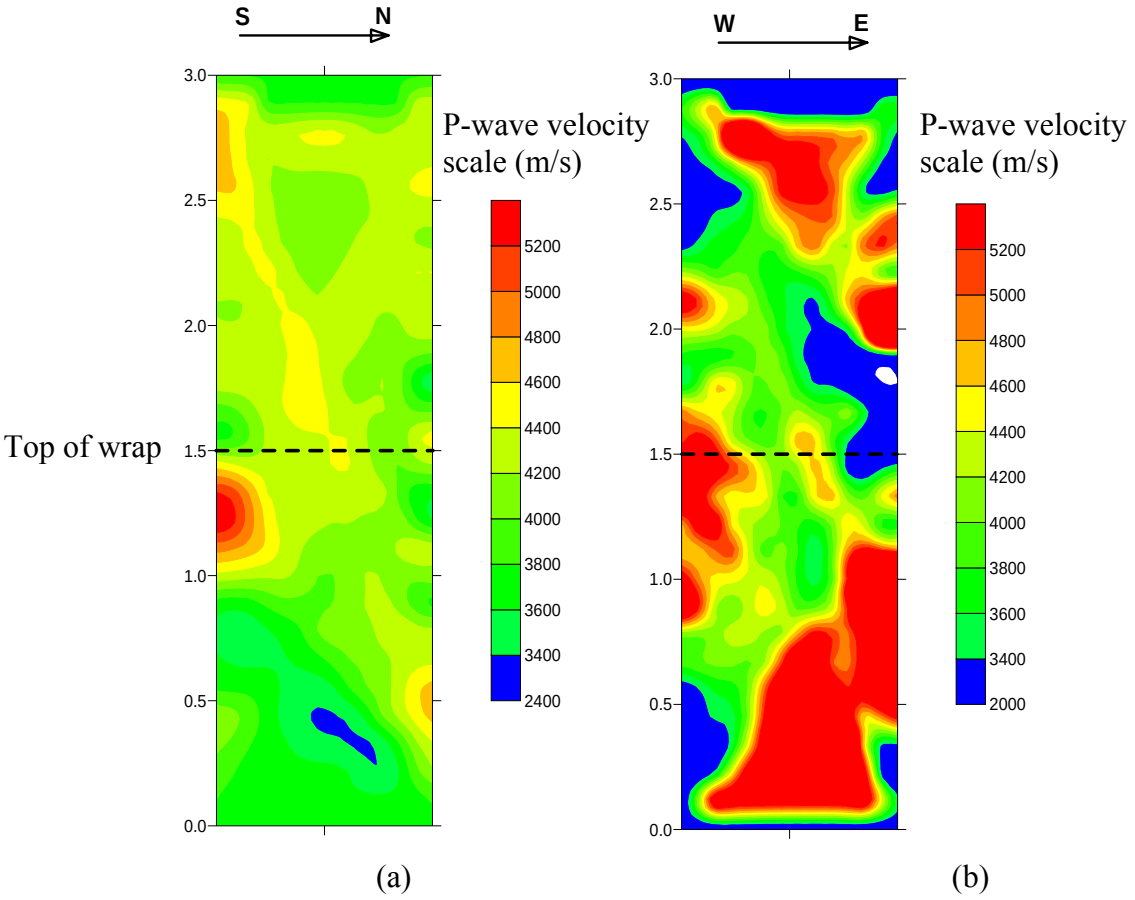

Figure 4.14: Horizontal P-wave velocity tomographic images of Bridge B-53-71 column B: (a) vertical parallel to traffic and (b) vertical plane perpendicular to traffic.

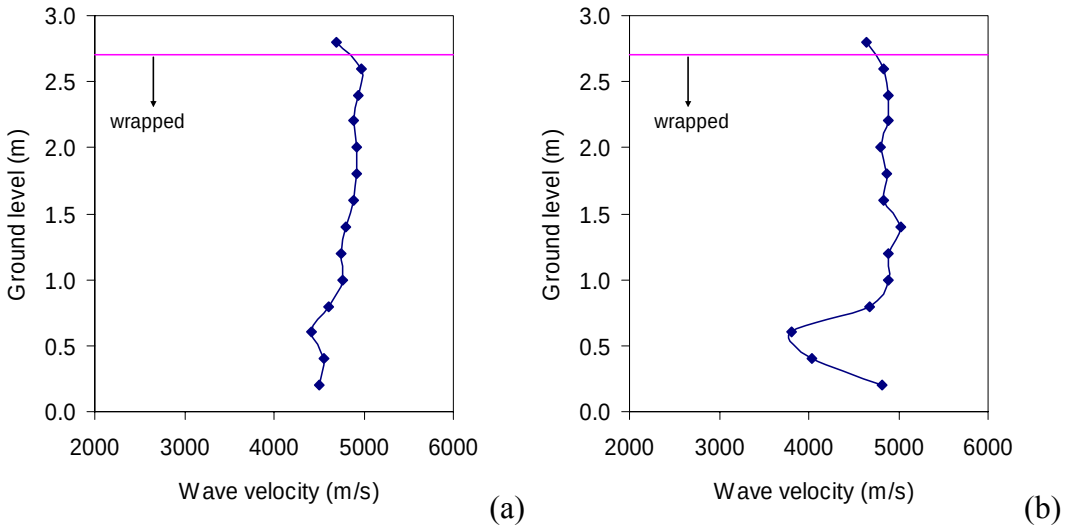

Figure 4.15: Horizontal P-wave velocity profiles in Bridge B-53-71 column C: (a) vertical parallel to traffic and (b) vertical plane perpendicular to traffic.

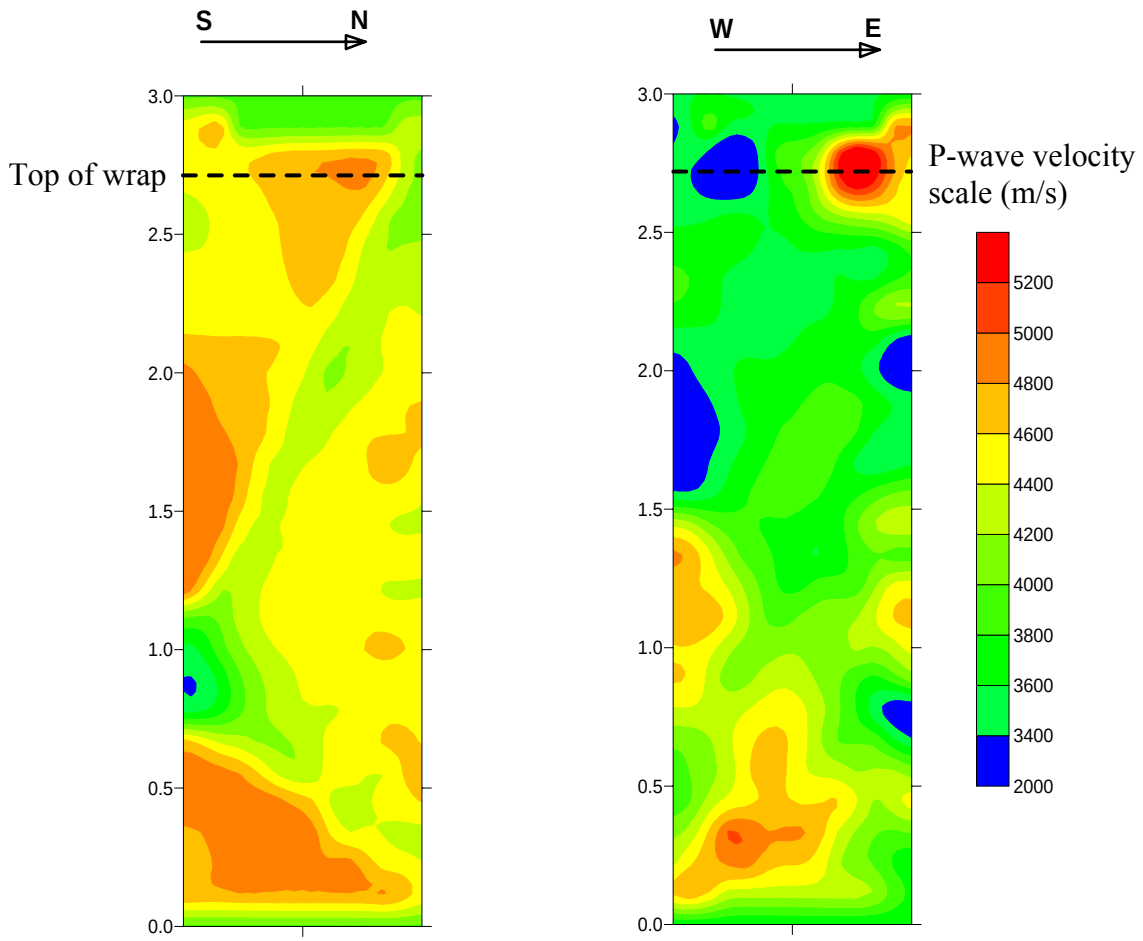

Figure 4.16: Horizontal P-wave velocity tomographic images of Bridge B-53-71 column C: (a) vertical parallel to traffic and (b) vertical plane perpendicular to traffic.

4.2.3 Bridge B-13-144: P-wave velocity results

P-wave velocity profiles and tomographic images were collected on two columns along of eastbound shoulder of Bridge B-13-144. Two of these columns (columns G and H) were treated with fiberglass wrap (Figure 4.17). These wrapped columns seem to be in very good condition, however P-wave velocity profiles and tomographic images indicate that the concrete is damaged in the bottom 1.5 m of both columns (Figure 4.18 and 4.19). WisDOT regular inspection reports also indicate that column G had experience fiberglass wrapping failure and needed replacement.

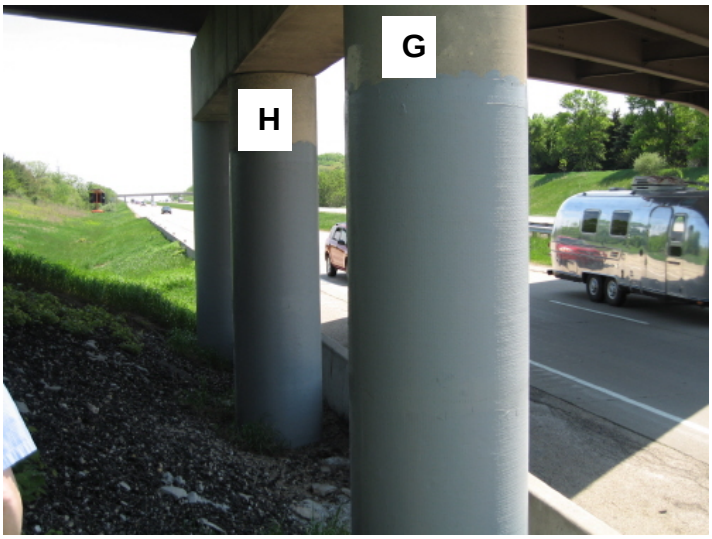

Figure 4.17: Tested columns in the Bridge B-13-144 (Southbound).

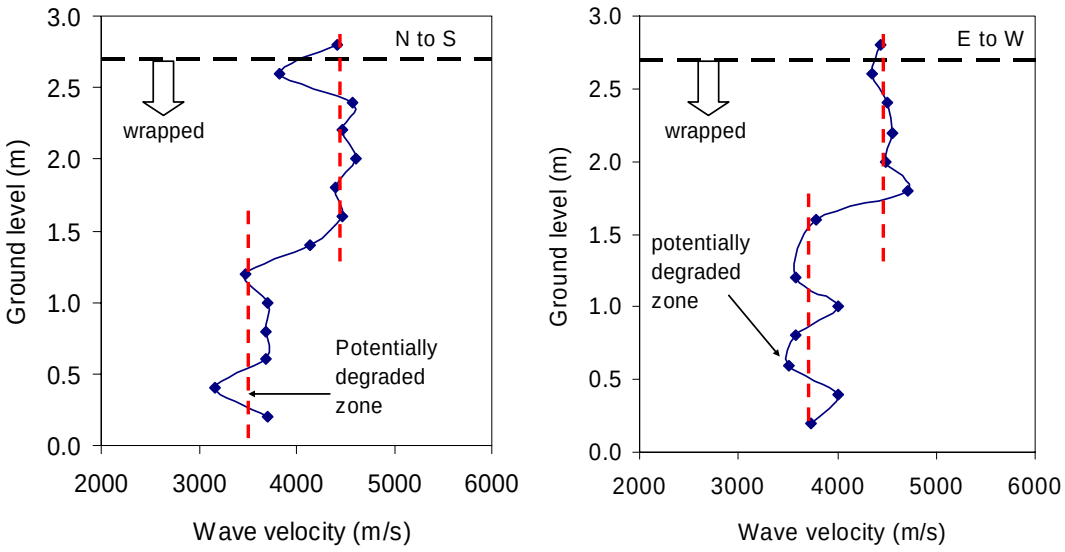

Figure 4.18: Horizontal P-wave velocity profiles in Bridge B-13-144 column H: (a) vertical parallel to traffic and (b) vertical plane perpendicular to traffic.

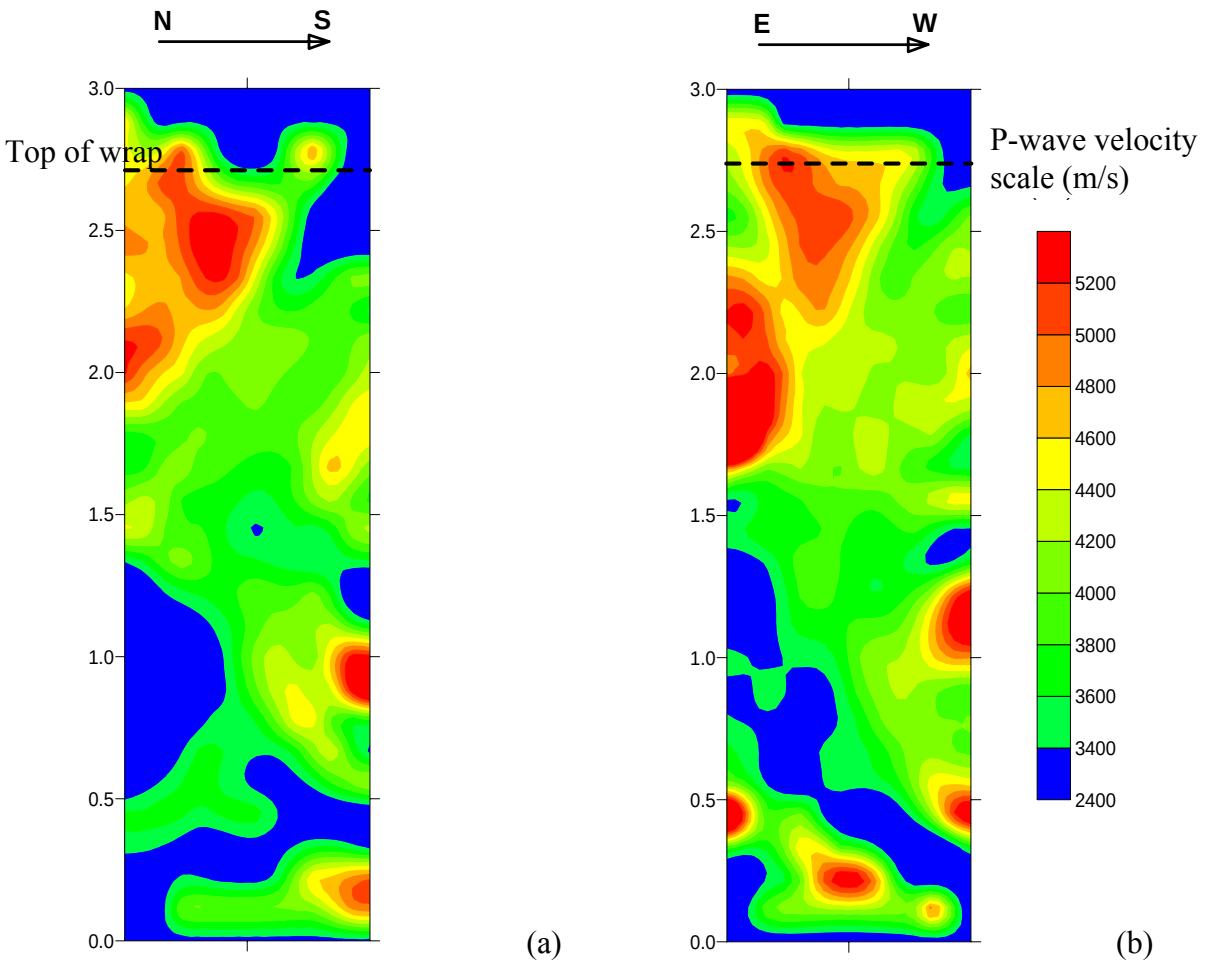

Figure 4.19: Horizontal P-wave velocity tomographic images of Bridge B-13-144 column H: (a) vertical parallel to traffic and (b) vertical plane perpendicular to traffic.

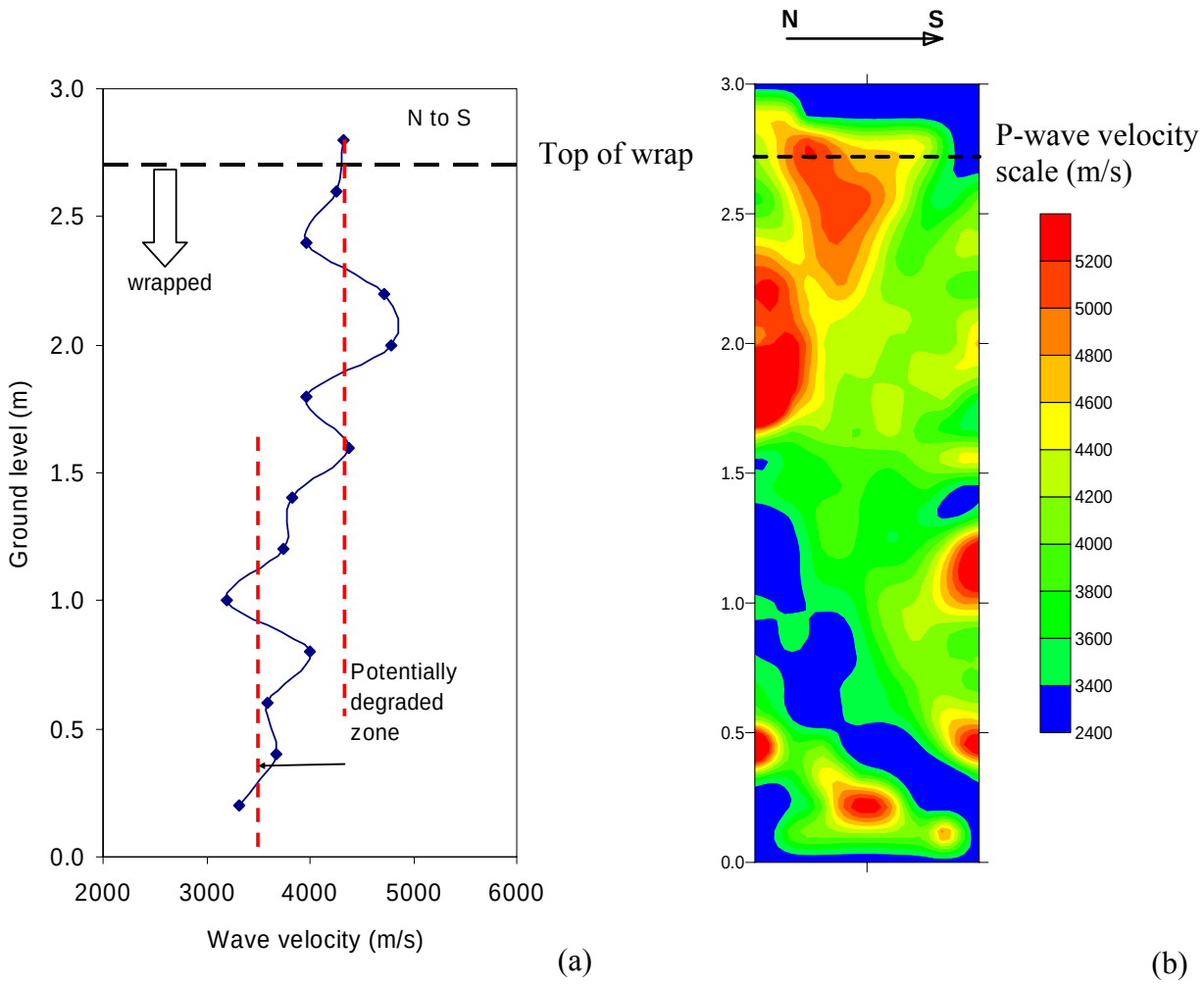

Figure 4.20: P-wave velocity results in Bridge B-13-144 column G along a vertical plane parallel to traffic: (a) P-wave velocity profile and (b) tomographic imaging.

4.3. Ground Penetrating Radar Measurements

A Sensors & Software pulseEKKO 100 Ground Penetrating Radar (GPR) system was used to collect data for the evaluation of electromagnetic properties (permittivity and conductivity) of the concrete columns. The main difference with elastic waves is that electromagnetic waves capture information about the volumetric water content and electrical conductivity distribution in the structural element. The drawback is that the EM waves interact with the steel reinforcement cluttering the collected data. The goal of this test was to evaluate distribution of volumetric water content (related to the measured electromagnetic wave velocity) and chlorine ion content (related to the attenuation of the collected signal). These results could be then related to potential

corrosion activity in the columns. That is, lower velocities indicate greater volumetric water content, while larger signal attenuations indicate greater electrical conductivity (i.e., Cl^- and water content in the columns).

The test setup consisted of two 200 MHz antennae connected through fiber optic cables to a driver and data acquisition consoled and driven by a laptop computer (Figure 4.21). The collected data were post processing, reduced and interpreted using the pulseEKKO View software.

Figure 4.21: GPR testing setup and data collection on a fiberglass wrapped column.

4.3.1 Bridge B-28-45: GPR tomography results

GPR data were collected in all three columns tested columns of Bridge B-28-45 (i.e., columns A, B and C). Figure 4.22 documents the GPR tomographic results along vertical planes: parallel and perpendicular to traffic directions. The lower electromagnetic wave velocity recorded along the midsection on north face of the column (Figure 4.22a) seems to indicate greater volumetric water content behind the fiberglass wrap. The location of this area of high volumetric water content

does not seem to coincide with the damaged areas predicted in the same column using the P-wave velocity tomography (see Figure 4.5). Furthermore, the high volumetric water content (that is, low electromagnetic wave velocity) in the cross section tomographic image (Figure 4.23) appears in the center of the column. This observation seems puzzling. Traffic splashing should show higher water content on the concrete surface however the surface may also dry faster.

Finally, Figure 4.24 shows the tomographic images of Bridge B-28-45 columns B and C (Column C does not have fiberglass wrap). Once again the results show greater water content areas (that is low electromagnetic wave velocities) at the center of the column in the lower section of the column or the top of column where little splashing would be expected.

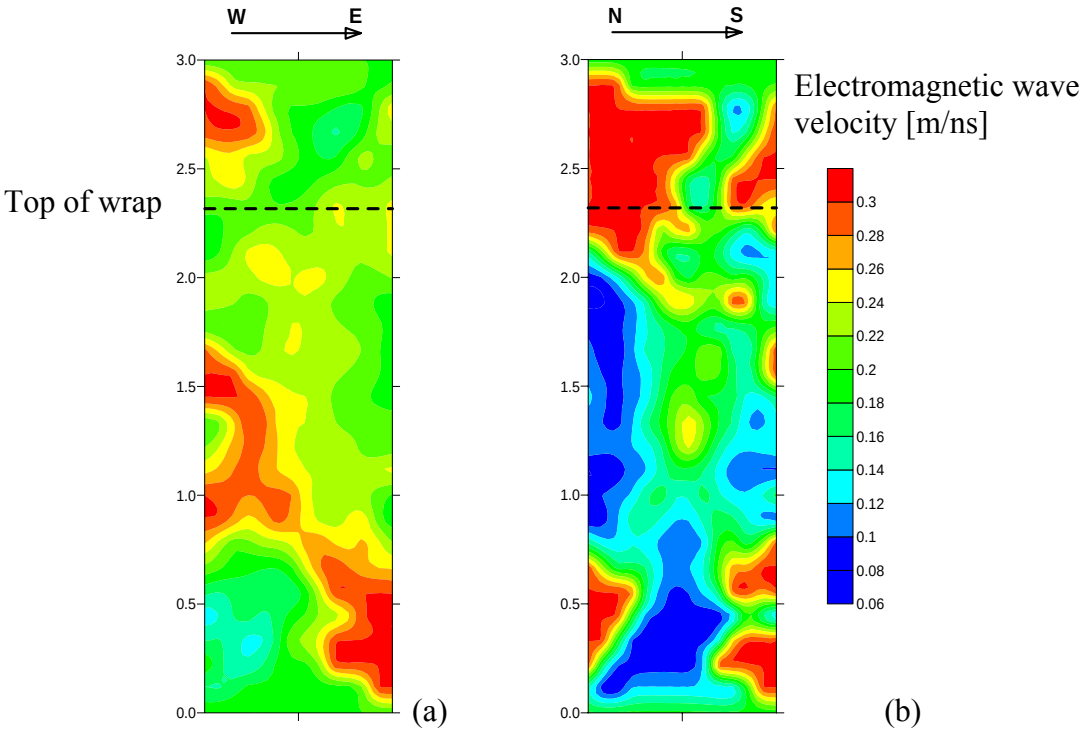

Figure 4.22: GPR tomographic images of Bridge B-28-45 Column A: (a) parallel to traffic and (b) perpendicular to traffic.

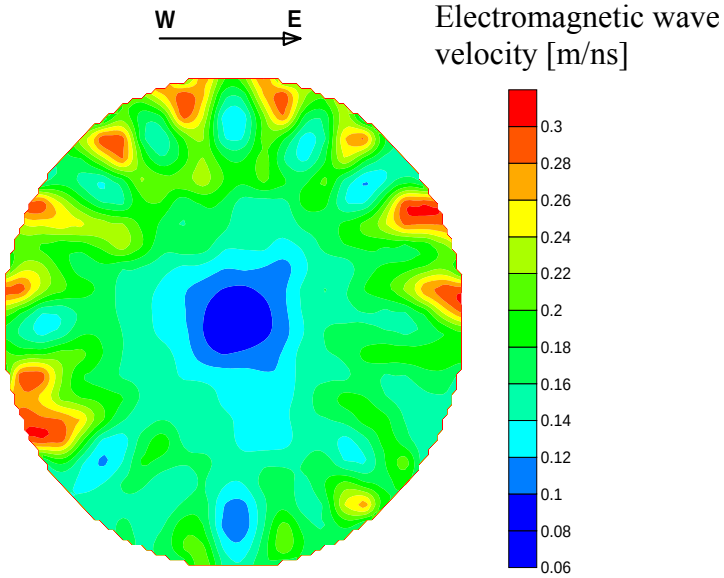

Figure 4.23: GPR tomographic images of Bridge B-28-45 Column A along 0.4 m high horizontal plane.

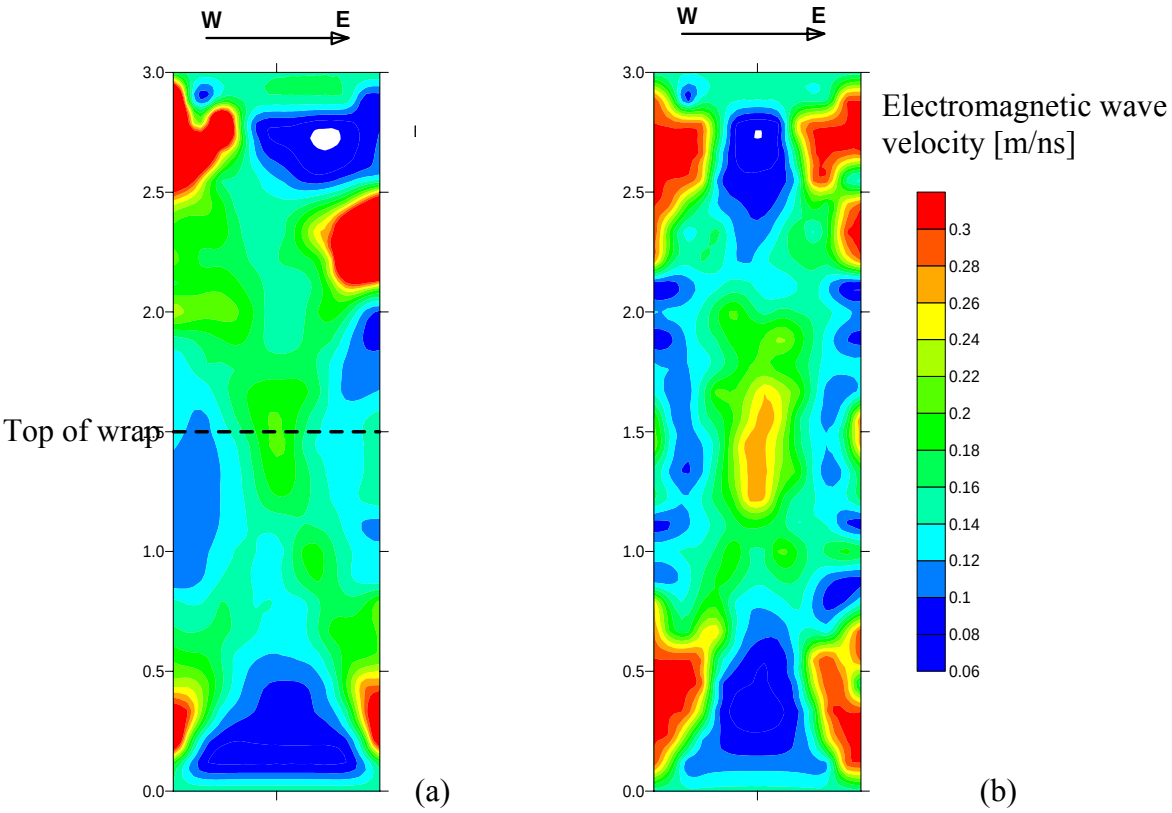

Figure 4.24: GPR tomographic images of Bridge B-28-45: (a) column B and (b) column C (parallel to traffic)

4.2.2 Bridge B-13-144: GPR tomography results

Figure 4.25shows tomographic images of Bridge B-13-144 columns H and G. Once again puzzling results are obtained. Areas with large water contents (that is, areas with low electromagnetic wave velocities) appear at the center of the column in the lower section of the column or the top of column where little splashing would be expected.

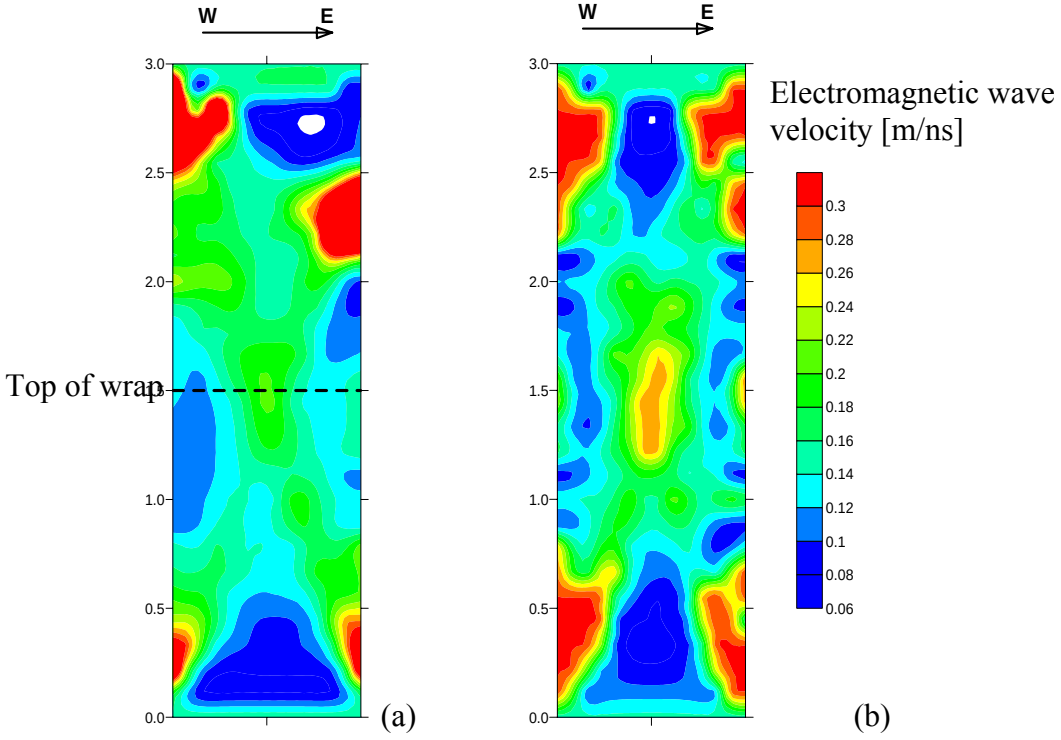

Figure 4.25: GPR tomographic images of Bridge B-13-144: (a) column H and (b) column G (plane parallel to traffic).

4.4. Half-Cell Potential Measurements

In addition to the P-wave and electromagnetic wave transmission tests, half-cell potential measurements were taken on all of the eight selected columns in bridges B-28-45, B-53-71, and B-13-144. These measurements were collected in order to determine the level of corrosion activity in the columns. Figure 4.26 shows the typical field test setup. The measurements were conducted in accordance with ASTM C876-91 using a copper-copper sulfate half-cell, wires, and a high-impedance voltmeter. Figure 4.27 shows the field procedure used to access the reinforcing bar and to collect half cell potential data. Half-cell measurements were taken throughout the columns in the unwrapped column (Bridge B-28-45 column C) and above and below the wrap in fiberglass wrapped columns (Bridge B-28-45 columns A and B, bridge B-53-71 columns A, B, and D, and bridge B-13-144 columns G). To monitor corrosion activity over time, half cell potential readings were collected both in 2007 and 2008 in bridge B-28-45 columns.

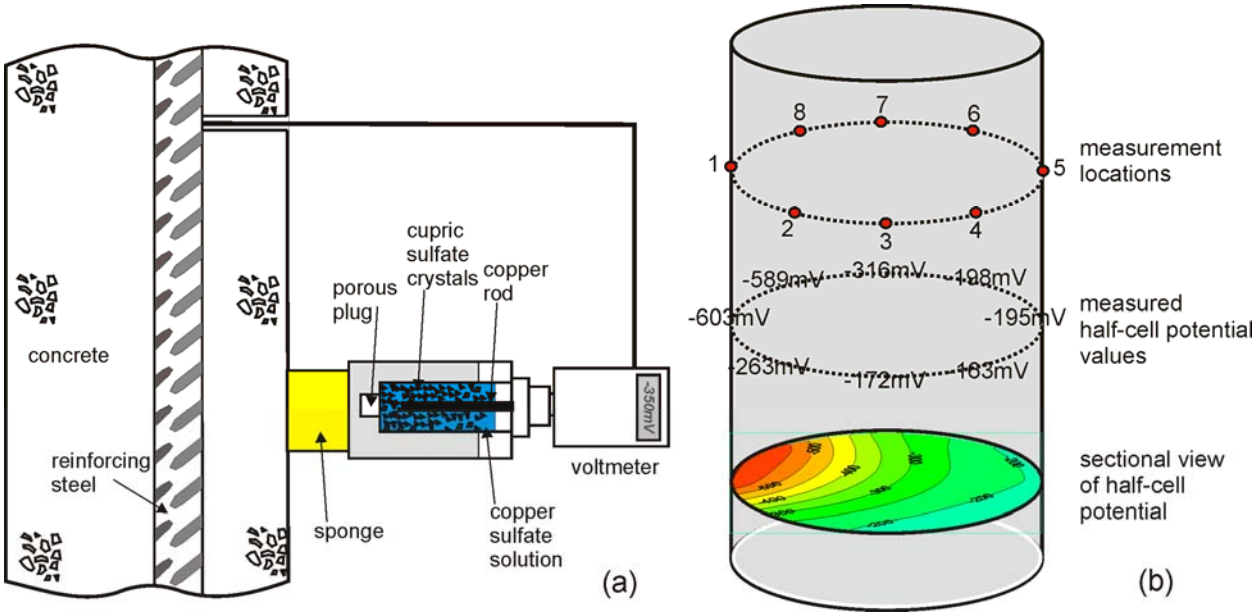

Figure 4.26: Copper to copper half-cell potential measurements on the reinforced concrete column: (a) testing set-up, and (b) measurement locations and presentation of the data.

Figure 4.27: Half-cell potential and Cl^- content data and sample collection: (a) Concrete column drilling. (b) Concrete powder collection for Cl^- content estimation. (c) Half-cell potential measurements. (d) Access to the concrete column below the fiberglass wrap. (e) Half-cell potential measurements below the fiberglass wrap. (f) Electrode connection to steel rebar.

4.4.1 Bridge B-28-45: Half-cell potential results

Half-cell potential measurements were collected in columns A, B, and C of bridge B-28-45. Data were collected in 2007 and then repeated in 2008 to evaluate the evolution of corrosion activity in fiberglass wrapped columns (columns A and B) and in a one untreated column (column C). Half-cell potential data in columns A and B were collected just below the fiberglass wrap (at the

column-ground level – Figure 4.27e) and just above the fiberglass wrap (at 2.4 m in column A and 2.8 m in column B). The impervious nature of the fiberglass prevented the collection of half-cell potential on the wrap. Half cell potential results for this bridge are summarized in Figures 4.28 to 4.32.

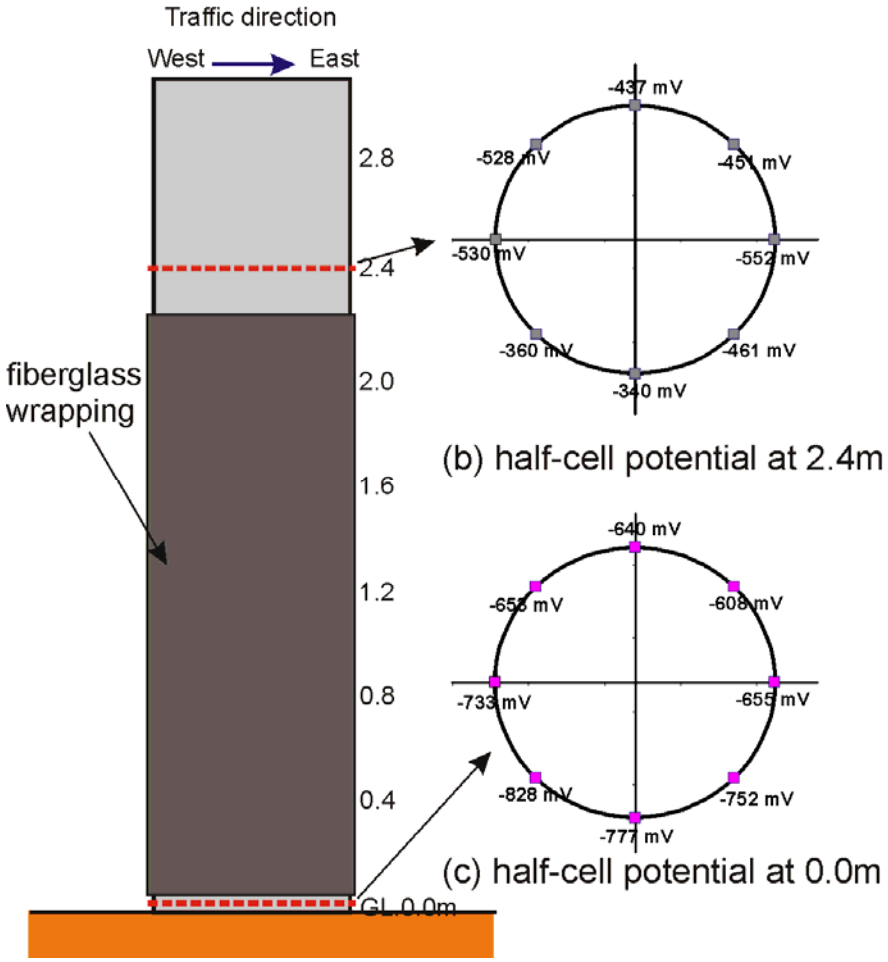

Figure 4.28: Half cell potential measurement in Bridge B-28-45 column A (fall 2007): (a) above wrap and (b) below wrap.

Figures 4.28 and 4.29 summarize half cell potential results for wrapped columns A and B collected in fall 2007. In both columns, the readings indicate strong corrosion activity (i.e., a 90% probability risk of corrosion - Table 2.4). The corrosion activity as indicated by the half cell potential measurements is particularly strong in column B. This activity is greater below the fiberglass wrap than above the wrap. This observation is expected as the salt solution splashing is

stronger at the bottom of the columns. Similar measurements were performed during the summer 2008. These results are summarized in Figures 4.30 and 4.31 and show a continuation of corrosion activity although the results are somehow smaller. The variation of the results may be caused by several environmental conditions such as changes in column moisture, temperature, etc.

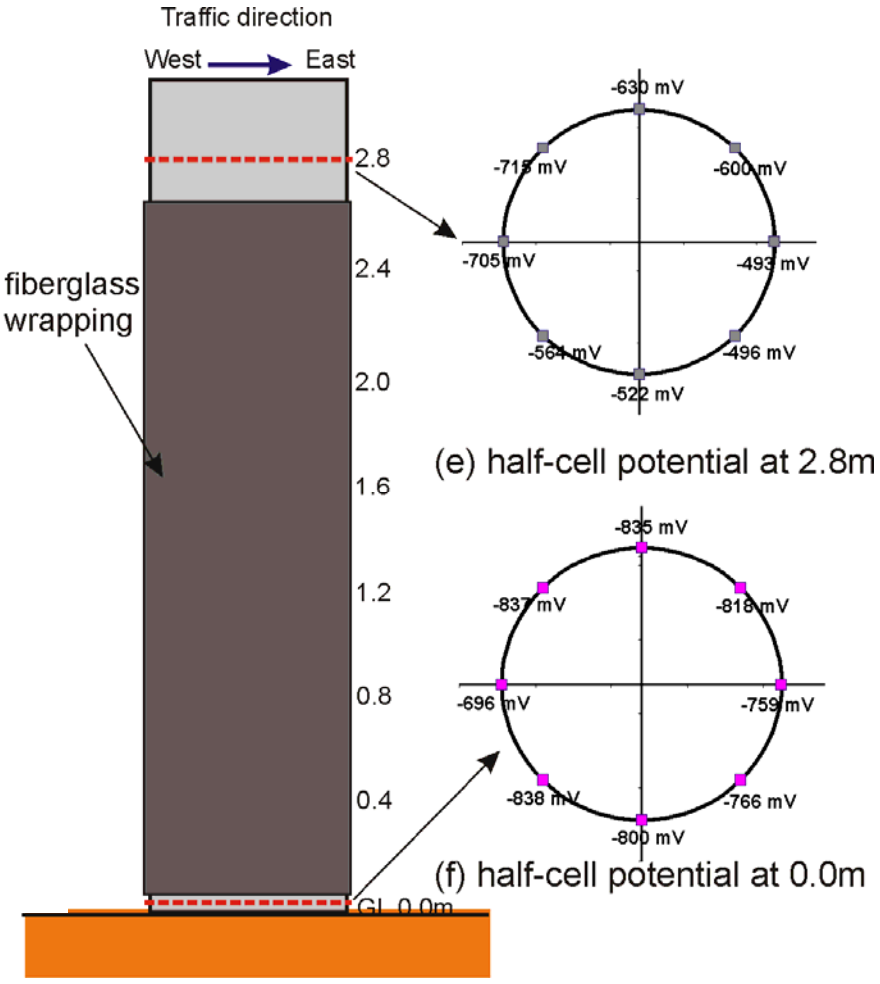

Figure 4.29: Half cell potential measurement in Bridge B-28-45 column B (fall 2007): (a) above wrap and (b) below wrap.

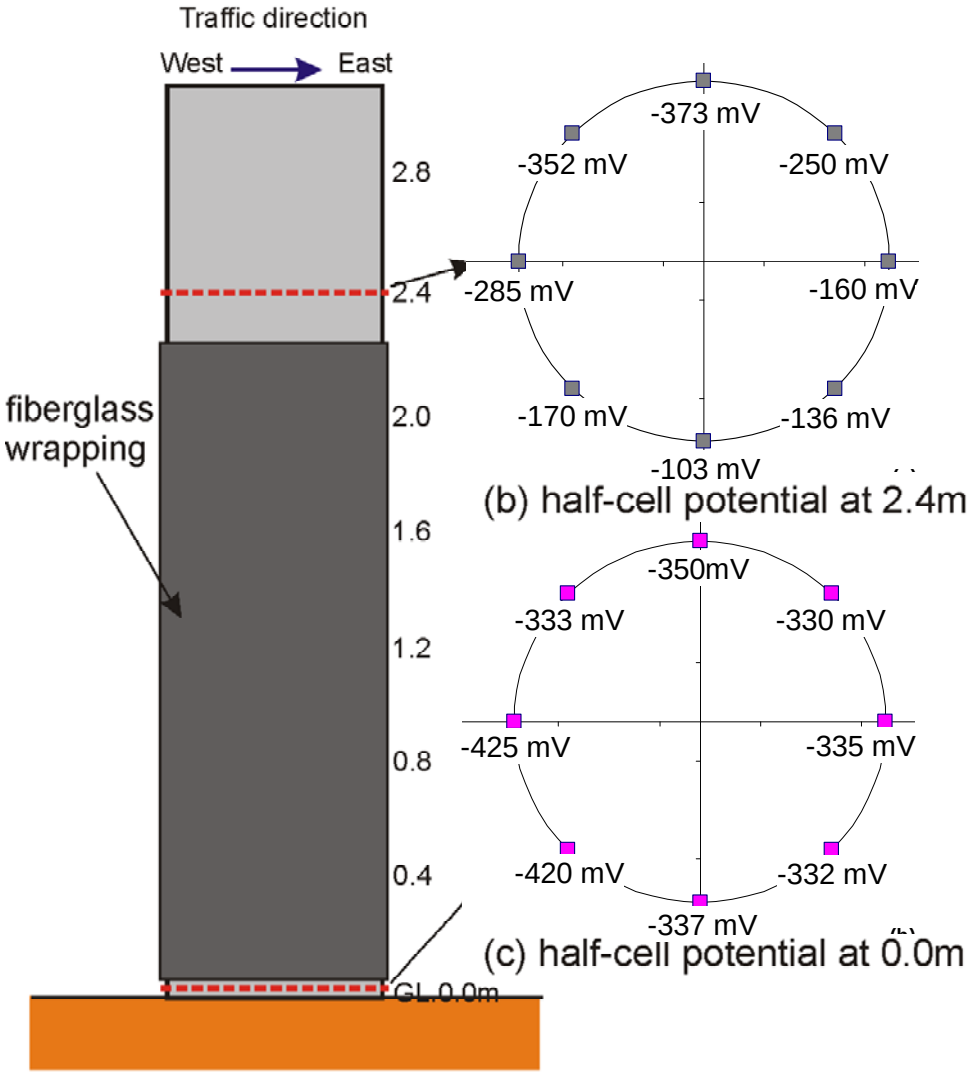

Figure 4.30: Half cell potential measurement in Bridge B-28-45 column A (summer 2008): (a) above wrap and (b) below wrap.

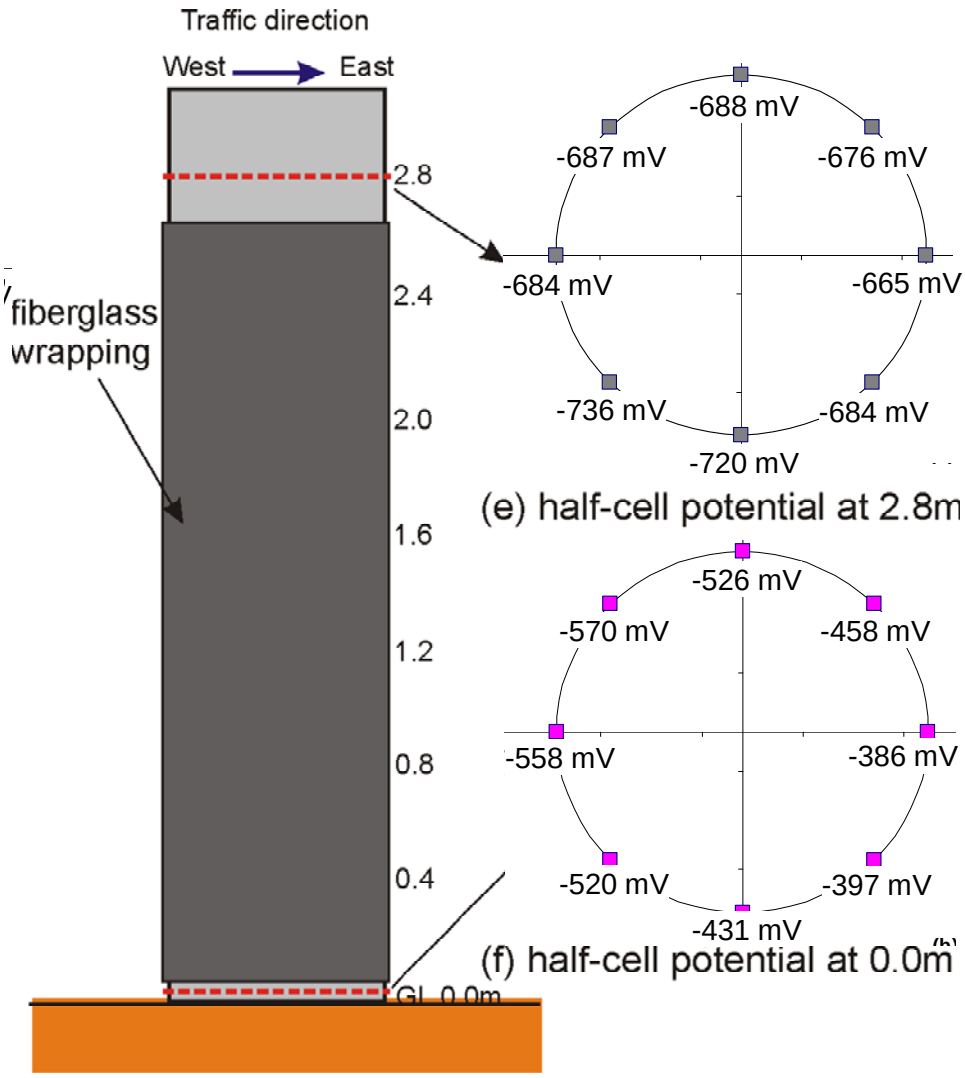

Figure 4.31: Half cell potential measurement in Bridge B-28-45 column B (summer 2008): (a) above wrap and (b) below wrap.

Half-cell potential readings were also taken on bridge B-28-45 unwrapped column C during fall 2007. These measurements shows greater negative values along the area with the corrosion distress (surface crack and discoloration – Figure 4.32). This area is also the surface of concrete that receives most of the deicing solution splashing (e.g., Figure 1.1). The half cell potential readings in the columns confirm the visual observations and show strong corrosion activity next and around the deteriorated concrete. It is also clear that the corrosion activity decreases at with height of the column as less saline solution splashing reaches at higher column elevations.

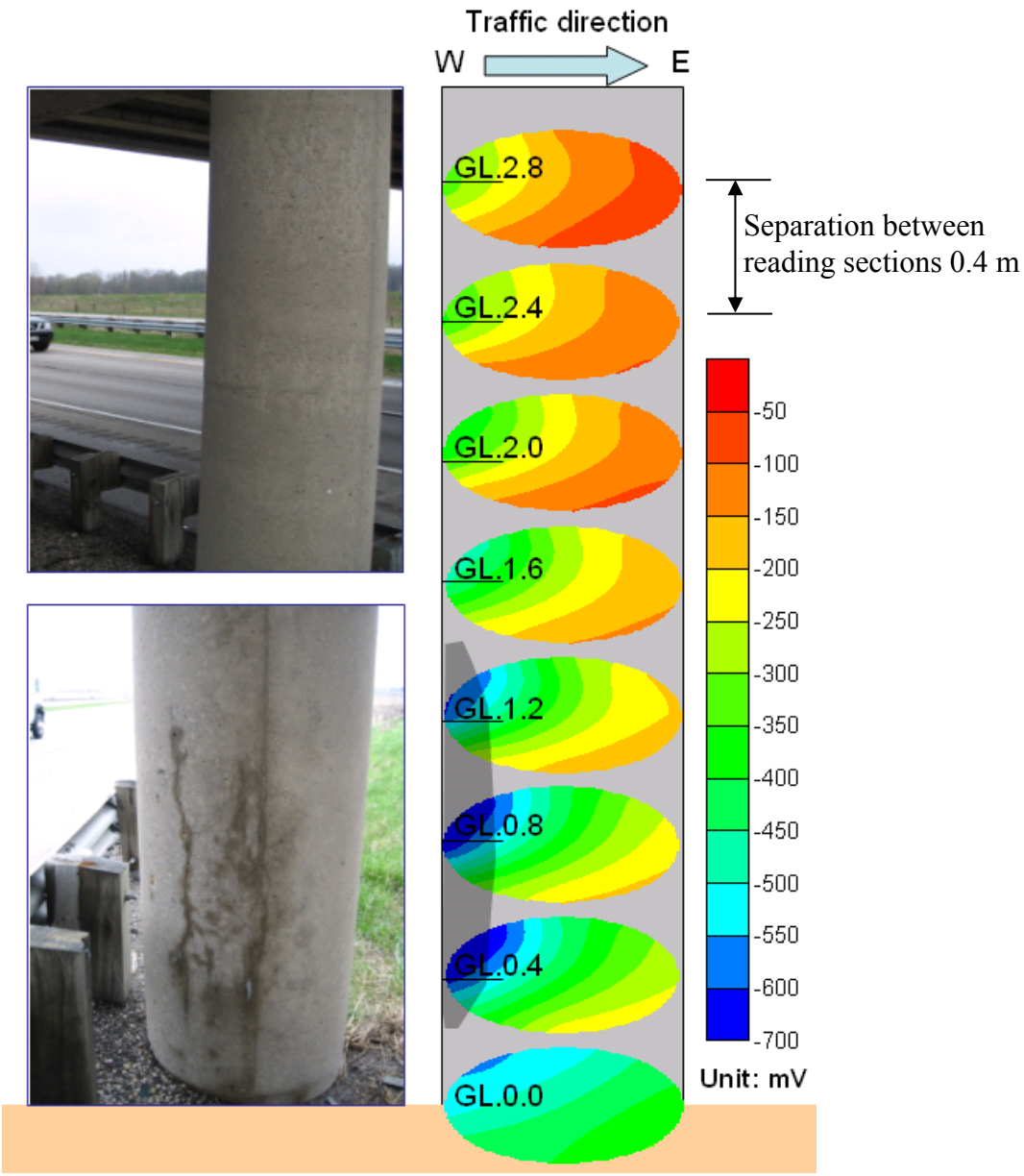

Figure 4.32: Half cell potential measurements in Bridge B-28-45 column C: View of the columns and half-cell potential measurement results (measurement at 0.2 m intervals above ground level - GL).

Half-cell potentials readings were also collected during summer 2008. Half-potential results collected in fall 2007 are compared to summer 2008 results in Figure 4.33. These data show a strong increase in the corrosion activity in one-year period. It is also important to note that half cell potential values collected in summer 2008 are clearly higher than the values obtained in the wrapped columns A and B.

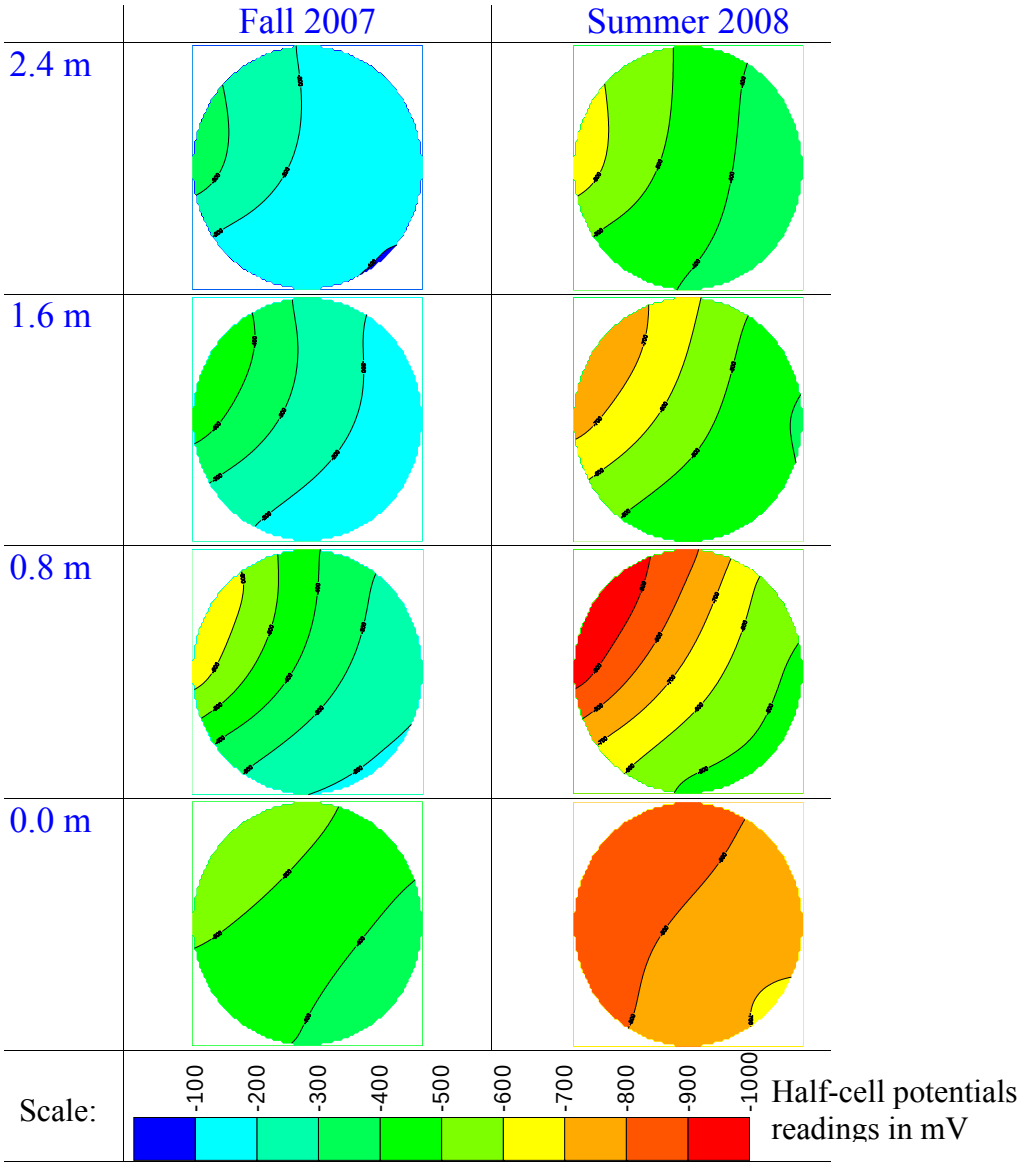

Figure 4.33: Half cell potential measurements in Bridge B-28-45 column C: Comparison of measurements collected on fall 2007 and summer 2008.

4.4.2 Bridge B-53-71: Half-cell potential results

Half-cell potentials reading were collected in Bridge B-53-71 column B during fall 2007. This column was wrapped with fiberglass up to the 1.4 m mark and then painted with epoxy up to the 1.6 m mark. The data collected just below and above the fiber glass wrap are presented in Figure 4.34. These data show high probability of corrosion activity (< -350 mV) just above and just above the wrap and facing the traffic direction. The activity levels are stronger just below the

wrap than above the wrap. These data are evidence of the continuing corrosion in spite of the fiberglass wrapping application. These results were confirm using half cell potential data from bridge B-53-71 column C. Figure 4.35 show half-cell data obtained just above and just below the fiberglass wrap. The bottom collected just below the fiberglass wrap show strong evidence of corrosion activity. It seems from these data that moisture and Cl^- are still reaching the columns maintaining the conditions for corrections activity.

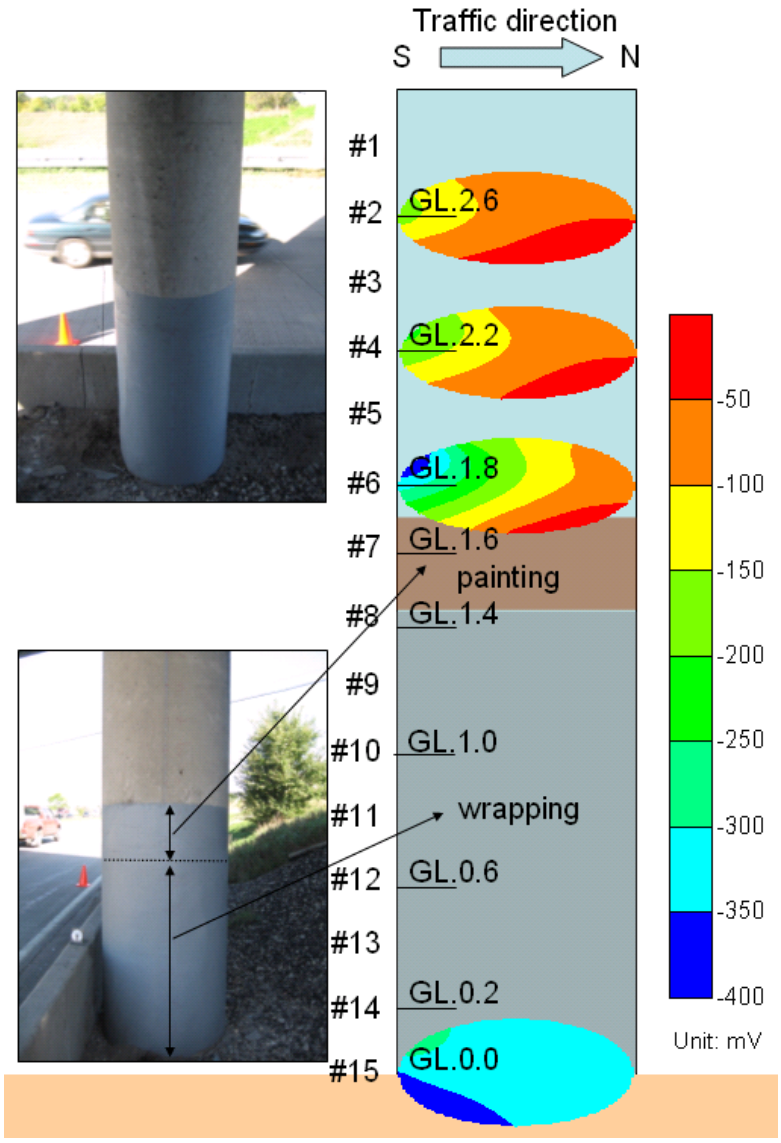

Figure 4.34: Half cell potential measurement in Bridge B-53-71 column B (fall 2007) at 0.2 m intervals above ground level (GL).

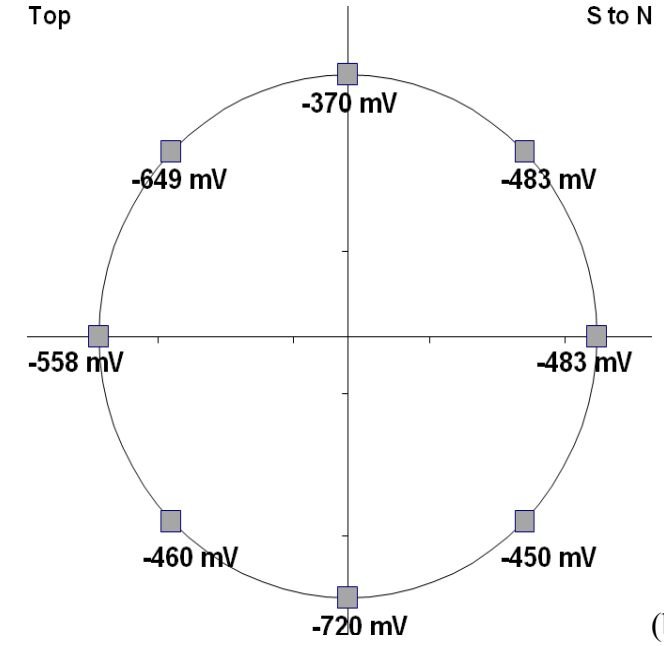

(b)

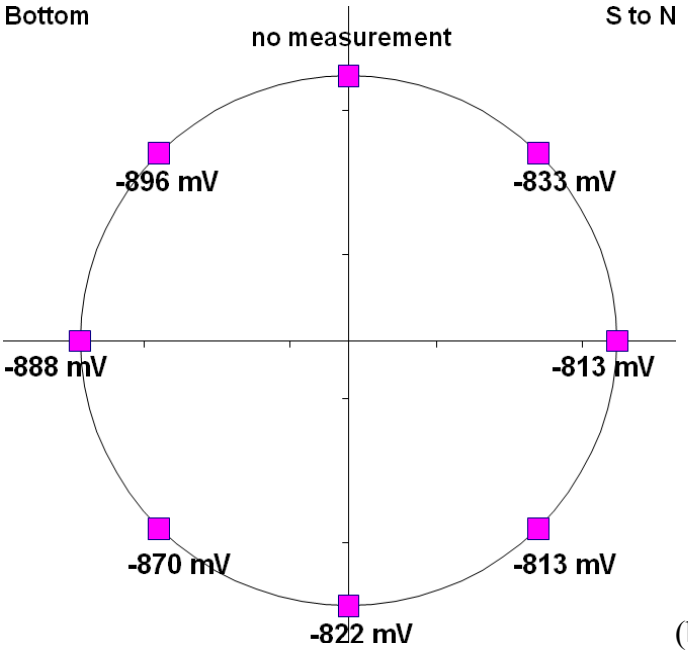

(b)

Figure 4.35: Half cell potential measurements in bridge B-53-71 column C: (a) just above the fiberglass wrap and (b) just below the fiberglass wrap.

4.4.3 Bridge B-13-144: Half-cell potential results

Finally half cell potential data were collected in Bridge B-13-144 column B during fall 2007. This column was wrapped and there was evidence of distress in the P-wave velocity survey (see Figure 4.18b). Figure 4.36 summarize the half cell potential data results. The data indicate high probability of corrosion. This activity seems to be especially high in the splash zone.

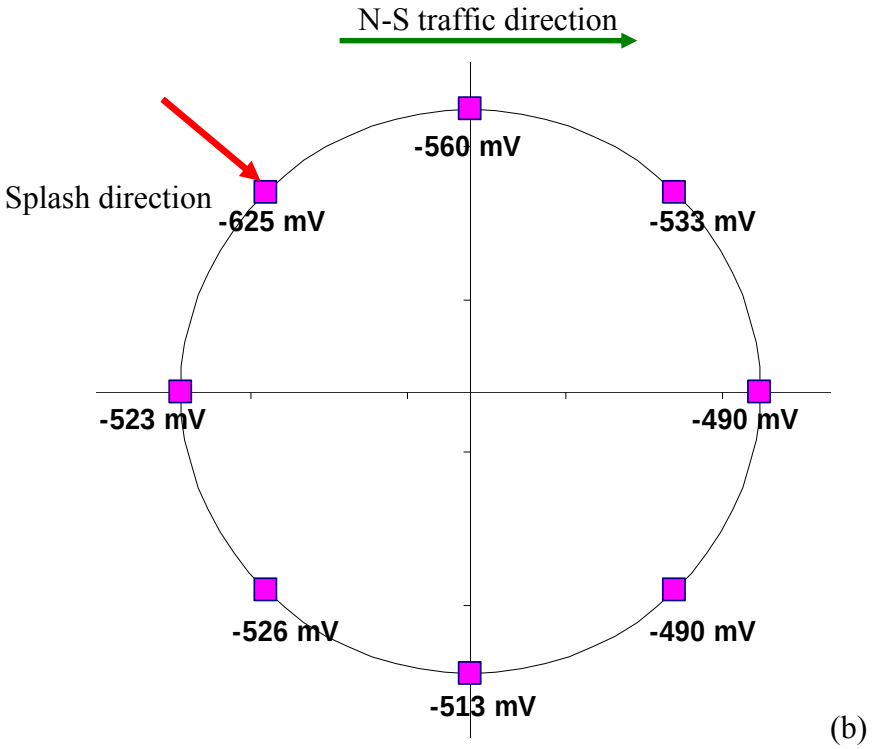

Figure 4.36: Half cell potential measurement in Bridge B-13-144 column G. Data collected just below the fiberglass wrap.

4.5. Half-Cell Potential Measurements

The chloride ion (Cl^-) concentration measurements were obtained from samples at various depths and locations in the columns in all three bridges studied. Concrete samples were taken on the traffic splash zones as well as on the shadow of traffic splashing surfaces and at different elevations to help understand and justified how different areas of the columns are attacked at different rates.

4.5.1. Sample collection

Concrete powder samples were collected in both wrapped and unwrapped columns. Powdery concrete samples were removed using a rotary hammer drill and collected using a portable vacuum cleaner (see Figure 4.26). Since three grams of concrete powder are necessary to perform Cl^- content test, approximately five to ten grams of material were gathered at different depths into the concrete. Collected samples were placed in a labeled plastic bag and taken to the laboratory for chloride ion testing as described in Section 2.4.5. Figure 4.36 show the sample extraction locations in all three bridges.

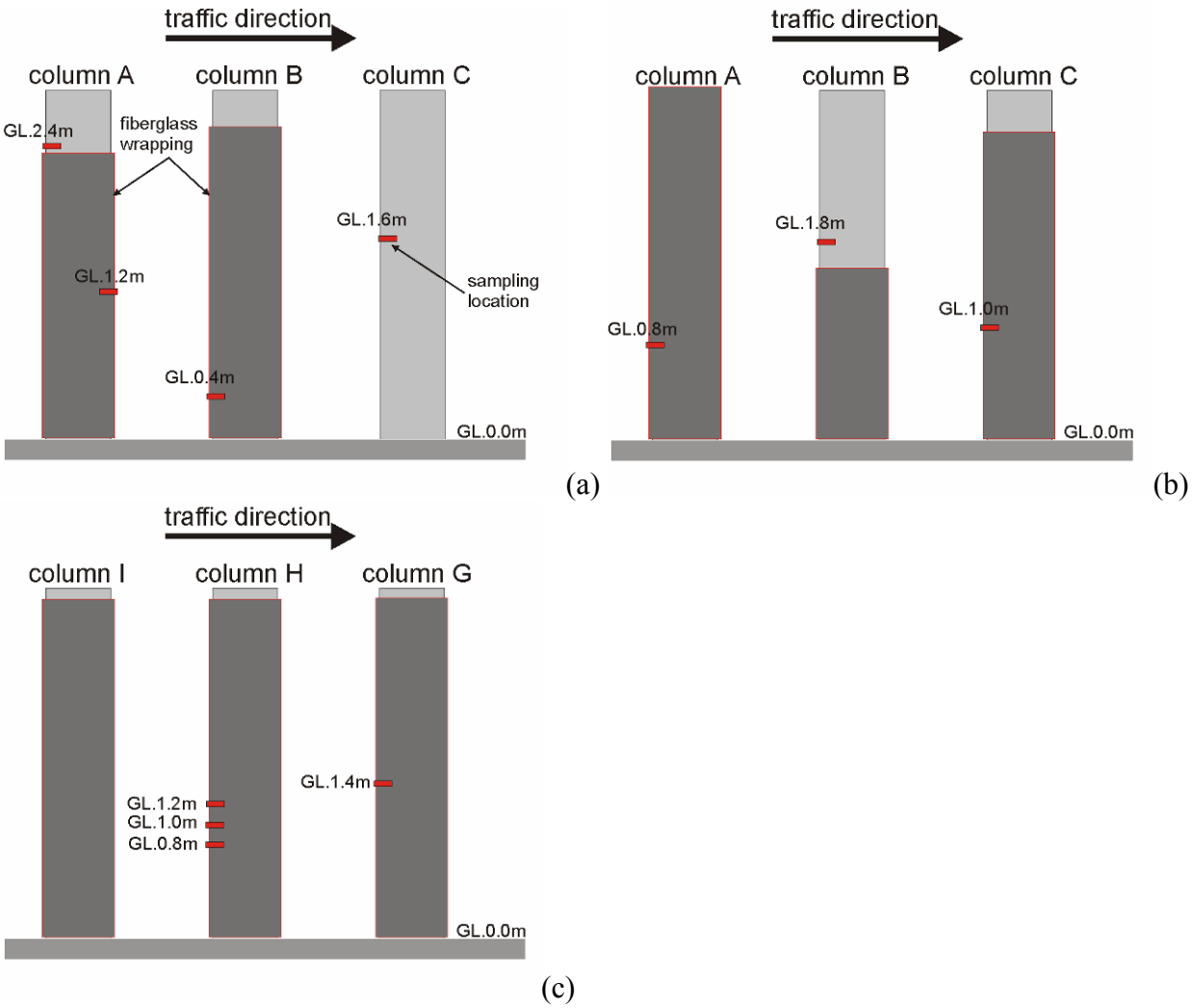

Figure 4.37: Location of extracted powder samples: (a) bridge B-28-45, (b) bridge B-53-71, and (c) bridge B-13-144.

4.5.2. Conceptual interpretation

An indicator of the corrosion potential of reinforcing bars in concrete is the amount of chloride content in the concrete (Cady and Weyers 1983). This value is typically limited in concrete elements. For example, the maximum water soluble chloride ion content recommended for conventionally reinforced concrete in a moist environment and exposed to chloride ions is 0.10 % (by weight of cement content - Berver et al. 2001; ACI 201.2R-77). However, the common threshold value documented in the literature to initiate corrosion in black rebars is 0.2 % (by weight of cement content – Pincheira et al. 2008).

To evaluate the progression of Cl^- into to concrete, the one-dimentional diffusion problem is commonly solved. The one-dimensional diffusion process is modeled using Fick's second law:

$$\frac{\partial C}{\partial t} = D_c \frac{\partial^2 C}{\partial z^2} \tag{4.1}$$

where C is the chloride concentration, z is the depth into the column, t is time, and D_c is the diffusion coefficient. The standard one-dimensional solution of the diffusion equation is:

$$C(z,t) = C_0 \cdot \left[1 - \mathrm{erf}\left(\frac{z}{2\sqrt{D_c \cdot t}}\right)\right] \tag{4.2}$$

where C(z,t) is the chloride concentration at depth z and time t, C_0 is the chloride concentration at the surface, and erf is the error function and it can be as the series expansion (Beyer 1987). It is expected that the Cl^- concentration decrease from the concrete surface towards the center of the columns. A reverse in the concentration distribution is an indication that the concrete may have been replaced during maintenance operations or during the application of the fiberglass wrapping. That is the damaged concrete is removed and new mortar with low Cl^- content is placed instead.

Finally, it should be considered that the surface Cl^- content is different in different parts of the columns. The Cl^- surface content is expected to decrease from the bottom to the top of the column and from the splash zone to the back of the columns. That is, the Cl^- content does not only changes with depth, but it also changes along the height and the diameter of the columns as controlled by the splashing pattern.

4.5.3. Cl^- Concentration Results

Table 4.1 summarizes the Cl^- results for concrete powder samples collected in fall 2007. The table presents the height of concrete sample extraction, the local Cl^- concentration, and the Cl^- concentration versus depth. The results are compared against typical diffusion results (that is, the Cl- concentration decreases versus depth) and the recommended maximum Cl^- concentration for this type of structures (Berver et al. 2001; ACI 201.2R-77).

Results from bridges B-28-45 and B-13-144 show that Cl^- measurements in the wrapped locations show an anomalous distribution: the Cl^- content is smaller closer to the surface than deeper into the columns. The reason for these lower measurement values is the presence of the newer mortar used to patch the damage area before the wrapping was applied. These out-of-trend points seem to show that the replacement of damaged concrete with new concrete improves the conditions against rebar corrosion as the Cl^- contaminated concrete is removed. However, the Cl^- content profile results from the B-53-71 bridge, which had experienced extensive corrosion damage, cannot show the effectiveness of fiberglass wrapping treatment. In these columns, there is no evidence of Cl^- content reduction after the application of the wrapping.

These results were confirmed with data collected during summer 2008. The comparison of the data collected in column B bridge B-28-45 in fall 2007 (Table 4.1) and summer 2008 (Table 4.2) show no significant increase in the Cl- content distribution over a year. This observation seems to indicate that fiberglass wrapping is an effective tool in arresting the access of additional chloride ion into the concrete. However, if fiberglass wrapping is applied on a corroding column, the treatment effectiveness may fall short of expectations. That is, corrosion activity may continue even after the application of the fiberglass wrap and additional maintenance may be required. Evidence of this problem was documented during the visual inspection of fiberglass

wrapped columns (B-11-17 – Figure 3.1). The same column was re-wrapped as the on-going corrosion process continued even after the column was treated with the fiberglass wrap.

Table 4.1: Chloride ion concentration results (Sampling: fall 2007)

Bridge	Column	Elevation (m)	Sample depth (cm)	Cl^- content (%)	Cl^- content distribution
B-28-45	A	1.2 (U)	2.54	0.069	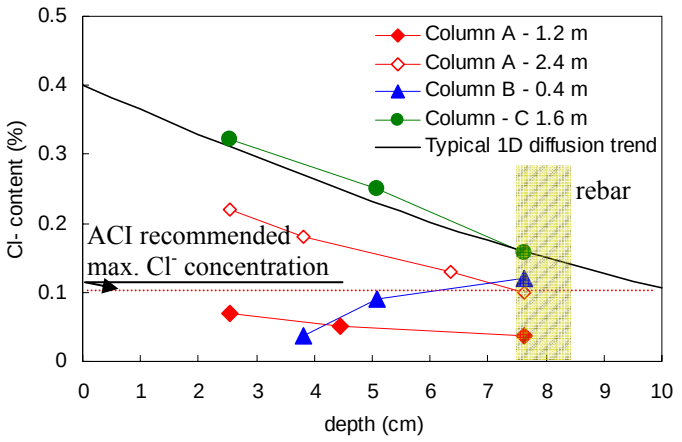
			4.45	0.050	
			7.62	0.037	
		2.4 (W)	2.54	0.220	
			3.81	0.181	
			6.35	0.129	
			7.62	0.099	
	B	0.4 (W)	3.81	0.037	
			5.08	0.091	
			7.62	0.121	
	C	1.6 (U)	2.54	0.321	
			5.08	0.251	
			7.62	0.157	
B-53-71	A	0.8 (W)	3.81	0.228	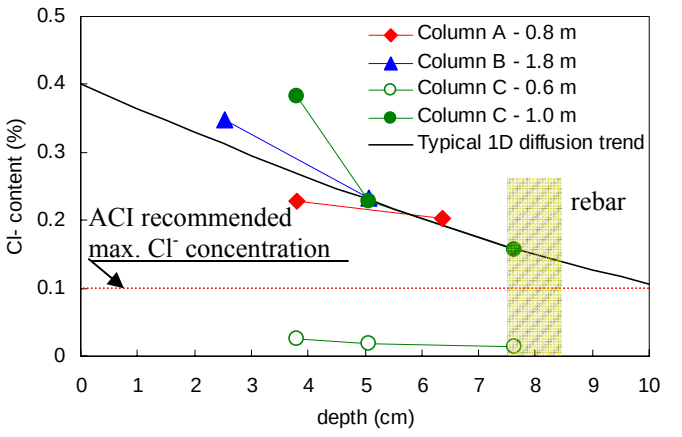
			6.35	0.203	
	B	1.8 (U)	2.54	0.347	
			5.08	0.232	
	C	0.6 (W)	3.81	0.025	
			5.08	0.019	
			7.62	0.014	
		1.0 (W)	3.81	0.382	
			5.08	0.229	
			7.62	0.157	
B-13-144	H	0.8 (W)	3.81	0.011	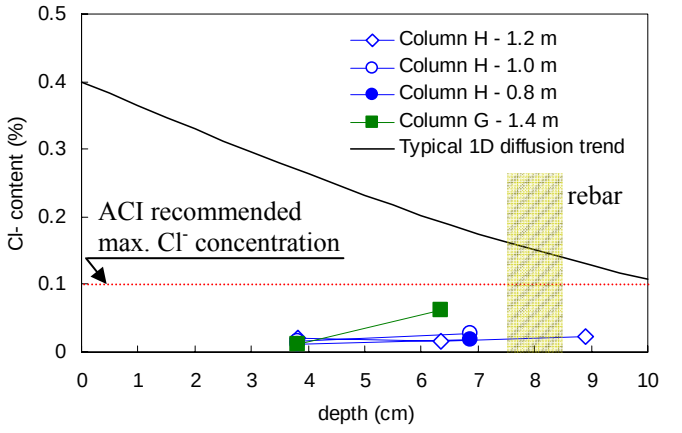
			6.86	0.018	
		1.0 (W)	3.81	0.017	
			6.86	0.028	
		1.2 (W)	3.81	0.021	
			6.35	0.017	
			8.89	0.022	
	G	1.4 (W)	3.81	0.012	
			6.35	0.061	

Note: W: wrapped column – U: unwrapped column

Table 4.2: Chloride ion concentration results (Sampling: summer 2008)

Bridge	Column	Elevation (m)	Sample depth (cm)	Cl^- content (%)	Cl^- content distribution
B-28-45	B	0.4 (W)	2.54	0.018	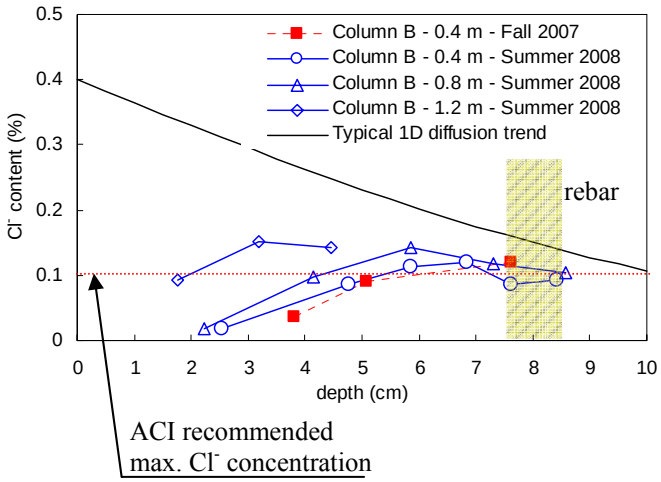
			4.78	0.086	
			5.87	0.112	
			6.83	0.119	
			7.62	0.087	
			8.41	0.092	
		0.8 (W)	2.24	0.017	
			4.14	0.097	
			5.87	0.142	
			7.32	0.118	
			8.59	0.103	
		1.2 (W)	1.75	0.092	
			3.18	0.151	
			4.45	0.142	
			7.62	0.157	

Note: W: wrapped column – U: unwrapped column

Chapter 5. Summary and Conclusions

This report summarizes the results of a research to evaluate the performance of fiberglass wrapping for reducing and arresting corrosion activity in damaged bridge concrete columns. The research team performed a complete visual inspection on thirteen columns Dane, Jefferson, Columbia and Rock counties in the State of Wisconsin. From these thirteen bridges, the research team selected eight columns in three different bridges for an in-depth study.

P-wave and electromagnetic wave travel-time data and tomographic images were used to evaluate the integrity of concrete column while half-cell potential measurements evaluated the level of corrosion activity in the selected columns. Concrete powder samples were collected to evaluate the distribution of Cl^- concentration in several of the columns studied. P-wave testing and half-cell potential measurement show that concrete damage and corrosion activity are located on the concrete surface that is splashed by the deicing solution (Figure 1.1) and is contaminated by chlorine ions. Cl^- content versus depth profiles provide information about the effectiveness of fiberglass wraps as barrier for chemical attacks and reduction of corrosion activity. Specific findings and conclusions follow:

- The P-wave travel time tomographic images of columns in bridge B-28-45 provide spatial information of damaged zone in concrete columns. Sectional and vertical tomographic images of wave velocity indicate that a most of the damaged occurs in the zone facing traffic. The tomographic images results are supported by visual inspection but also seem to indicate that the damage in the columns is deeper than the 3-in concrete cover
- In bridge B-28-45, half-cell potential measurements show that the corrosion activity continues even after the fiberglass was applied.

- The effectiveness of fiberglass wrapping was also evaluated by measuring Cl^- content profiles in three bridges. The results show that the patching used in damaged columns reduced the Cl^- content below the values recommended by ACI by replacing the contaminated concrete. However, in heavily damaged columns, the wrapping remediation does not seem to have reduced, the Cl^- concentration. This condition raises the possibility of continuing corrosion and the need to further maintenance.

Engineering recommendations

The data collected in this study indicate that fiberglass wrapping maintenance operations reduces the Cl^- ion content when the concrete cover is removed and replaced and it prevents the future ingress of de-icing salts. However, the maintenance technique does not reduce the potential for continuing corrosion activity if the driving mechanism (high Cl^- content and moisture remain). The technique should be complemented with other remediation operations, such as electrochemical removal of Cl^- (Bennett et al. 1993; Bilkul'chus 2005). These techniques aim at removing one of the drivers in the corrosion process by reducing the Cl^- content in the concrete. Furthermore, WisDOT officials should consider changing some of common fiberglass wrap maintenance practices, for example:

- The height of the fiberglass wrap treatment should be extended to at least one foot below the ground surface to reduce the likelihood of Cl^- and moisture intrusion to the concrete surface. Above the surface, the wrapping should be extended at least on foot above the maximum expected snow splashing (e.g., Figure 1.1).
- The practice of removing the damaged concrete and patching the columns with new mortar should be continued. However, WisDOT officials should also contemplate measuring Cl^-

content in the remaining concrete paste as high concentrations would continue corroding the rebars despite the fiberglass treatment and alternative treatment should be considered.

- Despite the effect of fibers was not studied in this project, WisDOT officials may consider painting the columns with epoxy resin (without using the fibers) to create an impervious barrier. This alternative treatment may have the same effect than the fiberglass treatment at lower cost and may allow preventing the initiation of the corrosion process. (The time of the epoxy painting application may be determined by the evaluation of diffusion parameters and Cl^- concentration in undamaged columns). WisDOT officials must be cautioned however that epoxy resin without fiberglass may experience cracking.
- Finally, WisDOT officials should also consider dryness and temperature during the application of the warp. Low moisture in the columns should help in reducing the corrosion activity as the wrap is applied.

References

Allen, R.T.L., S.C. Edwards, and J.D.N. Shaw, ed. (1993). *The Repair of Concrete Structures*, Second Edition, Blackie Academic & Professional, Glasgow, UK

Aster, R. C., Thurber, C. H., and Borchers, B. (2005). *Parameter Estimation and Inverse Problems*. Academic Press, 301 pages

Baiyasi, M. I. (2000). *Repair of corrosion-damaged columns using FRP wraps*, PhD Dissertation, Michigan State University.

Bennett, J., Fong, K. F., Schue, T. J. (1993). *Electrochemical Chloride Removal and Protection of Concrete Components: Field Trials*. Strategic Highway Research Program information. SHRP-S-669. URL: http://www.trb.org/publications/shrp/SHRP-S-669.pdf. 149 pages.

Bentur, A., Diamond, S., and Berke, N. S. (1997). *Steel corrosion in concrete*, Chapman & Hall, London, UK.

Berver, E.W., Jirsa, J. O., Fowler, D.W., Wheat, H.G., and Moon, T. (2001). *Effects of Wrapping Chloride Contaminated Concrete with Fiber Reinforced Plastics*, Center for Transportation Research Report 0-1774-2, October 2001.

Beyer, W. H. (1987). *Standard Mathematical Tables*, 28th edition, CRC Press, Boca Raton, FL.

Bikul'chus, G. (2005). "Chloride Removal from Reinforced Concrete and Relevant Loss of Strength". *Protection of Metals*. Vol. 41. No. 5, pp. 484–486.

Broomfield, J. P. (1997). *Corrosion of Steel in Concrete*, E. & F.N. Spon, London, UK.

Cady, P.D. and Weyers, R.E. (1983). "Chloride Penetration and the Deterioration of Concrete Bridge Decks", *Cement, Concrete and Aggregate*, Vol. 5, No. 2, pp. 81–87.

Daigle, M., Fratta, D., and Wang, L. B. (2005). "Ultrasonic and X-ray Tomographic Imaging of Highly Contrasting Inclusions in Concrete Specimens". *2005 GeoFrontier Conference*. Austin, TX.

Erki, M. A., and Rizkalla, S. H. (1993). "FRP reinforcement for concrete structures: a sample of international production". Concrete International, Vol.15, No.6, pp 48-53.

Fernandez, A.L. and Santamarina, J.C. (2003). "Design Criteria for Geotomographic Field Studies", *ASTM Geotechnical Testing Journal*, vol. 26, no. 4, pp. 410-420.

Google Maps (2008). URL: http://maps.google.com/. Accessed on August 25, 2008.

Gu, P., and Beaudoin, J. J. (1998). "Obtaining effective half-cell potential measurements in reinforced concrete structures." *Construction Technology Update No. 18*. National Research Council of Canada. 4 pages.

Khan, M. S. (1991). "Corrosion state of reinforcing steel in concrete at early ages." *ACI Materials Journal*, Vol. 88, No.1, pp.37-40.

Krautkrämer, J. And Krautkrämer, H. (1990). Ultrasonic Testing of Materials, Fourth Edition, New York, Springer-Verlag.

Leslie, J. R., and Cheesman, W. J. (1949). "An ultrasonic method of studying deterioration and cracking in concrete structures." *Journal of the American Concrete Institute*, Vol. 21, No. 1, pp. 17-36.

Li, C. Q., Lawanwisut, W. and Zheng, J. J. (2005). "Time-Dependent Reliability Method to Assess the Serviceability of Corrosion-Affected Concrete Structures". *Journal of Structural Engineering.* Vol. 131, No. 11, pp. 1674-1680.

Mehta, P. K. (1986). *Concrete, Structure, Properties, and Materials*. Prentice-Hall, Englewood Cliffs, New Jersey.

Mirmiran, A., Shahawy, M., Nanni, A., and Karbhari, V. (2004). "Bonded Repair and Retrofit of Concrete Structures Using FRP Composites," *NCHRP Report 514*, National Cooperative Highway Research Program, Transportation Research Board, Washington, D.C., 2004.

Nanni, A., and Lopez, A. (2004). "Validation of FRP composite technology through field testing" *16th World Conference on Nondestructive Testing*. Montreal, Canada. August 30-September 3, 2004.

Neale, K. W., Demers, M., and Labossière, P. (2005). "FRP protection and rehabilitation of corrosion-damaged reinforced concrete columns". *Int. J. Materials and Product Technology*, Vol. 23, Nos. 3/4, pp. 348-371.

Neville, A. M. (1996). *Properties of Concrete*. Fourth Edition, Wiley, New York.

Perkins, P.H. (1997). *Repair, Protection and Waterproofing of Concrete Structures*. E.& F.N. Spon, London, UK.

Pincheira, J. A., Amarayo, A., Kim, K.-S., and Fratta, D. (2008). *Corrosion Protection Performance of Epoxy-Coated Reinforcing Bars*. Minnesota Department of Tranportation Report No. MN/RC 2008-47. 224 pages.

Prada, J., Fratta, D., and Santamarina, J. C. (2000). "Tomographic Detection of Anomalies with Limited Data Sets - Velocity and Attenuation". *ASTM Geotechnical Testing Journal*, Vol. 23, No. 4, pp. 472-486.

Ryall, M. J. (2001). *Bridge Management*. Boston: Butterworth-Heinemann.

Santamarina, J.C., in collaboration with Klein, K. and Fam, M. (2001). *Soils and Waves*. J. Wiley and Sons, Chichester, UK, 488 pages.

Santamarina, J. C. and Fratta, D. (2005): *Discrete signals and inverse problems: an introduction for engineers and scientists*, John Wiley and Sons, Chichester, UK.

Sbartai, Z. M. (2007). "Using Radar Direct Wave for Concrete Concrete Assessment: Correlation with Electrical Resistivity". *Journal of Applied Geophysics.* Vol. 62, No. 4, pp. 361-374.

Tang, B. M. (2003). "FRP composites technology brings advances to the American bridge building industry.", *Proceedings of the 2nd International Workshop on Structural Composites for Infrastructure Applications*, Cairo, Egypt; December 16-18, 2003.

Teng, M.-H., Sotelino, E. D., and Chen, W.-F. (2003). "Performance evaluation of reinforced concrete bridge columns wrapped with fiber reinforced polymers.", *Journal of Composites for Construction,* Vol. 7, No. 2, pp.83-92.

Tyfo Fiberwrap Systems (2008). Company Web Site. URL: http://www.fyfeco.com/. Accessed on August 20, 2008.

Vaysburd, A. M, and Emmons, P. H. (2000). "How to make today's repairs durable for tomorrow – corrosion protection in concrete repair." *Construction and Building Materials*, Vol. 14, No. 4, 189-197.

Watson, R. J. (2000). "Wrapping it Up," *ASTM Standardization* News, February, pp. 22-25.

Wootton, I. A., Spainhour, L. K., and Yazdani, N. (2003) "Corrosion of steel reinforcement in carbon fiber-reinforced polymer wrapped concrete cylinders", *Journal of Composites for Construction*. Vol. 7, No. 4, pp. 339-347.

Wisconsin Highway Research Program
University of Wisconsin-Madison
1415 Engineering Drive
Madison, WI 53706
608/262-2013
www.whrp.org